

Alma Mater Studiorum – Università di Bologna

DOTTORATO DI RICERCA IN

Oncologia, Ematologia e Patologia

Ciclo XXX

Settore Concorsuale di afferenza: 06/D3

Settore Scientifico disciplinare: MED06

**New therapeutic approaches in sarcoma:
Immunomodulation and tumor microenvironment**

Presentata da: Dott.ssa. Emanuela Palmerini

Coordinatore Dottorato

Relatore

Chiar.mo Prof. Pier-Luigi Lollini

Chiar.mo Prof. Pier-Luigi Lollini

Esame finale anno 2018

..to my family and Leonardo...

*'I always find beauty
in things that are odd and imperfect
- they are much more interesting'.
[Marc Jacobs]*

INDEX

1 - ABSTRACT.....	7
2 - INTRODUCTION	9
2.1 - Sarcoma.....	9
2.1.1 - Osteosarcoma.....	9
2.1.2 - Synovial sarcoma	16
2.2 - Immune system overview	23
2.3 - The immune contexture in human tumors	25
2.3.1 - The immune contexture: characteristics.....	25
2.3.2 - Clinical impact of the immune contexture.....	28
2.3.2.1 - Intratumoural lymphoid infiltrates	28
2.3.2.2 - Intratumoural PD-L1 expression	29
2.4 - VEGFR, neoangiogenesis and immunotherapy	32
2.4.1 - VEGFR inhibitors as immune-modulators in sarcomas.....	34
2.4.2 - Immunotherapy in sarcomas.....	37
2.5 - CXCR-4 and tumor microenvironment.....	42
2.5.1 - CXCR4 expression in sarcomas	44
2.5.2 - CXCR4 mechanism of action and ‘chemosensitizer’ potential	47

3 - AIM OF THE STUDY	51
3.1 - AIM 1: Immune contexture in osteosarcoma and synovial sarcoma	51
3.2 - AIM 2: Anti-VEGFR and anti-PD-1 activity in osteosarcoma and synovial sarcoma.....	51
3.3 - AIM 3: Anti-CXCR4 activity in osteosarcoma and synovial sarcoma	51
4 – MATERIALS AND METHODS	53
4.1 - Aim 1: Immune contexture in osteosarcoma and synovial sarcoma	53
4.1.1 - Osteosarcoma.....	53
4.1.1.1 - Pre-treatment (bioptic samples)	53
4.1.1.2 - Post-induction chemotherapy (surgical samples)	55
4.1.1.3 - Statistical Analysis	55
4.1.2 - Synovial sarcoma	56
4.1.2.1 - Design and patients	56
4.1.2.2 - Data collection.....	56
4.1.2.3 - Histology and molecular studies.....	56
4.1.2.4 - FISH analysis	56
4.1.2.5 - RT-PCR analysis.....	56
4.1.2.6 - Immunohistochemistry staining.....	57
4.1.2.7 - Statistical analysis.....	58

4.2 - Aim 2: Anti-VEGFR and anti-PD-1 activity in osteosarcoma and synovial sarcoma...	58
4.2.1 - Human Cells.....	58
4.2.2 - Cell lines	58
4.2.3 - Chemicals and Reagents.....	59
4.2.4- Cell proliferation assay	59
4.2.5 - PD-L1 expression on sarcoma cell lines by flow cytometry	60
4.2.6 - Mixed lymphocyte reaction (MLR)	60
4.2.7- Flow cytometry immunophenotyping	61
4.2.8 - Cell apoptosis assay	62
4.2.9 - Statistical analysis.....	62
4.3 - Aim 3: Anti-CXCR4 activity in osteosarcoma and synovial sarcoma	62
4.3.1 - Cell lines and chemicals	62
4.3.2 - Isolation and culture of human bone-marrow mesenchymal stem cells (BM-MSC)	63
4.3.3 - CXCR4 and SDF1 expression in sarcoma cell lines	63
4.3.4 - t(X;18) SS18(SYT)-SSX1 in synovial sarcoma by RT-PCR.....	64
4.3.5 – Cell viability and sensitivity	64
4.3.6 - Cell apoptosis assay	66
4.3.7 - Wound healing assay	67
4.3.8- Statistical analysis.....	67

5 - RESULTS	68
5.1 - Aim 1: Immune context in osteosarcoma and synovial sarcoma	68
5.1.1 - Osteosarcoma.....	68
5.1.1.1 - Tumoral microenvironment components prior chemotherapy (bioptic samples).....	68
5.1.1.2 - Tumoral microenvironment post-induction chemotherapy (surgical samples)	73
5.1.2 - Synovial sarcoma	74
5.2 - Aim 2: Anti-VEGFR and anti-PD-1 activity in osteosarcoma and synovial sarcoma	77
5.2.1 - Sunitinib malate inhibit proliferation in sarcomas	77
5.2.2 - Sarcoma cell lines express PD-L1	78
5.2.3 - PD-1 blockade hamper sarcoma-induced-PD1 expression on lymphocytes.....	78
5.2.4 - Nivolumab activity on <i>activated</i> T-lymphocytes	82
5.2.5 - Sunitinib induce apoptosis in sarcoma	85
5.2.6 - Sunitinib and PD-L1 in sarcoma	86
5.3 - Aim 3: Anti-CXCR4 activity in osteosarcoma and synovial sarcoma	88
5.3.1 - SYT-SSX translocation in synovial sarcoma cell lines	88
5.3.2 - CXCR4 and SDF-1 (CXCL12) expression in sarcoma cell lines	88
5.3.3 - SDF-1 (CXCL12) expression in different media	90
5.3.4 - Treatment with MDX1338 and AMD3100 reduce SW983 and U2OS proliferation.....	92
5.3.5 - Treatment with MDX1338 and AMD3100 does not change CXCR4 expression	94
5.3.6 - Treatment with MDX1338 and AMD3100 reduces SW982 and U2OS cells	

migration	95
5.3.7 -Treatment with MDX1338 and AMD3100 promote SW982 and U2OS cells apoptosis.....	97
5.3.8 - Doxorubicin – CXCR4 inhibitor combined treatments	99
6 - DISCUSSION	103
7 - CONCLUSIONS.....	115
8 - BIBLIOGRAPHY.....	117
9- ACKNOWLEDGMENTS.....	142

1- ABSTRACT

High-grade sarcomas are a heterogeneous group of aggressive tumors arising in bone and soft tissues. They are usually treated with surgery combined in some cases with chemotherapy. Drugs active in osteosarcoma include adriamycin (ADM), cisplatin (CDDP), ifosfamide (IFO) and methotrexate (MTX), while ADM and IFO represent standard chemotherapy for synovial sarcomas. The survival of sarcomas has minimally improved in the past decades, and after relapse treatment options are limited.

Tumors grow within an intricate network of epithelial cells, vascular and lymphatic vessels, cytokines, chemokines and infiltrating immune cells. T- lymphocyte and antigen-presenting cells (APCs) interactions are bi-directional and mediated by ligands such as programmed cell death ligand 1 (PD-L1) on APCs and PD1 on lymphocytes. PD-L1 is expressed also by several tumors. PD-1 inhibitors such as pembrolizumab or nivolumab have been approved for many tumors and PD-L1 expression on tumoral cells has been associated with response in some of the studies. However, few data on the prognostic and predictive role of infiltrating immune cells and PD-1/PD-L1 system in sarcoma are available.

Stromal cells present in the tumor microenvironment express high levels of CXCL12 protein, directly stimulating proliferation and migration of CXCR4-expressing cancer cells. CXCR4/CXCL12 signalling therefore is an attractive therapeutic target in cancer, since CXCR4 inhibition might sensitize cancer cells to conventional chemotherapy.

Finally, another key element of the tumor microenvironment involves its vasculature. Tumor angiogenesis is related to suppression of T cell-mediated tumor rejection. There are numerous examples that demonstrate a simultaneous activation of angiogenesis and immunosuppression. The overall goal of this project is to characterize the osteosarcoma and synovial sarcoma tumor

microenvironment, to assess how the infiltrating immune cells can affect the prognosis of patients and to assess the activity of immune modulating (anti-PD-1), migration inhibitors (anti-CXCR4) and antiangiogenic (anti-VEGFRs, anti-PDGFRs) compounds in an in vitro sarcoma model.

2- INTRODUCTION

2.1 - Sarcomas

Sarcomas are a heterogeneous group of mesenchymal neoplasmas that can be grouped into two general types, primary bone sarcoma and soft tissue sarcoma. Most frequent primary bone sarcomas include osteosarcoma, Ewing sarcoma and chondrosarcoma; most frequent soft tissue sarcomas include synovial sarcoma, liposarcoma, leiomyosarcoma, and angiosarcoma. The survival rate of sarcoma patients increased with the emergence of effective chemotherapy regimens and the development of surgical techniques. However, metastasis still occurs in 20%-55% of these patients, and it remains the main cause of death. Efforts have been made in the last twenty years to improve survival outcomes of sarcoma patients, but changes of the chemotherapy drugs, the doses and the administration schemes did not significantly improve prognosis (1). Advanced treatment methods are urgently needed. Identification of effective prognostic factors is important to get a better understanding of the pathogenesis of bone and soft tissue sarcoma, and to develop new effective treatment methods.

2.1.1 - Osteosarcoma

Osteosarcoma is a high-grade malignant tumor composed of mesenchymal cells producing osteoid and immature bone.

Almost constantly intramedullary, rarely it may originate at the bony surface. Osteosarcoma may sometimes presents with skip or more distant skeletal metastases, but it can be also skeletally multifocal at presentation. There are, consequently, several varieties of osteosarcoma whose anatomo-clinical presentation, treatment and prognosis, however, are not as distinctive as to

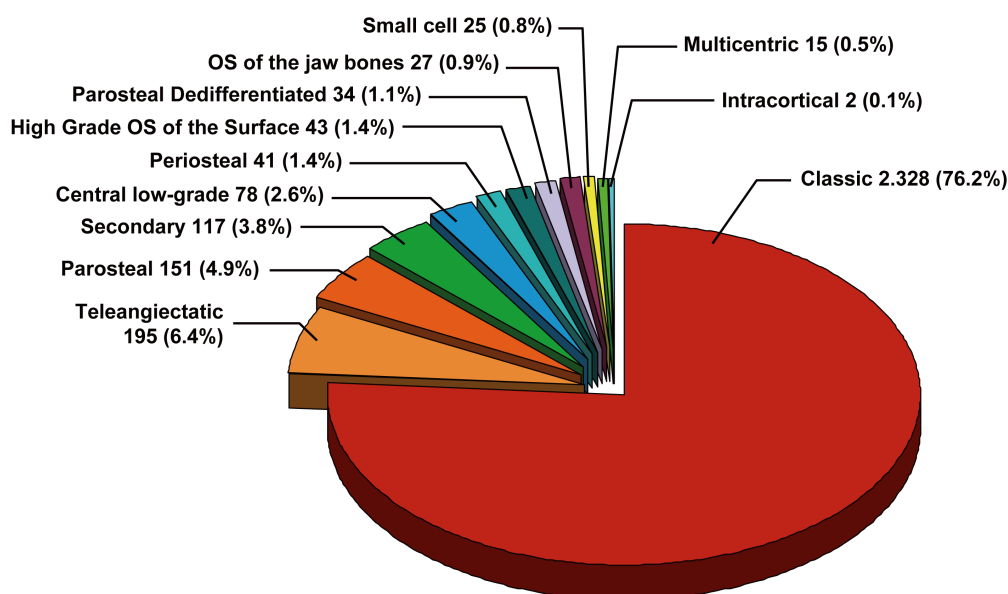
justify a separate classification. Other low grade osteosarcoma types, instead, are different in their clinical, pathologic and therapeutic-prognostic features, and are classified as separate entities (periosteal OS, parosteal OS, low-grade central OS)(Table 1, Figure 1) (2,3).

Table 1. Varieties and their prevalence on 100 cases

High Grade osteosarcoma (OS) varieties ~90 %	
▪ Classic Osteosarcoma	75
▪ Teleangiectatic OS	6/7
▪ OS of jaw bones	4
▪ Secondary OS	4
▪ Small cell OS	<1
▪ OS of bone surface	½
▪ Multifocal OS	0.5
▪ Intracortical OS	0.05
Low Grade OS varieties ~10 %	
▪ Parosteal	5
▪ Central	2.5
▪ Periosteal	1.5

Figure 1. The Istituto Ortopedico Rizzoli series: varieties and their prevalence on 100 cases

OSTEOSARCOMAS - 3.056 cases



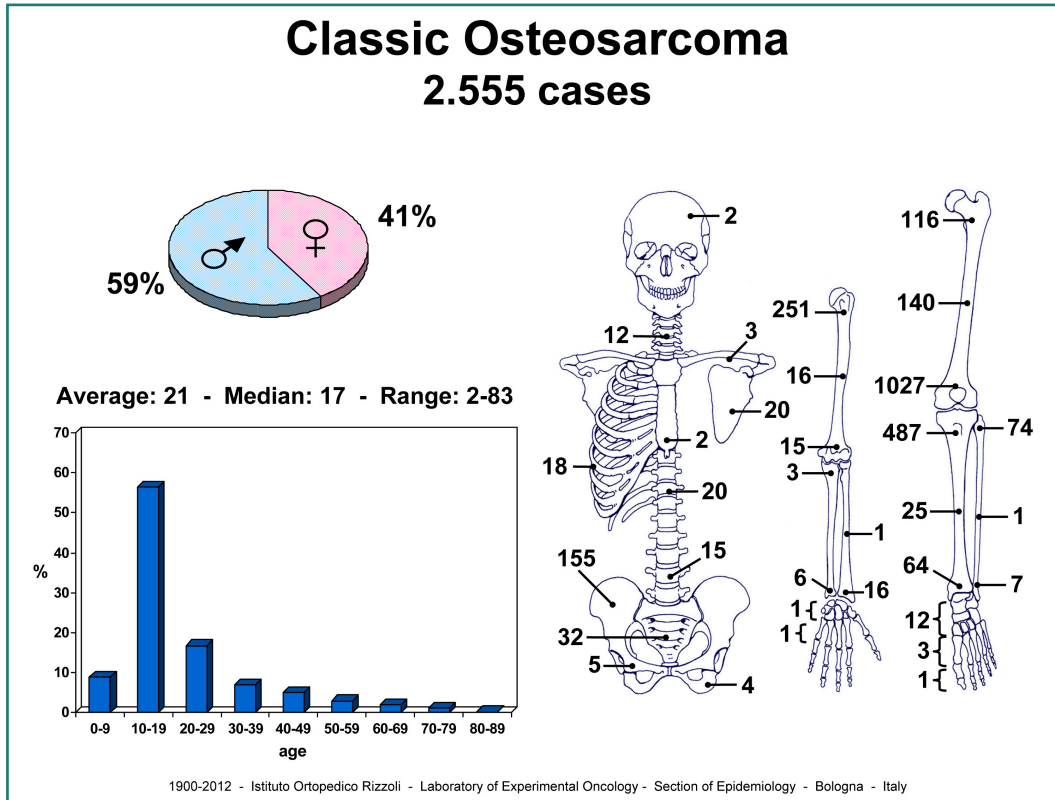
Epidemiology: High-grade osteosarcoma is the most frequent primary malignant tumor of bone, excluding myeloma. Its prevalence is of 2-3 cases/million/year (only 0.2% of all malignancies). Males are more commonly affected (1.5-2:1). Most cases occur between 10 and 20 years of age (Figure 2). Older patients are usually diagnosed with osteosarcoma secondary to radiation, Paget disease of bone, or develop chondrosarcomas or other primary bone tumors (2).

Localization: 70% of osteosarcomas are localized around the knee or shoulder. Other locations are proximal or mid-femur, ilium, mid and distal tibia, proximal fibula, spine, and exceptionally in the hand and foot. Osteosarcoma usually grows in the metaphysis or meta-diaphysis but tends to invade the epiphysis even in presence of a growth plate (2).

Clinical: Pain is usually the first symptom, often referred to trauma. In few weeks it increases and painful swelling appears. High temperature and limited joint motion are advanced signs. Pathologic fracture may occur in osteolytic forms. Alkaline phosphatase is frequently elevated. Less frequently,

also LDH may be increased (2).

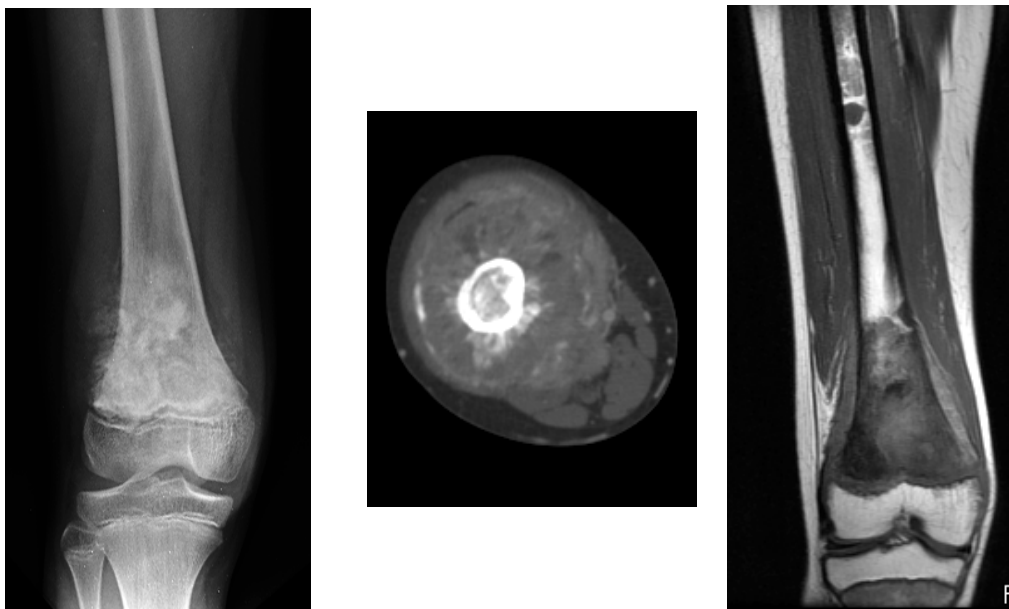
Figure 2. Gender, site and age distribution of osteosarcoma (1)



Imaging: The plain x-ray is usually diagnostic. Typically, osteosarcoma starts intra-medullary, but breaches the cortex and expands in the soft tissues. It is usually a combination of radiolucency and radiodensity, sometimes it is entirely eburneous with edges always faded. The pure osteolytic form is typical of the teleangiectatic variety. The tumor soft tissue extension shows irregular, cloud-like radiodensities, and/or stripes of density perpendicular to the cortex (sunray image). Occasionally, it is purely radiolucent and it can be appreciated only by CT and MRI. At the periphery of the area where the tumor breaches the cortex, a triangular buttress of immature bone (Codman's triangle) is seen. This is due to reactive bone acutely produced by the periosteum. Isotope bone scan is intensely hot even beyond the radiographic limits of the tumor. Rarely, it may reveal skips or distant bone metastases. CT demonstrates intraosseous and extraosseous extension of the tumor and

intratumoral radiodensities. With MRI, most osteosarcomas exhibit the usual pattern of low T1, and high T2 signal. MRI is the best way to determine medullary tumor borders, epiphyseal invasion, skip metastases. Contrast CT and MRI show the relationship with vessels, but in some cases, an angiogram may be more reliable (Figure 3). Patient work-up always includes CT of the lungs where metastases may appear as radiodense round nodules (2,3).

Figure 3. Radiograph, CT and coronal T1W MR image showing a high grade osteosarcoma of the distal femur.



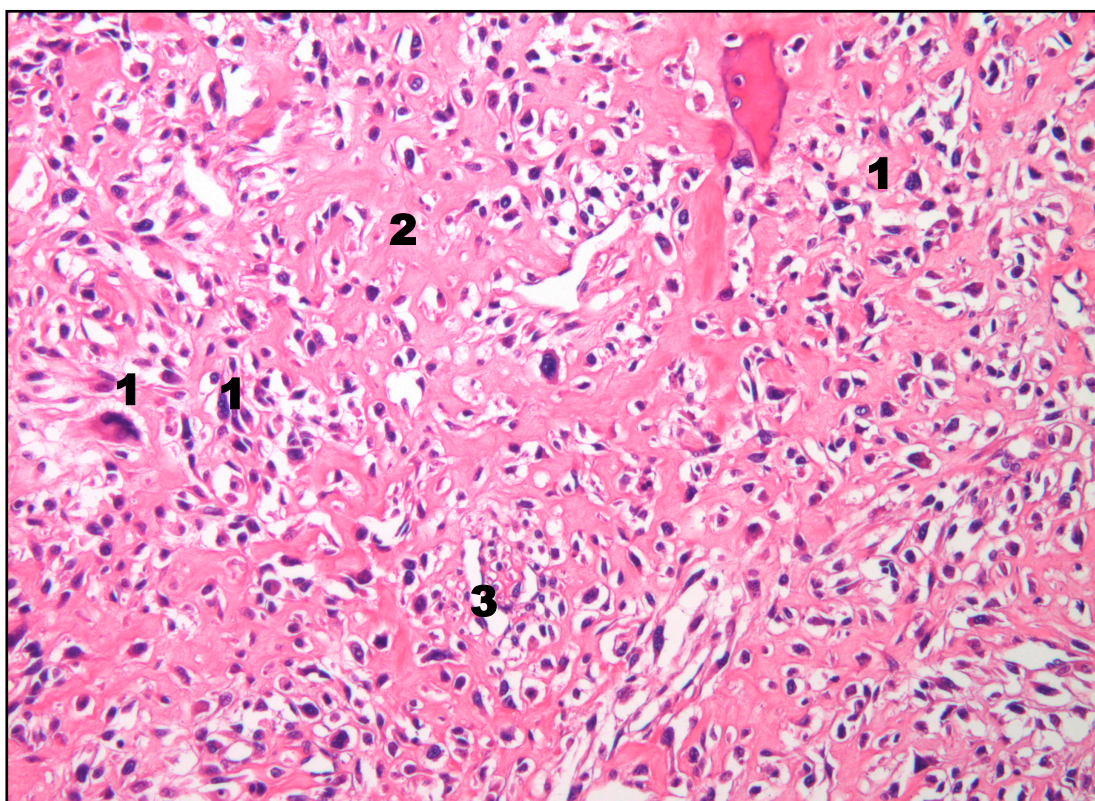
The tumor is metaphyseal, heterogeneous, forms bone, destroys part of the cortex, and invades soft tissues. A skip metastasis is detected on MR in the medullary cavity.

Histopathology: Osteosarcoma is fleshy-soft in cellular areas with little matrix, firm and rubbery in fibroblastic areas with collagen production, gritty to stone-hard in osteogenic areas, cartilaginous to myxoid in chondroblastic areas (2, 4-6). Hemorrhage, necrosis and cystic alterations are common. The most relevant diagnostic feature is constant permeation of marrow spaces, trapping host trabecular bone along its margins, predominantly. Cortex is also permeated and usually breached.

An endosteal and periosteal production of reactive bone is associated. Osteosarcoma may invade the joint capsule and ligaments. Rarely, osteosarcoma plugs are found in the adjacent veins. Skip metastases, usually in the same but also in the adjacent cross-joint bone may be detected in a small percentage of cases.

Microscopically, osteosarcoma has a wide range of histological presentations, but the characterizing feature is represented by high-grade sarcomatous cells producing osteoid and woven bone (Figure 4). The less osteogenic areas of the tumor (usually the periphery) are highly cellular and show more clear-cut features of high-grade malignancy as compared to more osteoid or bone rich central areas of the tumor. Cells are large, with striking pleomorphism, hyperchromia, prominent nucleoli, frequent atypical mitoses, although some 10% of cases may show little anaplasia and lead to confusion with benign entities such as osteoblastoma, chondroblastoma, giant cell tumors, and a few others. Tumor osseous matrix varies from slender lace-like seams of osteoid to islands or dense sheets of woven bone. No regular trabeculae rimmed by osteoblasts are produced by osteosarcoma cells. Where osteosarcoma is intensely sclerotic, cells are scarce, small, with no mitoses; tissue is scarcely vascular and may be necrotic. In these areas, features of malignancy may be absent and diagnosis of OS is suggested by the permeative pattern of the tumor. Occasionally, osteosarcoma is extensively fibro-histiocytic (identical to a UPS), or chondroblastic (as a high-grade chondrosarcoma), or fibroblastic (similar to a fibrosarcoma). The osteoid-osseous production, which identifies the osteosarcoma, may be found only in the microscopic study of the entire specimen. Reactive giant cells are seen, particularly in areas of hemorrhage. Particularly at the periphery of the tumor reactive osteogenesis associates and should not be confused with tumorous osteogenesis. Histochemical stains show a high content of alkaline phosphatase in osteosarcoma cells. Ploidy study indicates that most of osteosarcoma are aneuploid, although a few cases may be diploid.

Figure 4. High grade osteosarcoma histology



Sarcomatous tissue with cells producing osteoid and bone.

- 1- Sarcomatous tissue. The aspects of the high-grade malignancy are fairly evident: large, pleomorphic and hyperchromic cells are seen.
- 2- Neoplastic osteoid and osseous material, shaped with an absolutely anarchical architecture. It is nearly impossible to find trabeculae bordered by a regular row of osteoblasts.
- 3- Abundant blood vessels. They do not have their own well-formed and continuous wall. In some areas, vessels are directly walled by sarcomatous cells.

Clinical Course and Staging: Osteosarcoma has a rapid course (2, 7-12). At presentation, 80% of patients with osteosarcoma are stage II-B; only 5% are stage II-A. About 15% of osteosarcoma are stage III. In the era before chemotherapy, 80 to 90% of osteosarcoma patients died of metastases, notwithstanding ablation of the primary tumor. Thus, it can be said that in 80-90% of cases occult micrometastases are present at diagnosis. Metastatic spread occurs primarily to the lungs.

Treatment: Treatment of osteosarcoma is based on chemotherapy and surgery of both the primary

tumor and the metastases. Postoperative chemotherapy (adjuvant) started in 1971, pre- and postop chemotherapy (neoadjuvant) was introduced in 1978. Presently, most effective drugs are Adriamycin (ADM), high dose Methotrexate (HDMTX), Cisplatinum (CDDP), and Ifosfamide (IFO). Based on post-induction chemotherapy staging study, surgery is performed. The entire tumor is sampled histologically and examined to quantify tumor necrosis. Good response is indicated by necrosis from 90 to 100%. Postop chemotherapy is continued, starting 1-2 weeks after surgery, and lasting from 4 to 6 months. Usually, the same drugs as used preoperatively are given in good responders. In poor responders, different drugs are administered or added in more prolonged trials. For the treatment of metastatic disease surgery and high-dose ifosfamide or gemcitabine and taxotere have been used (7,8). In second line setting, prospective trials with agents such as pemetrexed or sorafenib and sorafenib/everolimus have shown modest activity in osteosarcoma, but none were deemed worthy of further development (9-11).

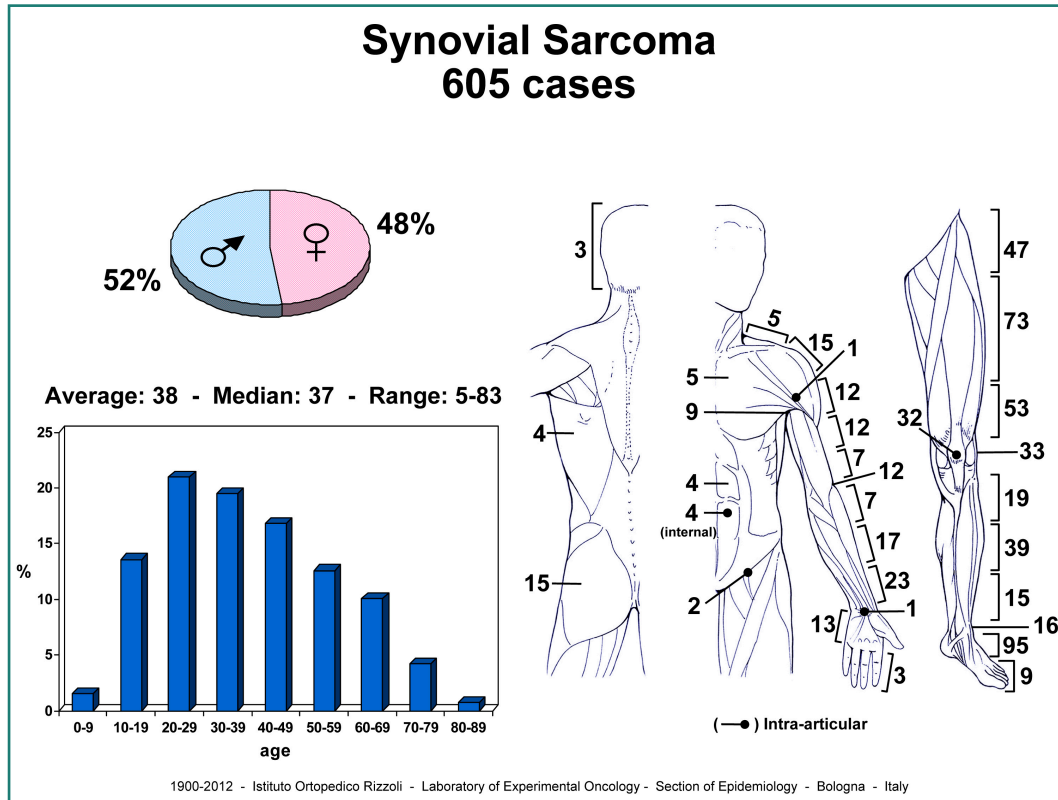
Prognosis: Without chemotherapy, the 10-year survival rate is 10 to 15%. With current chemotherapy the 10-year survival rate has improved to about 70%, for osteosarcoma non-metastatic at presentation and involving the appendicular skeleton (2,12). Also, local recurrence rate after conservative surgery is around 5% after conservative surgery. Metastases (mainly to the lungs) usually occur in the first 2-3 years. There are, however, rare cases of metastases occurring even 5 to 10 years after treatment. The second most frequent site for metastases is the skeleton (2).

2.1.2- Synovial sarcoma

Synovial sarcoma is a malignant tumor whose cells were once thought to arise from synovium, but their occurrence independent of any joint and their immunohistochemical pattern speak to a tumor that has no relationship to synovium (2).

Epidemiology: 5-10% of all sarcomas of soft tissues. Males. 15-40 years old (Figure 1) (2).

Figure 1. Gender, site and age distribution of synovial sarcoma (ref 2)



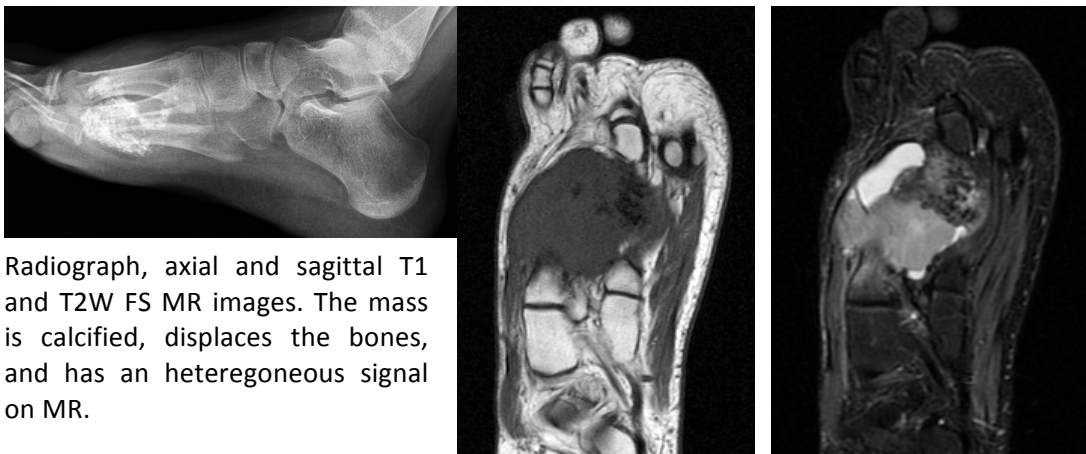
Location: 80% extremities. Lower limb (60% - thigh, knee, foot, ankle), upper limb (23% - forearm, wrist, shoulder). Only 10% within a joint. Usually, close to a major joint, intimately related to tendons, tendon sheaths, bursae, beyond the confines of the joint capsule.

Clinical: A palpable deep-seated mass, often with pain. Pain may be the first symptom of the disease. Tumor grows slowly and insiduously and the duration of symptoms ranges from 2 to 4 years, although in some cases they have been noted for as long as 20 years.

Imaging: On x-ray, a round or oval, lobulated swelling of moderate density near a joint is seen. Usually, bone is uninvolved. Periosteal reaction, bone erosion or bone invasion is seen in a minority of patients (15-20%). Multiple, small and spotty calcifications, or cloudy and faded shadow or massive and dense radiopacities of bone formation (40%). Radiopacities are more

frequent in the periphery. On angiography, tumors are richly hypervascularized. On CT, an infiltrating soft tissue mass is seen, with slightly higher density than muscle, markedly enhanced, with easily detected calcifications, cortical erosion, joint invasion when tendons or ligaments are involved. On MRI – tumors are nearly always (90%) hypointense on T1, hyperintense on T2, less commonly with fluid levels (15%). Marked inhomogeneity, enhancement and septation are seen on T2. A triple signal pattern on T2 (30%): white-like fluid, gray-like fat, dark-like fibrous tissue. Small high signal areas on T1 (45%) are foci of hemorrhage. This and the triple pattern are suggestive of synovial sarcoma (13, 14).

Figure 2. Radiologic presentation of a synovia sarcoma in a foot.

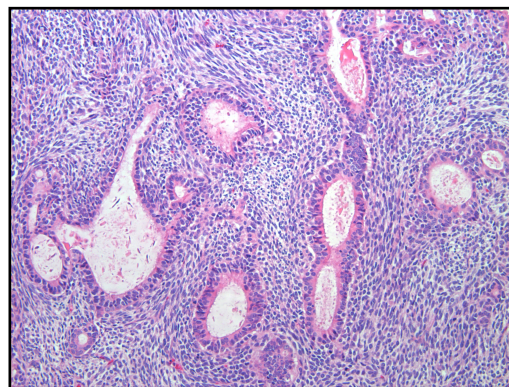


Radiograph, axial and sagittal T1 and T2W FS MR images. The mass is calcified, displaces the bones, and has an heterogeneous signal on MR.

Histopathology: Slow-growing lesions are a firm, lobular mass fairly well circumscribed, attached to surrounding tissues, from yellow to gray-white. More rapidly growing lesions are a soft, globose mass poorly encapsulated, with a variegated, friable or shaggy appearance, from mottled pink yellow to light brown, with frequent necrosis, hemorrhage and cystic areas. Calcifications are rarely seen. Two different types of cells are seen: epithelial and spindle cells, in four patterns: 1) biphasic type: two cellular components; 2) monophasic fibrous type: only spindle cells; 3) monophasic epithelial type: only epithelioid cells; 4) poorly differentiated type (20%). In the biphasic synovial sarcoma there is a balanced distribution of the two components. Epithelioid cells are globose, cubic

or cylindrical, with large vesicular nuclei, abundant pale cytoplasm, with well-defined limits. They are disposed in solid cords, whorls, nests, islands and border irregular pseudoglandular, cleftlike or cystlike spaces with granular or homogeneous secretions. Fibrous cells are well-oriented, plump, spindle-shape, have a uniform appearance, with scant and indistinct cytoplasm and oval, dark nuclei. They form solid, compact masses with irregular nodular arrangement. A fine net of collagen fibers surrounds the single cells of the fibrous component. Mitotic figure are infrequent (1).

Figure 3. Biphasic synovial sarcoma: granular and spindle cell component intermixed in the same tumor.



In monophasic/fibrous type synovial sarcoma, spindle cells are the most prominent feature of the lesion and only a minute focus of epithelial cells may be observed. Monophasic/epithelial type synovial sarcoma is rare and presents a pseudoglandular feature with poorly developed spindle cells pattern prevalence. In poorly differentiated synovial sarcoma there are solidly, packed, oval or spindle, poorly differentiated cells; cells are usually small in size and appear neither clearly fibroblast nor epithelioid cell. Mitotic figures are frequent, richly vascularized with hemangiopericytoma like pattern. Biphasic synovial sarcoma usually does not require immunohistochemistry for diagnosis. Monophasic and poorly differentiated synovial sarcoma show cytokeratin expression in most cases, although it can be quite focal and confined to only rare cells in an entire section. EMA may be positive in some cytokeratin-negative cases. S-100 protein expression is present in 20% of SS but

CD34 expression is not seen. More than 70% of synovial sarcomas are CD99 positive, particularly the poorly differentiated synovial sarcoma. There is nuclear expression of TLE-1. The balanced reciprocal translocation t(X;18)(p11.2;q11.2) is found in more than 90% resulting in fusion of the SYT gene on chromosome 18 with the SSX1, SSX2, or rarely SSX4 gene on the X chromosome (15).

Course and Staging: Local recurrence is common even 10 years later if inadequate surgery was performed. Metastases develop in about 50% of cases. The tumor usually presents as AJCC stage IIB (15).

Treatment: Surgery aims at obtaining wide margins, also sacrificing functionally important structures or amputating the limb. Wide conservative surgery may be difficult for the characteristic growth of the tumor (16). It may be useful to associated adjuvant chemotherapy and pre- or postoperative radiation therapy. Excision of the regional lymph nodes can be considered for selected patients; sentinel node biopsy may be worthwhile in selected patients. Overall 10-year survival varies from 15 to 35%. Favorable prognostic factors are: <5cm, youth, women, distal extremities, calcifications, <15 mits/10HPF, degree of glandular differentiation, no intravascular plugs (16).

In patients with recurrent disease, the post-relapse survival is very poor, with a 5-year OS of about 20–30% after lung recurrence, and very few patients live after 3 years in case of multiple site recurrences (12, 16). No standard treatment strategies are defined in this setting, due to the scanty literature on this specific subject (17).

Nonetheless, Karavasilis et al. (18) in a series of 488 advanced STS, including SS, concluded that palliative chemotherapy should be regarded as a standard treatment option, with approximately half of patients deriving benefit.

New target have been explored in synovial sarcoma, but only the pazopanib study (PALETTE) (19)

among all studies listed in Table 1 (17) translated into drug approval for metastatic soft tissue sarcomas in Europe.

Table 1. Clinical trials of emerging therapeutic targets in the treatment of synovial sarcoma.

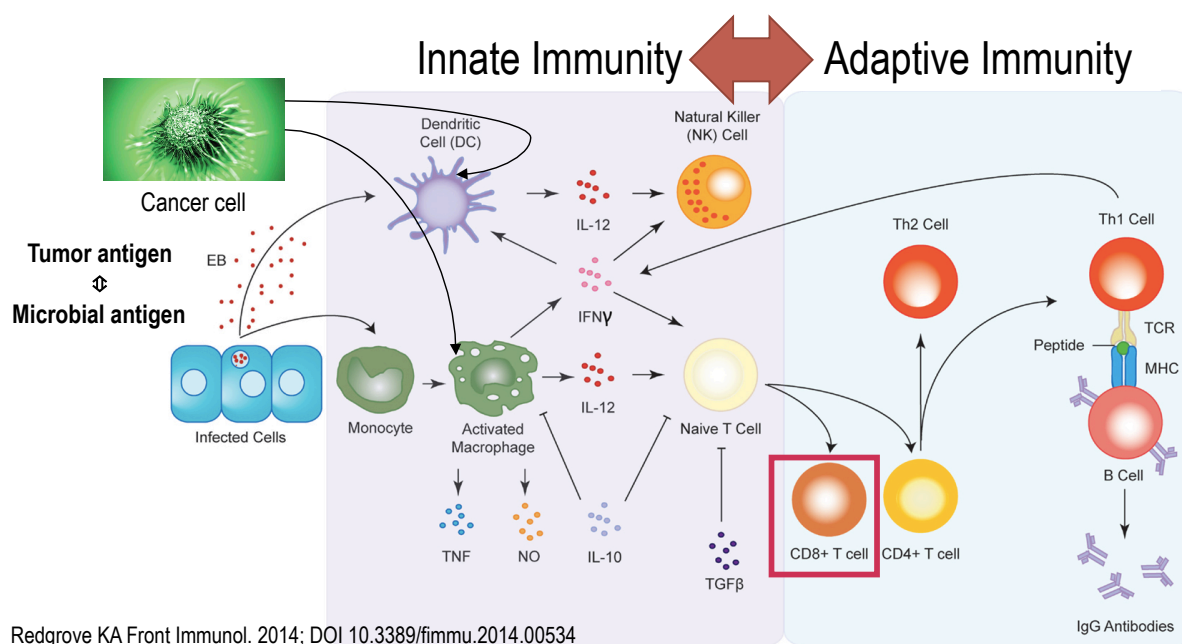
Study (year)	Agent	Targets	Study design	SS Outcome	No. of SS patients in study
Maki <i>et al.</i> (2009)	Sorafenib	Raf-1; PDGFR-b; VEGFR-2,3; FLT3; KIT	Phase II; 122 pts with recurrent or metastatic sarcoma received sorafenib at 400 mg bid	6 SD 3 months PFS 42%	12
Santoro <i>et al.</i> (2012)	Sorafenib	Raf-1; PDGFR-b; VEGFR-2,3; FLT3; KIT	Phase II; 100 patients with advanced STS pretreated with doxorubicin received sorafenib at 400 mg b.i.d.	2 PR	7
Martín-Liberal <i>et al.</i> (2013)	Sorafenib + ifosfamide	Raf-1; PDGFR-b; VEGFR-2,3; FLT3; KIT	Phase I, 12 pts, pretreated STS; doses recommended: ifo 6 g/m ² ; sorafenib at 400 mg b.i.d.	7 SD lasting more than 3 months (not reported for SS)	1
Sleijfer <i>et al.</i> (2009) [44]	Pazopanib	VEGFR-1,2,3; PDGFR-a,b;c-KIT	Phase II; 142 pts; intermediate, high-grade advanced STS, II or III line; pazopanib 800 mg daily; pts stratified in to adipocytic STS, leiomyosarcoma, SS and all others	18 (49%) SS pts achieved the primary endpoint of progression-free rate at 12 weeks; 5 PR, 4 of this lasting from 415–812 days	37
van der Graaf <i>et al.</i> (2012)	Pazopanib	VEGFR-1,2,3; PDGFR-a,b; c-KIT	Phase III; randomized to placebo, 369 metastatic STS pts, no adipocytic, II or more line; pazopanib 800 mg daily (PALETTE)	SS patients showed a PFS rate not statistically different from the other histotypes (hazard ratio for SS vs other sarcoma 0.82 (0.51–1.32))	uk
D'Adamo <i>et al.</i> (2005)	Bevacizumab	VEGF	Phase II; 17 patients with metastatic STS; doxorubicin 75 mg/m ² , bevacizumab 15 mg/kg q3 weeks	SD after 5 cycles	1
Verschraegen <i>et al.</i> (2012)	Bevacizumab + Docetaxel + Gemcitabine	VEGF	Phase Ib; 20 patients with metastatic STS, I line; bevacizumab 15 mg/kg q3, gemcitabine 1500 mg/m ² , docetaxel, 50 mg/m ²	1 PR, 1 SD	2
George <i>et al.</i> (2009)	Sunitinib	VEGFR-1,2,3; PDGFR-a/b; KIT; FLT3; RET; and CSF-1	Phase II; 53 pts with advanced non-GIST STS; sunitinib 37.5 mg daily	1 of 4 SS pts had SD at 16 weeks	4
Fox <i>et al.</i> (2010)	Cediranib	VEGFR-1,2,3; c-KIT	Phase I; 16 patients (8–18 years old) with refractory solid tumors including STS; MTD 12 mg/m ² /day	One patient had a PR with 67% tumor reduction	2
Ray-Coquard <i>et al.</i> (2008)	Gefitinib	EGFR	Phases I–II; 46 SS refractory to doxorubicin	10 SD, 6 months PFS 6%	46, EGFR IHC+; no amplification/mutation
Ha HT <i>et al.</i> (2013)	Cetuximab	EGFR	Phase II, 21 metastatic STS and bone sarcomas	ORR: 0%	7, EGFR IHC+
Weigel <i>et al.</i> (2013)	Cetuximab	EGFR	Phase I, pediatric solid tumors	ORR: 0%	2, EGFR UK
Olmos <i>et al.</i> (2010)	Figitumumab	IGF1R	Phase I expansion cohort, 29 pts with STS and Ewing's	1 tumor shrinkage	5
Schöffski <i>et al.</i> (2013)	Cituxumab	IGF1R	Phase II, 113 pretreated advanced and metastatic STS and Ewing family, cituxumab 10 mg/kg/every other week	18% 3 months PFS; 1 PR, 6 SD (2 lasting more than 12 weeks)	13, IGF1R UK
Demetri <i>et al.</i> (2013)	Ridaforolimus	mTOR	Phase III, randomized to placebo, maintenance study in advanced STS pts, responding to chemotherapy after four cycles; ridaforolimus 40 mg daily (SUCCEED)	23 SS patients in the ridaforolimus arm and 37 in placebo arm; PFS: 28% RR reduction associated with ridaforolimus (hazard ratio = 0.72; p = 0.0001)	60
Schuetze <i>et al.</i> (2012)	Sirolimus + Cyclophos	mTOR	Phase II, 46 pts, metastatic bone and STS, pretreated; sirolimus 12 mg po day 1, 4 mg daily subsequently + cyclophosphamide 200 mg daily po, every other week	1 pt progression-free at least 6 months	3
Schwartz <i>et al.</i> (2013)	Temsirolimus + Cituxumab	mTOR IGF1R	Phase II, 388 pts, metastatic STS and bone sarcoma, First line; weekly treatment with cixutumumab (6 mg/kg iv.) and temsirolimus (25 mg, iv. flat dose) in 6-week cycles	ORR: 0%; 3 tumor shrinkage	18, 78% IGF1R+
Robbins FA <i>et al.</i> (2011)	Genetically engineered lymphocyte reactive with NY-ESO-1	NY-ESO-1 cancer/testis antigen antigen	Phase II, 17 pts, metastatic melanoma and SS, doxorubicin resistant, HLA-A2+; cyclophosphamide (60 mg/kg/day for 2 days) and fludarabine (25 mg/m ² /day for 5 days)	4 PR	6
Maki <i>et al.</i> (2013)	Ipilimumab	Anti-CTLA-4 (NY-ESO-1)	Phase II, 6 pts, metastatic SS	ORR: 0%; 3 months PFS: 0%	6

Flt: Fms-like tyrosine kinase 1; ORR: Overall response rate; OS: Overall survival; PFS: Progression-free survival; MTD: Maximum tolerated dose; PDGFR: PDGF receptor; PR: Partial response; Raf: Oncogenic kinase initially isolated from a transforming mouse virus; SD: Stable disease; SS: Synovial sarcoma; STS: Soft tissue sarcoma; VEGFR: VEGF receptor.

2.2 - Immune system overview

Knowledge about the immune system is essential for understanding the principles underpinning cancer immunotherapy. There are two types of immune responses against microbes: called innate and adaptive immunity (Figure 1) (20).

Figure 1. Innate versus Adaptive Immune Response



Innate immunity, whose main components are phagocytic cells (neutrophils and macrophages) and natural killer cells, provides the initial defence against invading microbes during infection (20). Small molecular proteins called cytokines mediate many activities of the cells involved in innate immunity. In addition to cytokines, dendritic cells (DCs) and macrophages play critical roles in the activation of innate immunity. These components also have a role in communicating with acquired (adaptive) immunity (20). The key components of adaptive immunity, following the initial innate immunity, are T and B-lymphocytes. The lymphocytes play a central role in eliminating infectious pathogens, virus infected cells, and cancer cells and also in generating antigen-specific memory cells (99). Adaptive immunity consists of humoral and cell-mediated immunity.

T lymphocytes recognize short peptides as antigens presented by major histocompatibility complexes (MHCs) on the cell surface of DCs (21). CD8 and CD4 T cells recognize antigen in the context of MHC class I and class II molecules, respectively. Primed and activated T cells differentiate into mature effector cells while undergoing clonal expansion. The effector CD8 T cells recognize virus infected cells and tumor cells and eliminate them from the body. The differentiation of naïve CD8 T cells into effector and memory CD8 T cells is mediated by the “help” of CD4 T cells or by DCs (22). DCs, B cells, and macrophages are professional antigen-presenting cells (APCs) (22).

2.3 - The immune contexture in human tumors

All immune cell types may be found in a tumor, including macrophages, dendritic cells, mast cells, natural killer (NK) cells, naive and memory lymphocytes, B cells and effector T cells (including various subsets of T cell: T helper cells, regulatory T (T_{Reg}) cells, T follicular helper (T_{FH}) cells and cytotoxic T cells).

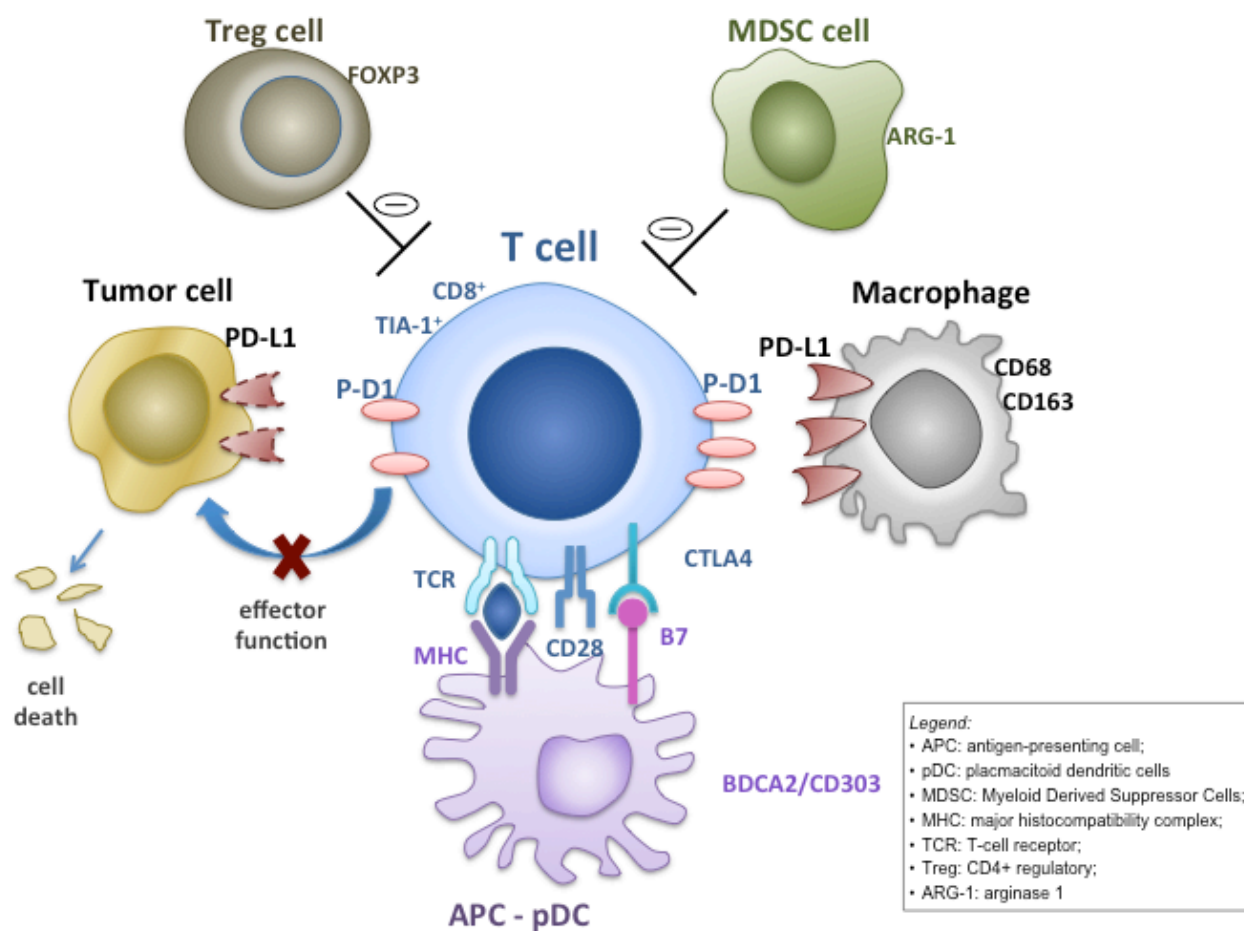
These immune cells can be located in the core (the centre) of the tumour, in the invasive margin or in the adjacent tertiary lymphoid structures (TLS).

The analysis of the presence, location and density of the different immune cell populations (which has been termed the 'immune contexture') in large annotated collections of human tumours has allowed the identification of components of the immune contexture that are beneficial, as well as those that are deleterious, to patients (23).

2.3.1 - The immune contexture: characteristics

Histopathological analyses of human tumours have provided evidence that variable numbers of infiltrating immune cells are found in different tumours of the same type, and are found in different locations within and around a tumour (Figure 1, Glossary)

Figure 1. Mechanisms for intratumoral programmed cell death ligand-1 (PD-L1) expression.



Adaptive focal expression of PD-L1 by macrophages (CD68+/CD163+) occurs at the interface of tumor cell nests with immune infiltrates secreting pro-inflammatory factors such as interferon- γ . The ligation of PD-L1 on macrophage and, in some histotypes, on tumor cells, with programmed cell death protein 1 (PD-1) molecules will down-modulate T cell function, essentially creating a negative feedback loop that reduces antitumor immunity (the so called 'tumor shield' effect), eventually reducing CD8 tumoricidal function.

Macrophages, mast cells, granulocytes and myeloid- derived suppressor cells (MDSCs) are found in most cases infiltrating or surrounding tumour beds both in the core and at the invasive front of the tumour. It is well established that chronic inflammation and the presence of M2 macrophages favour tumour growth and spreading (24). Lymphocytes are not randomly distributed but are located in specific areas. Therefore, NK cells are found in the stroma and are not in contact with tumour cells. B cells are mostly found in the invasive margin of growing tumours and in TLS that are adjacent to tumour beds (25). T cells, particularly CD8⁺ T cells, may be located in the

invasive margin but can also be in the tumour core. Immature dendritic cells are distributed in the tumour core, in contact with tumour cells or in the surrounding stroma. Mature dendritic cells concentrate in TLS, in close contact with naive T cells (25).

The fact that functional populations of immune cells are located in different areas of a tumour, and that this distribution varies between cancer types, suggests that different immune cell populations may have different roles in tumour control. Moreover, the variable density and location of these immune cells between tumours in different individuals with the same cancer type prompted the investigation of whether the immune context might affect clinical outcome.

Glossary

Cytotoxic T cells

CD3⁺CD8⁺ effector T cells with cytotoxic granules that contain perforin and granzymes, which are released on interaction with target cells expressing cognate antigen. This leads to the death of target cells by apoptosis.

Dendritic cells

Cells that capture microorganisms or dead tumour cells and that process them to present antigen to T cells in secondary or tertiary lymphoid organs. They express high levels of co-stimulatory molecules, which allows them to activate naive T cells.

High endothelial venules

Specialized venules that occur in secondary lymphoid organs, except the spleen. They allow continuous transmigration of lymphocytes as a consequence of the constitutive expression of adhesion molecules and chemokines at their luminal surface.

Macrophages

Can be subdivided according to their cellular properties and cytokine secretion profiles. M1 macrophages secrete

pro-inflammatory cytokines (IL-1, IL-6 and TNF), release reactive oxygen and reactive nitrate species and have a pro-inflammatory role. M2 macrophages secrete IL-4, IL-10, IL-13 and TGFβ and have an anti-inflammatory role, promote angiogenesis and favour tumour progression.

Memory T cells

CD3⁺CD4⁺CD45RO⁺ and CD3⁺CD8⁺CD45RO⁺ cells that have encountered antigen and that respond faster and with increased intensity on antigenic stimulation compared with naive T cells.

Myeloid-derived suppressor cells

(MDSCs). Heterogeneous population of polymorphonuclear and monocytic CD11b⁺GR1⁺ cells that inhibit T cell activation.

Naive T cells

CD3⁺CD4⁺ and CD3⁺CD8⁺ cells that differentiate into effector T cells (CD4⁺ T helper cells or CD8⁺ cytotoxic T cells) in secondary lymphoid organs or TLS after stimulation with three signals: antigen, co-stimulatory molecules and cytokines.

Regulatory T (T_{Reg}) cells

Population of CD3⁺CD4⁺ T cells that inhibit effector B and T cells. Some produce cytokines with immunosuppressive activities; for example, IL-10 and TGFβ. They have a central role in suppressing anti-self immune responses to prevent autoimmune diseases.

Tertiary lymphoid structures

(TLS). Ectopic lymphoid aggregates that are generated during the process of chronic immune stimulation and that exhibit the structural characteristics of secondary lymphoid organs.

T helper cells

Populations of CD3⁺CD4⁺ effector T cells that secrete cytokines with differential activities. T_H1 cells produce IL-2 and IFNγ and favour cellular immunity (acting on CD8⁺ cytotoxic T cells, NK cells and macrophages). T_H2 cells produce IL-4, IL-5 and IL-13 and favour humoral immunity (acting on B cells). T_H17 cells produce IL-17A, IL-17F, IL-21 and IL-22 and favour anti-microbial tissue inflammation (acting on epithelial and endothelial cells, fibroblasts and immune cells).

2.3.2 -Clinical impact of the immune contexture

2.3.2.1 - Intratumoural lymphoid infiltrates

Virchow commented on the interaction between leukocytes and tumour cells in his monograph of 1863 (26). Today, we are still unravelling the complexities of the interaction between cancer and the host immune system. Different components of the immune system can either promote or combat tumour growth. The potential for the immune system, in particular CD8⁺ cytotoxic T lymphocytes, to control or eradicate tumours has been shown in laboratory models. In a study of human colorectal carcinoma (CRC) specimens detailing the relationship between T cell densities at the invasive tumour margin and those in the centre of the tumour, high densities of CD3⁺CD8⁺CD45RO⁺granzyme⁺ T cells (that is, antigen-experienced cytolytic T_{eff} cells) were associated with a lower likelihood of tumour relapse and improved overall survival (27). Moreover, coordinated pathological analysis of CD3⁺ T cell densities outperformed internationally accepted clinical staging criteria (Union for International Cancer Control (UICC)-TNM) in predicting disease-free survival and overall survival in multivariate analysis (27). In a survey of the literature on the prognostic importance of T cell infiltrates in different tumour types, the association of CD8⁺ T cells with improved prognosis was seen in 97% (58/60) of the reports analysed (28).

Table 1 summarizes the effect of T cells on solid tumor clinical outcome (29-53). A strong lymphocytic infiltration has been reported to be associated with good clinical outcome in many different tumour types, including melanoma, and head and neck, breast, bladder, urothelial, ovarian, colorectal, renal, prostatic and lung cancer.

On the other hand most of the studies in sarcomas either failed to demonstrate any correlation

(51,52), or were inhomogenous for stage of the patients included (53).

Table 1. Immune infiltrate and cancer outcome

Cells	CD8 ⁺ T cells	T _{Reg} cells
Melanoma	Good ^{29,30}	None ³¹ , Poor ³²
Head and neck cancer	Good ³³	Good ³³
Breast cancer	Good ³⁴	None ³⁵ , Poor ³⁶
Bladder cancer	Good ³⁷	Good ³⁸
Ovarian cancer	Good ³⁹	Good ⁴⁰ , Poor ⁴¹
Oesophageal cancer	Good ⁴²	
Colorectal cancer	Good ²⁷	Good ⁴³
Renal cell carcinoma	Good ⁴⁴ , Poor ⁴⁴	Poor ⁴⁵
Prostatic adenocarcinoma	Good ⁴⁶	
Lung carcinoma	Good ²⁵	Poor ⁴⁷
Pancreatic cancer	Good ⁴⁸	Poor ⁴⁹
Brain cancer		None ⁵⁰
Soft tissue sarcoma	None ⁵¹	
Osteosarcoma	None ^{52, 53}	

CD8+ T cell infiltrate was also among the first predictive biomarkers explored for immune checkpoint-blocking therapies. Specifically, in the context of anti-PD1 therapy for melanoma, CD8+ T cell density at the invasive tumour edge has been correlated with response to anti-PD1 treatment (54)

2.3.2.2 - Intratumoural PD-L1 expression

Beyond enumerating, localizing and phenotyping CD8⁺ T_{eff} cells and other tumour-infiltrating immune cell types, the next layer of biomarker investigation involves examining specific defence mechanisms that tumours can use to guard against immune attack. A dominant mechanism that is relevant to anti-PD1 drug response is PD-L1 expression. PD-L1 is normally expressed by a subset of macrophages and can be induced on activated lymphocytes (T, B and NK cells), endothelial cells and other non-malignant cell types in an inflammatory microenvironment, as part of a physiological process to down-modulate ongoing host immune responses in peripheral tissues (52-57). However, tumour cells and associated stromal cells can also express PD-L1, thereby turning off T_{eff} cells (56). In some cancers, PD-L1 expression is constitutively driven by aberrant signalling pathways or chromosomal alterations. For example, PTEN mutations causing PI3K–AKT pathway activation in a subset of glioblastoma cases (58), can result in broad expression of PD-L1 on the surface of the majority of the tumour cells.

PD-L1 may also be expressed in the TME by a mechanism termed *adaptive immune resistance* (59) a phenomenon in which tumour and stromal cells adapt to attack from infiltrating T cells by expressing the immune inhibitory ligand PD-L1. In this scenario, PD-L1 expression is driven by inflammatory cytokines such as interferon- γ secreted by tumour antigen-specific T cells.

The first scientific support for the concept of adaptive immune resistance was provided by Taube and colleagues in a study focused on human melanoma samples (60). In this study, four distinct archetypes of tumour–host interaction were demonstrated: 1) broad, constitutive tumour cell PD-L1 expression in the absence of a substantial host immune response, consistent with the aforementioned genetically driven constitutive PD-L1 upregulation; 2) PD-L1 expression focally and geographically associated with the host anti- tumour immune response; 3) tumours that had immune cell infiltrates but lacked PD-L1 expression; and 4) tumours that lacked both an immune

response and PD-L1 expression.

Notably, intratumoural PD-L1 expression was associated with improved overall survival in this melanoma study, contrary to expectations based on its known immunosuppressive function (60). This paradox is explained by a mechanism in which cytotoxic T lymphocytes upregulate PD-1 expression when they encounter tumour antigens (*adaptive response to IFN γ*): PD-L1 in this context may be considered as a marker of active immune response.

Further complexity has arisen with regard to the cell type (or types) expressing PD-L1. Certain cancers, such as melanoma, SCCHN, and breast cancer, frequently express PD-L1 on the surface of tumour cells as well as on infiltrating immune cells (60-62). In contrast, in other tumours such as CRC and gastric carcinoma, PD-L1 is observed almost exclusively on tumour- infiltrating immune cells and is only rarely expressed on tumour cells themselves (63-65). Such differential expression may reflect the variable susceptibility of tumour cells and infiltrating immune cells to cytokines and other stromal factors in the tumour milieu (666).

PD-L1 in sarcomas

In a study by Kim JR et al, there were 58% of PD-1 and 65% PD-L1 positive expression in a series of 105 soft tissue sarcoma patients with localized disease (67). PD-1 expression was measured in lymphocytes and PD-L1 in tumor cells. Interestingly, the authors found a significant correlation with survival, with a 5-year event –free survival (EFS) rates for PD-1⁻/PD-L1⁻, PD-1⁺/PD-L1⁻ or PD-L1⁺ of 90%, 74% and 13% respectively (64). By contrast, in a study from MSKCC, reporting on a series of 50 soft tissue sarcoma, only 12% and 22% of tumors had PD-L1 and PD-1 positivity respectively and no significant association with clinical end points was detected (68). Movva S et al reported 50% of PD-L1 positivity in a large series including 2539 sarcoma cases (69). Last, Toulmonde et al, among 328

localized soft tissue sarcomas with genomic complexity, including low grade tumor, reported a PD-L1 rate of 19.5%, with no survival implication (51).

Collectively, in these studies, the range of PD-L1 positivity in STS is wide (12-58%) reasons such as the inclusion of different histotypes (large prevalence of GIST in the study by MSKCC) the different methodology used (namely, the antibodies used: Dako in MSKCC series (68), Santa Cruz in Kim series (64), Pharmingen in Movva series (69), Ventana clone SP142 in the study by Toulmonde (51); and also different scoring or procedure such as TMA or whole section) might explain it.

Dealing with bone tumors, a 74% PD-L1 positive expression on tumor cells was demonstrated in a series of 38 osteosarcoma patients with localized and metastatic disease (70). In this study PD-L1 gene expression by RT-PCR assay was performed on total RNA of the same samples: the median overall survival for PDL1-low patients was 89 months (29 cases), and 28 months for PDL1-high patients (9 cases) ($P = 0.054$) (70). Another study on localized and metastatic osteosarcoma demonstrated an expression of PD-L1 in 7% and 25% of TMA or whole sample respectively in a series of 54 patients (52). The event free-survival (EFS) in this series was significantly improved for PD-L1 negative cases, but no clinical information, included stage, of patients analysed was provided. Moreover, PD-L1 expression was assessed in a large series of conventional, mesenchymal, clear cell and dedifferentiated chondrosarcomas using tissue microarrays: interesting PD-L1 expression was absent in conventional ($n = 119$), mesenchymal ($n = 19$) and clear cell ($n = 20$) chondrosarcomas, while 9/22 (41%) dedifferentiated chondrosarcomas displayed PD-L1 positivity: PD-L1 expression was not prognostic in this series (71).

2.4 - VEGFR, neoangiogenesis and immunotherapy

The dynamic interactions between tumour cells and immune cells are dependent on the local

network of blood and lymphatic vessels. A dense vascular network may allow potential metastatic cells to escape the primary tumour but, conversely, could also favour the infiltration by immune cells provided that the relevant chemokines are produced. Vascular endothelial growth factor A (VEGFA), a cytokine that is produced by tumour cells, is a major inducer of tumour-associated neovascularization, which present specific features as compared with normal vascularization (Table 1).

Table 1. Normal vs. Tumor Vasculature

Normal	Tumor
Organized	Disorganized
Evenly distributed and nonpermeable	Twisted and leaky
Properly matured	Immature
Supporting cells present (eg, pericytes)	Fewer supporting cells
Appropriate expression of membrane proteins	Inappropriate expression of membrane proteins (eg, integrins)
Independent of cell survival factors	Dependent on cell survival factors (eg, VEGF)

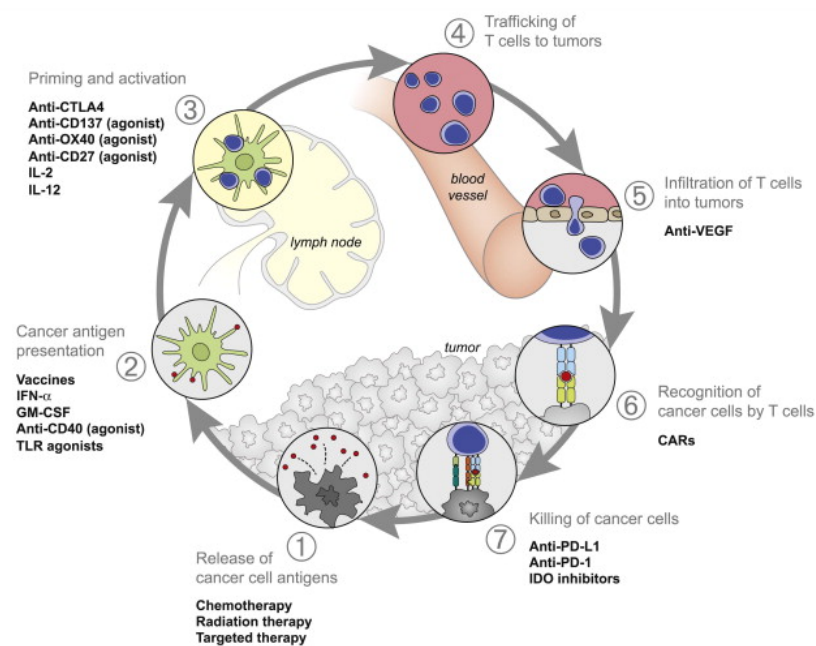
Angiogenesis is involved in tumor development from the initial stages of cancer formation to the growth of distant metastases. Importantly, VEGF is overexpressed not only by tumor cells, but also by any hypoxic cells in the tumor, including tumor stromal cells, fibroblasts, and macrophages, which are particularly responsive to hypoxia (72). A tumor that is not yet hypoxic is usually avascular and dormant. When it undergoes the “angiogenic switch,” VEGF expression is elevated, vasculature is established via capillaries, and the tumor begins an exponential growth phase. This phase is associated with greatly increased metastatic potential because platform metastasis can easily occur via the newly generated blood vessels (72).

VEGF is also important in the metastatic process. When tumor cells gain entry into blood vessels,

they travel to other tissues and form metastatic nodules. However, these nodules are initially poorly vascularized until they undergo a similar angiogenic switch, when they develop vasculature and start to grow exponentially. Anti-VEGF monoclonal antibodies have been developed that target VEGF-D, VEGF-C, and VEGF receptors (VEGFR). Anti-VEGFR antibodies are currently in phase I and II clinical trials, and anti-VEGFR3 antibodies appear to inhibit some forms of angiogenesis.

More recently, it has been speculated that anti-VEGF treatments might represent an important actors in the Cancer-Immunity Cycle (Figure 1) (73).

Figure 1. Therapies that Might Affect the Cancer-Immunity Cycle



Our institution, in collaboration with the Italian Sarcoma Group, and Spanish Sarcoma Group (GEIS), has recently activate the first trial using sunitinib, an anti-TKI, including VEDFR, as immunomodulator in sarcomas: ‘Phase I-II trial of sunitinib plus nivolumab after standard treatment in advanced soft issue and bone sarcomas (EudraCT Number: 2016-004040-10). The aim of this project is to assess in vitro the potential immunomodulation properties of this approach.

2.4.1 – VEGFR inhibitors as immune-modulators in sarcomas

VEGF, v-akt murine thymoma viral oncogene homolog (AKT), platelet-derived growth factor (PDGF), mitogen-activated protein kinase (MAPK), are variably expressed in osteogenic sarcoma, and VEGF pathway was found to be a critical signaling pathway in osteogenic sarcoma (74).

Sunitinib is a small molecule receptor tyrosine kinase (RTK) inhibitor that blocks signaling of multiple RTKs, including vascular endothelial growth factor receptor (VEGFR), platelet-derived growth factor receptor (PDGFR), Kit, and Flt-3, colony stimulating factor receptor type 1 (CSF-1R) and the glial cell-line derived neurotropic factor receptor (RET) (75).

Sunitinib is approved by the FDA for the treatment of patients with gastrointestinal stromal tumors after disease progression on or intolerance to imatinib, for the treatment of patients with advanced renal cell carcinoma, and for the treatment of pancreatic neuroendocrine tumors (pNET) (76).

The approved dose for these indications is 50 mg orally daily for 4 weeks, followed by 2 weeks off.

This compound has been also shown effective in soft tissue sarcomas, with partial responses described in synovial sarcomas, leiomyosarcoma, angiosarcoma (77) and activity described for desmoplastic sarcomas (78), alveolar soft part sarcomas (79) and extraskeletal myxoid chondrosarcomas (80). There are no published studies on the use of sunitinib in bone sarcomas, with limited pre-clinical evidence of sunitinib potential for effective treatment of metastasizing osteosarcoma (81).

Sunitinib might exert immunostimulatory activity through the modulation of the ratio of immunostimulatory versus immunoregulatory cells. In fact, In addition to its pro-angiogenic function, VEGF has immune modulating properties, which include increasing the influx of lymphocytes and DCs into the tumour, while decreasing the intratumoural frequencies of TReg cells

and myeloid-derived suppressor cells (MDSCs) (82-84). Furthermore, high expression of *VEGFA* counteracts the beneficial effects of T_H1 cells or cytotoxic T cells by suppressing the expression of interferon regulatory factor 1 (*IRF1*) and granulysin (*GNLY*), respectively (85). In addition, *VEGFA* is known to inhibit dendritic cell maturation, which may result in the induction of suppressor rather than of effector cells, which hampers the necessary balance of immune cells at the tumour site. Indeed, treatment with anti-*VEGFA* chemotherapy drugs, such as sunitinib, sorafenib or bevacizumab, results in a decrease of T_{Reg} cells and MDSCs both in the periphery and in the tumours of some patients (86). The analysis of a cohort of patients with metastatic renal cell cancer who were treated with sunitinib or bevacizumab revealed that patients with a decrease in circulating T_{Reg} cells after two or three treatment cycles had a significantly longer overall survival than patients with no decrease in circulating T cells (87).

Some of the immunomodulatory treatments, including VEGFR inhibitors are summarized below (Box 1).

Box 1 Immunomodulatory treatments that modify the immune context

Anti-angiogenic drugs decrease the levels of myeloid-derived suppressor cells (MDSCs), as well as circulating and intratumoural regulatory T (T_{Reg}) cells, which modulate anti-tumour immunity^{87,88,89}.

Immunogenic chemotherapies, such as oxaliplatin, which induce calreticulin expression on the tumour cell membrane, result in an increased uptake of the tumour cell by phagocytic cells and improved antigen presentation, which helps to clear cancer cells^{90,91}.

Immune checkpoint-blocking antibodies (which target cytotoxic T lymphocyte-associated antigen 4 (CTLA4), programmed cell death protein 1 (PD1), PD1 ligand 1 (PDL1) and CD137, for example) and specific depletion of T_{Reg} cells⁹² increase the infiltration of the tumour microenvironment by T cells, particularly $CD8^+$ T cells, which increases immune responses to tumour cells^{93,94}.

Emerging data on chemotherapy/TKIs and immunotherapy combination, showed that the drugs schedule may play a role, with best responses observed in sequential versus concurrent approach (59, 95, 96).

2.4.2 - Immunotherapy in sarcomas

Historically, Coley reported a case of unresectable small-cell sarcoma of the neck in 1891. The sarcoma completely regressed after a severe episode of erysipelas. He reported that a systemic response against erysipelas influenced the patient's tumor (97). The mechanism by which erysipelas caused tumor regression was unclear at that time.

However, it is now understood that the activation of innate immunity through Toll-like receptors (TLRs) by erysipelas followed by activation of acquired immunity specific to sarcoma may contribute to the underlying mechanism (98). Thus, the case described by Coley was the first to demonstrate that the immune system might be involved in the spontaneous regression of sarcomas. Over the past 100 years, his work encouraged many scientists to work on cancer immunology, in an attempt to find a cure for cancers (99, 100).

The myriad of genetic and epigenetic alterations that are characteristic of all cancers provide a diverse set of antigens that the immune system can use to distinguish tumour cells from their normal counterparts.

Tumor antigens recognized by the immune system are categorized into cancer testis antigens (CTAs), melanocyte differentiation antigens, mutated proteins, overexpressed proteins, and viral antigens (101). Several types of CTAs have been identified in patients with sarcomas (Table 1).

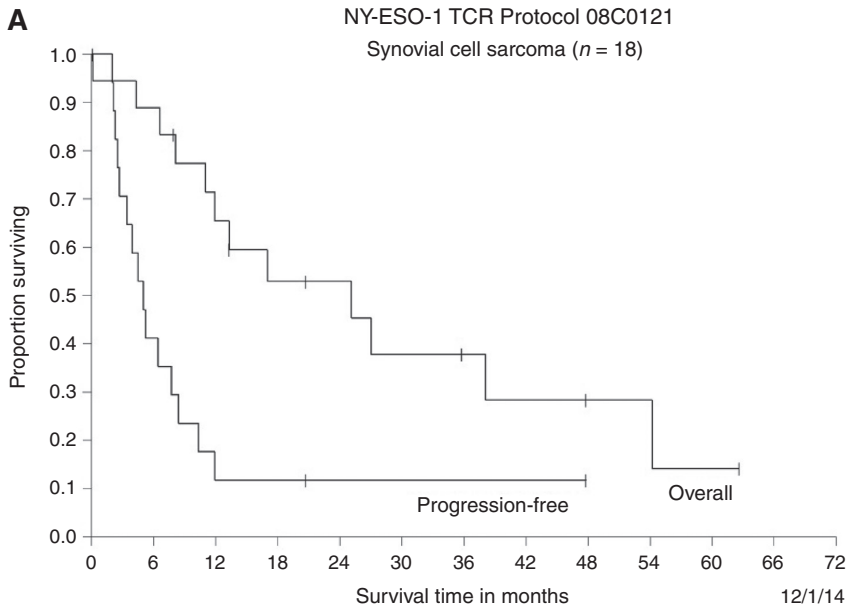
Table 1. Cancer testis antigens in bone and soft tissue sarcomas (101)

Sarcoma subtypes	Expression of cancer testis antigens						
	NY-ESO	LAGE	MAGE-A3	MAGE-A4	MAGE-A9	PRAME	SSX-2
Bone sarcomas							
Osteosarcoma [14]	+	+	+	+			
Ewing's sarcoma [14]	+	+	+	+			
Chondrosarcoma [14]	+	+	+	+			
Soft tissue sarcomas							
Synovial sarcoma [15]	+	+	+	+	+	+	+
Malignant fibrous histiocytoma, pleomorphic spindle cell sarcoma [15]	+	+	+			+	+
Liposarcoma [15]	+	+	+	+	+		+
Leiomyosarcoma [15]		+	+	+	+	+	

Because tumor antigens are potential targets that induce cytotoxic immune responses, many clinical trials have utilized tumor antigens as vaccines for decades.

In 2011 Robbins et al published the first-in-human clinical trial utilizing the adoptive transfer of autologous peripheral blood mononuclear cells (PBMC), transduced with a high-affinity TCR directed against an HLA-A*0201–restricted NY-ESO-1 epitope, in 6 cases with NY-ESO-1 positive synovial sarcomas. This trial demonstrated a good response in terms of response rate (102). However, results are preliminary (18 cases treated so far in the up-date publication, 103) and the procedure cannot be adopted in all patients (HLA-A*02:01 and NY-ESO-1 restricted trial). Figure 2 shows the progression-free survival (PFS) and overall survival (OS) curves (103).

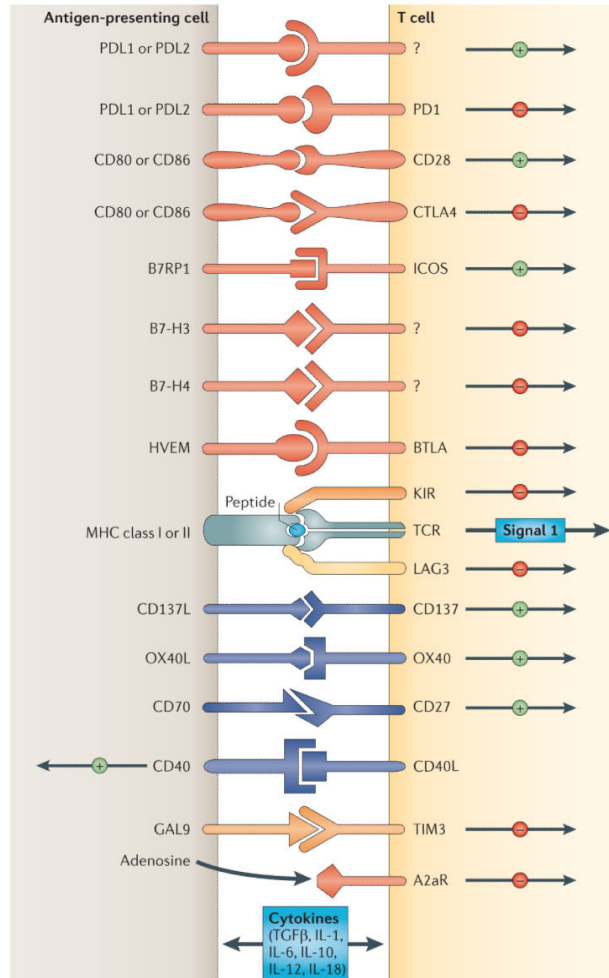
Figure 2. Progression-free survival (PFS) and overall survival (OS) in synovial sarcoma



Although antitumor immunity is induced in patients with cancer vaccines, recent advancements in cancer immunity have revealed the presence of immune-inhibitory mechanisms.

In fact, the ultimate amplitude and quality of the T cells response, which is initiated through antigen recognition by the T cell receptor (TCR), is regulated by a balance between co-stimulatory and inhibitory signals (that is, immune checkpoints) (Figure 3) (104).

Figure 3. Co-stimulatory and inhibitory signals (immune checkpoints) in cancer immunotherapy (adapted from Pardoll et al, ref 104).



Under normal physiological conditions immune checkpoints are crucial for the maintenance of self-tolerance (that is, the prevention of autoimmunity) and also to protect tissues from damage when the immune system is responding to pathogenic infection.

Cancer, are able to deregulate the expression of immune-checkpoint proteins, such as PD1

(programmed cell death protein 1) and its ligand (PD-L1) or T-lymphocyte-associated antigen 4 (CTLA-4), a protein receptor expressed on T cells, that downregulates T cell activation.

Tumor cells upregulate the expression of PD-L1, and the interaction of PD1 with PD-L1 downregulates the function of T cells within the tumor microenvironment. Therefore these immune checkpoints represent an important immune resistance or *tolerance* mechanisms for tumor cancer escape and are emerging as an important therapeutic target for many tumors.

In the last years many studies with immune checkpoints inhibitors were performed in sarcomas with pembrolizumab (anti-PD1) (105), which was considered active in some histologic subtypes (liposarcoma dedifferentiated and UPS), nivolumab (anti-PD-1) (combined with pazopanib, an anti-VEGFR/PDGFR in some case) (106) and ipilimumab (anti-CTLA4) (considered negative) (107).

Last, CMB305, a prime-boost vaccine approach against NY-ESO-1-expressing tumors, was combined with anti-PD1 compound (atezolizumab) in 36 patients with NY-ESO-1+ synovial sarcoma or myxoid/round-cell liposarcoma: the combination had an increase PFS as compared with atezolizumab alone but the duration of the response was short (2.6 months median PFS) (108)

2.5 - CXCR-4 and tumor microenvironment

Tumor progression is a multistep process during which tumor-associated stromal cells perform an intricate cross-talk with tumor cells to supply appropriate signals that may promote tumor survival, proliferation and aggressiveness.

An increasing number of preclinical cancer studies underscore the importance of the microenvironment in tumorigenic potential of epithelial cells (109) The tumour microenvironment consists of resident non-cancerous cells (stromal fibroblasts, endothelial cells and immune cells),

connective tissue and extracellular matrix, altogether supporting tumour structure, angiogenesis and growth (110).

A tumor can influence its microenvironment by releasing extracellular signals, promoting tumor angiogenesis and inducing the inflammatory response, while the immune cells in the microenvironment can affect the growth and evolution of cancer cells. The relationship between cancer cells and their microenvironment contributes to tumor heterogeneity (111).

Mesenchymal stem cells (MSCs) are non-hematopoietic multipotent stromal cells that are involved in tissue homeostasis and regeneration. Early studies demonstrated that bone marrow-derived mesenchymal stem cells (BM-MSCs) possess a remarkable ability to home in to tumor sites and putative immune-privileged status that renders them suitable carriers for delivering anti-tumor agents to the tumor microenvironment (112). However, BM-MSCs have also been identified as pro-active tumor stroma-associated cells that are implicated in promoting cell survival, angiogenesis, invasion, and metastasis in addition to the evasion of the immune system (113).

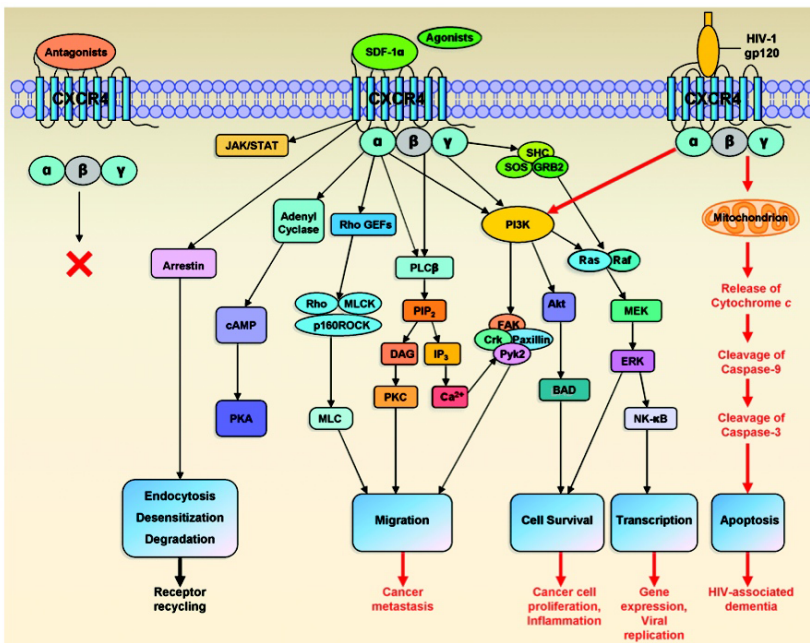
The cross-talk between tumor cells and stromal cells induced the production of growth factors, cytokines and chemokines that can specifically attract BM-MSCs to invade the tumor

microenvironment, as has been shown in breast (114) and other solid tumors.

BM-MSC-derived chemokines, such as chemokine ligand 1 (CXCL1), CXCL2 or CXCL12 (also known as stromal cell-derived factor 1 (SDF-1)), have been shown to promote cancer cell proliferation through the related receptors chemokine receptor 2 (CXCR2) and 4 (CXCR4) in a number of cancer models (115, 116).

The CXCR4 belongs to the large superfamily of G protein-coupled receptors and has been identified to play a crucial role in a number of biological processes, including the trafficking and homeostasis of immune cells such as T lymphocytes (Figure 1) (117)

Figure 1. CXCR4 intracellular signaling pathways



CXCR4 has been found to be a prognostic marker in various types of cancer, including leukemia and breast cancer, and recent evidence has highlighted the role of CXCR4 in prostate cancer (117). Furthermore, CXCR4 expression is upregulated in cancer metastasis, leading to enhanced signaling (117).

The CXCR4/CXCL12 (SDF-1) axis has additionally been identified to have a role in normal stem cell homing. In fact BM-MSCs express CXCR4, indicating that the CXCR4/SDF-1 axis may direct the trafficking and metastasis of these cells to organs that express high levels of SDF-1, such as the lymph nodes, lungs, liver, and bone (117).

High levels of CXCL12 expressed by cancer cells and tumor-associated stromal cells directly stimulated the proliferation and invasiveness of breast cancer cells in an autocrine and paracrine manner (118). Moreover, in mouse models of human breast cancer (118), and prostate cancer (119), high CXCL12 levels in the tumour attract CXCR4-positive inflammatory, vascular and stromal cells into the tumour mass, where they will eventually support the tumour growth by secreting growth factors, cytokines, chemokines and pro-angiogenic factors. CXCL12 is physiologically mainly expressed by mesenchymal stromal cells in various organs and tissues, such as the liver, lungs, lymphatic tissues and bone marrow (119).

Preclinical mouse models of human multiple myeloma, acute lymphocytic leukaemia, chronic lymphocytic leukaemia and non-Hodgkin B-cell and T-cell lymphoma have shown that CXCR4 positive cancer cells can be recruited to CXCL12-rich mesenchymal stroma niches (119,120).

2.5.1 - CXCR4 expression in sarcomas

Several studies have reported that BM-MSCs promoted the progression of osteosarcoma through different mechanisms involving CXCR4 (121, 122). Furthermore a metanalysis on CXCR4 expression in samples of patients with bone and soft tissue sarcomas was recently published (11 articles published from 2005 to 2015) (123). Baseline characteristics of the included 11 studies are summarized in Table 1 (124 – 135).

Table 1. Characteristics of eligible studies included in CXCR4 in sarcoma meta-analysis

Study	Patient source	Study period	Follow-up duration (range), months	Method	Antibody for IHC			CXCR4 cut-off	Histology type	Mean age (range), years	Number of patients	CXCR4 +, %	Study design	HR estimation	NOS score
					Type	Source	Dilution								
Palmerini 2015[14]	Italy	1976-2008	72 (12-360)	IHC	MC	Abcam	1:1000	>1%	SYS	37 (11-63)	88	35.2	Re S	Provided in article	8
Lu Y 2015[15]	China	2007-2009	Minimum 36	IHC	PC	Abcam	NR	SS	OS	20 (12-56)	96	68.8	Pro S	Provided in article	9
Guan G 2014[16]	China	2007-2009	34 (5-65)	IHC	MC	R&D	1:75	SS	OS	16.5 (8-48)	107	34.6	Pro S	–	8
Miyoshi 2014[17]	Japan	1976-2007	17 (1-233)	IHC	MC	BD	1:100	SS	RS	NR (0-71)	78	48.7	Re S	Provided in article	7
Guo M 2014[18]	China	2003-2007	NR	IHC	NR	Abcam	1:200	>1%	OS	NR	98	46.9	Re S	Available data	7
Berghuis 2012[19]	Netherland	NR	60 (0-181)	IHC	NR	Abcam	NR	SS	ES	19 (1-43)	30	73.3	Re M	Survival curve	8
Baumhoer 2011[20]	Switzerland	1974-2010	42 (0-287)	IHC	NR	Epitomics	1:500	SS	OS	16.3 (4-88)	159	49.1	Re M	–	7
Lin F 2011[21]	China	2002-2006	Minimum 24	IHC	PC	Epitomics	1:400	>1%	OS	22.4 (7-67)	56	69.6	Re S	Survival curve	7
Oda 2009 (STS)[22]	Japan	1988-2004	41.5 (2-288)	IHC	MC	BD	1:100	SS	STS	NR	112	51.8	Re M	Provided in article	8
Oda 2006 (OS)[23]	Japan	1974-2004	38.5 (9-145)	IHC	MC	BD	1:100	SS	OS	15 (7-69)	30	33.3	Re M	Available data	8
Laverdiere 2005[24]	USA	1998-2000	41 (1-329)	RT-PCR	–	–	–	–	OS	16 (4-77)	47	63.8	Re S	Survival curve	7

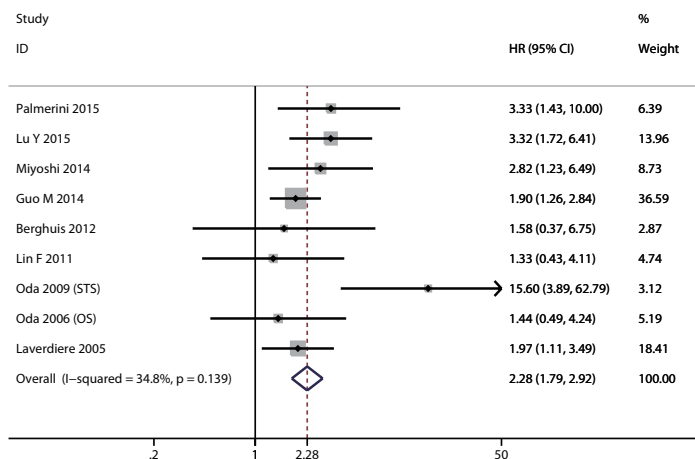
IHC immunohistochemistry, *NR* not reported, *RT-PCR* reverse transcription-polymerase chain reaction, *MC* monoclonal, *PC* polyclonal, *SS* score system combining intensity and percentage, *SYS* synovial sarcoma, *OS* osteosarcoma, *RS* rhabdomyosarcoma, *ES* Ewing sarcoma, *STS* soft tissue sarcoma, *Re* retrospective, *Pro* prospective, *S* single center, *M* multi center, *NOS* Newcastle-Ottawa Scale

The sample size of the studies included in the meta-analysis ranged from 30 to 159 patients, and a total of 901 sarcoma patients were included.

Overall 455/901 (50%) of patients presented CXCR4 overexpression, but the rate of CXCR4 overexpression was wide (ranging from 33.3% to 69.6%), possibly due to the different stage of the patients included in the different series (123).

A total of 9 studies with 635 patients were included in the analysis of overall survival. Under fixed-effect model, the pooled HR was 2.28 (95% CI: 1.79–2.92, $P < 0.001$), suggesting that overexpression of CXCR4 was an indicator for poor overall survival (Figure 2).

Figure 2. Meta-analysis of the effect of CXCR4 overexpression on overall survival (ref 123)



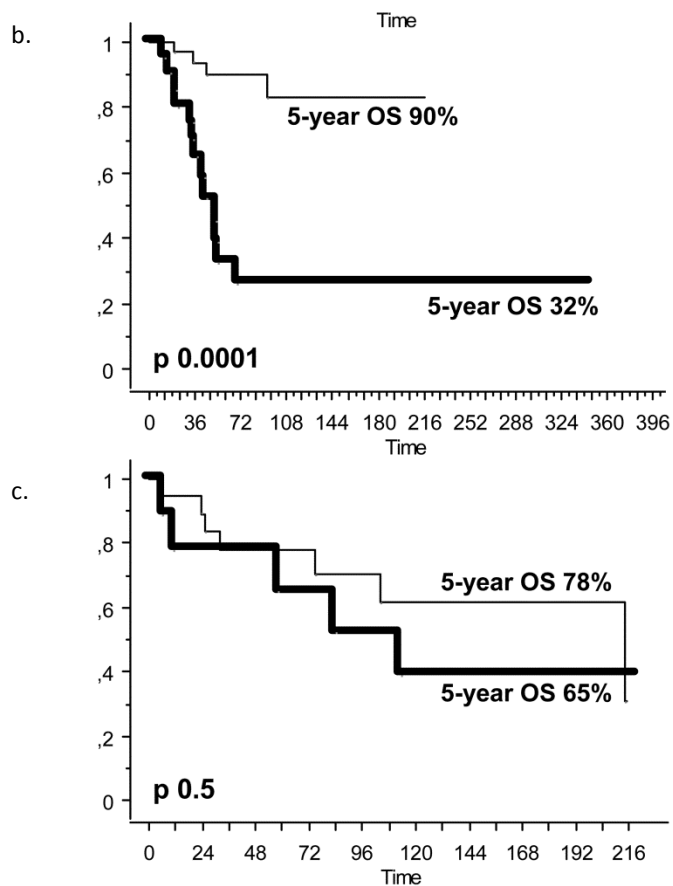
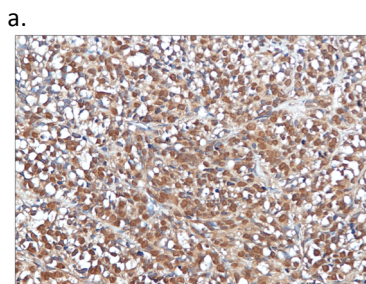
When the analysis was stratified by histological subtypes (bone sarcoma comprising osteosarcoma and Ewing sarcoma, and soft tissue sarcoma including synovial sarcoma and rhabdomyosarcoma), statistical analysis method (multivariate analysis and univariate analysis) and CXCR4 measuring method (IHC or RT-PCR), the significant correlation to poor overall survival was also observed except for that in Ewing sarcoma and RT-PCR groups (123).

Furthermore, in the study by our group including only patients with synovial sarcoma and no metastases at diagnosis, the CXCR4 impact on survival was specifically observed in the subgroup of patients undergoing chemotherapy, suggesting CXCR4 role in resistance to chemotherapy (Figure 3) (124).

Figure 3. 5-year overall survival in patients with localised synovial sarcoma according to CXCR4 expression:

- CXCR4 negative
- CXCR4 positive

a) immunohistochemical expression of CXCR4;
 b) patients undergoing surgery and chemotherapy;
 c) patients undergoing surgery alone



2.5.2- CXCR4 mechanism of action and ‘chemosensitizer’ potential

The recruitment of CXCR4 positive cancer cells mimics the homing of normal stem cells to the bone marrow (Figure 4).

Various mechanisms of action of CXCR4/CXCL12 axis in tumor biology have been proposed (135):

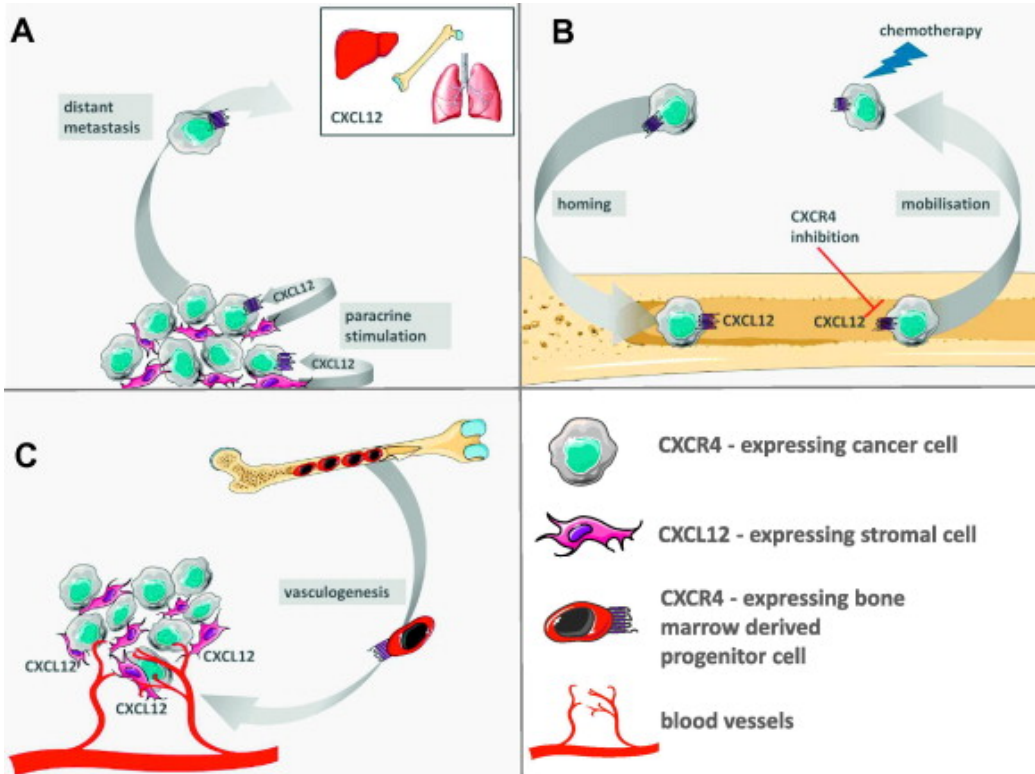
A. CXCR4/CXCL12 regulation of primary tumor growth and metastasis. Tumor associated stromal cells (pink) constitutively express CXCL12. This paracrine signaling stimulates the proliferation and survival of CXCR4-positive tumor cells (grey). Moreover, CXCR4-expressing tumor cells migrate along the CXCL12 gradient to distant organs showing peak levels of CXCL12 expression, eventually leading to metastases (118).

B. Tumor cells utilize CXCR4 to access the CXCL12-rich bone marrow microenvironment that favors

their growth and survival. High levels of CXCL12 secretion by bone marrow stromal cells are essential for homing of CXCR4-expressing tumor cells. CXCR4 antagonists can inhibit the cross-talk between tumor and stromal cells and mobilize cancer cells from this protective microenvironment, making them more sensitive to conventional drugs (standard chemotherapy): ‘chemosensitizer effect’ (120).

C. High expression of CXCL12 by tumor cells and tumor-associated stromal cells forms a local gradient of the chemokine in the tumor region. CXCR4-expressing bone marrow derived progenitor cells are thus recruited to the tumor, where they contribute to the process of vasculogenesis by supporting newly formed blood vessels and by releasing other pro-angiogenic factors (136).

Figure 4. Multiple functions of chemokine receptor 4 (CXCR4)/chemokine ligand (CXCL12) axis in tumor biology



As initially shown in an acute promyelocytic leukaemia mouse model, cancer cells that home to bone marrow reside in a microenvironment, which protects them in a CXCR4-dependent manner from chemotherapy (120). In other words, CXCR4/CXCL12 mediated invasion of tumor cells in the stromal layer allows their direct attachment to stromal cells. Activated adhesion molecules, such as $\alpha_v\beta_3$ integrins, provide malignant cells with pro-survival signaling in vitro. This is thought to lead to adhesion-mediated drug resistance (137), with the acquisition of a quiescent phenotype that is thought to be a feature that allows cancer cells to avoid chemotherapeutic toxic activity (*quiescent* = *chemoresistant* phenotype) (138, 139).

The above findings indicate that CXCR4/CXCL12 signaling events present in the bone marrow niche can, directly or indirectly, contribute to resistance to chemotherapy in leukaemia (140) and solid tumors (141).

Since the CXCL12-CXCR4 interaction is considered crucial for attracting tumor cells to the bone marrow niche, CXCR4 inhibitors have been explored as chemosensitising agents in the field of leukaemia treatment (140-142).

Most results on chemosensitisation by CXCR4 inhibition have been obtained in haematological mouse models. Therefore the findings in these models might not directly be applicable to the situation of solid tumours. Nonetheless, there is growing evidence that CXCR4-positive solid tumour cells, analogous to leukaemic cells, also interfere with the microenvironment that favours their survival during anticancer therapy (144, 145). In an in vivo mouse model of human melanoma lung metastases, the CXCR4 antagonist T22 was able to sensitize melanoma cells for immune-augmenting low dose cyclophosphamide and anti-CTLA4 monoclonal antibody therapy, resulting in 70 and 50% fewer lung metastases, respectively, when compared to cyclophosphamide and anti-

CTLA4 monoclonal antibody alone (144).

In conclusion, numerous preclinical studies support the usage of CXCR4 antagonists in cancer, in order to sensitize tumour cells to current chemotherapeutic therapies by disrupting CXCR4-dependent tumour-stroma interactions (140-145).

3 - AIM OF THE STUDY

The overall aim of this project is to analyse current evidence on tumor microenvironment and immune-infiltrate role in sarcomas, and to provide some insights in this field with both patient-derived tissue studies and in vitro studies of tumor microenvironment–targeted agents activity on osteosarcoma and synovial sarcoma cell lines.

3.1 – AIM 1: Immune context in osteosarcoma and synovial sarcoma

PD-1/PD-L1 immune checkpoint blockade provides clinical benefits in a variety of solid tumors.

We hypothesized that immune infiltrates were associated with superior survival, and examined primary osteosarcoma and synovial sarcoma tissue microarrays (TMAs) to test this hypothesis. Also, we analysed the role of the PD-1/PD-L1 expression in tumor microenvironment of sarcomas.

3.2 – AIM 2: Anti-VEGFR and anti-PD-1 activity in osteosarcoma and synovial sarcoma cell lines

We hypothesized that the ability of PD-1/PD-L1 immune-checkpoint inhibitors to reduce cancer immunological tolerance might be increased by immunomodulators. Therefore, by using a co-culture system with sarcoma cell lines, lymphocytes and dendritic cells, we assessed the effect of anti-VEGFR/PDGFR inhibitors (sunitinib) in combination with anti-PD1 agents (nivolumab).

3.3 – AIM 3: Anti-CXCR4 activity in osteosarcoma and synovial sarcoma cell lines

Based on the fact that the anti-tumor mechanism of CXCR4 inhibitors (AMD3100 and MDX1338) alone or in combination with chemotherapy were not assessed in sarcoma, we hypothesized that

AMD3100 and MDX1338 were more effective than chemotherapy alone in the treatment of sarcoma.

Here, we measured the expression of CXCR4 and SDF-1 on osteosarcoma and synovial sarcoma cell lines and then evaluated the effect of combined treatment of AMD3100 and MDX1338 and adriamycin on the migration, proliferation and apoptosis of sarcoma cells in vitro.

4 - MATERIALS AND METHODS

4.1 - Aim 1: Immune context in osteosarcoma and synovial sarcoma

4.1.1 - Osteosarcoma

4.1.1.1 - Pre-treatment (bioptic samples)

After EC approval, tissue samples obtained from biopsies performed prior chemotherapy in 129 patients were collected. Patients were prospectively treated at Istituto Ortopedico Rizzoli from 04/2001 to 11/2006 within protocol ISG-OS1, with surgery and a chemotherapy based on methotrexate, cisplatin, adriamycin and ifosfamide as described (146), were collected.

The clinical characteristics of the patients were the following: the median age was 16 years (range 4-39 years), with paediatric patients (59/86, 67%) and male gender (53/86, 62%) being most represented. High LDH levels and high AP at baseline were detected in 36/86 (42%) and 18/86 (21%) of patients respectively. All patients underwent neo-adjuvant chemotherapy and surgery as per protocol. A good pathologic response ($\geq 90\%$ necrosis) was achieved by 45/86 (52%) of the patients.

All samples underwent decalcification as previously described (147). For tissue microarray (TMA) construction, a slide stained with hematoxylin and eosin was prepared from each formalin-fixed, paraffin-embedded (FFPE), and representative tumor regions were morphologically identified and marked on each slide. Tissue cylinders with a diameter of 1.0 mm were punched from the marked areas of each block and brought into a recipient paraffin block. Five TMAs were constructed. Each tumor sample was represented by a minimum of 1 core to a maximum of 5 cores.

From TMA blocks, 4 micron-sections were cut. This histological sections were coloured with haematoxylin eosin and the tumor microenvironment was characterized by applying

antibodies directed against fixation resistant epitopes of CD68 (tumor associated macrophages: TAM), CD3, CD8, CD20 (T tumor infiltrating lymphocytes: TILs), FOXP3 (T regulatory lymphocytes: T-regs), Tia-1 (cytotoxic T cell), BDCA-2/CD303 (plasmacytoid dendritic cells: pDC), Arginase-1 (myeloid derived suppressor cells: MDSC) proteins. PD-1 expression on immune-cells (IC), and PD-L1 on both tumour cells (TC) and IC was also investigated. The antibody reactivity, source as well as the antigen retrieval protocols were reported in Table 1.

Table 1. Immunohistochemistry antibody reactivity, sources as well as the antigen retrieval protocols, dilutions and revelation systems.

antibody	clone	Origin	dilution	antigen retrieval		revelation system		
CD3	SP7	Neomarkers	1:60	PT-link Flex	EnVision	Dako Real	Detection system	
CD8	144B	Dako	1:100	PT-link Flex	EnVision	Dako Real	Detection system	
CD20	L26	Dako	1:300	PT-link Flex	EnVision	Dako Real	Detection system	
FOXP3	Sp97	Abnova	1:100	PT-link Flex	EnVision	Dako Real	Detection system	
TIA-1	2G9	Immunotech	1:300	PT-link Flex	EnVision	Dako Real	Detection system	
BDCA-2/CD303	124B3.13	Dendritics	1:100	PT-link Flex	EnVision	Dako Real	Detection system	
Arginase-1	polyclonal	GeneTex	1:3200	PT-link Flex	EnVision	Dako Real	Detection system	
PD-1	NAT-1	Prof. Roncador (Madrid)	1:4	PT-link Flex	EnVision	Dako Real	Detection system	
PD-L1	SP263	Ventana, Roche	RTU	Ventana Conditioning (CC1)	Cell 1	Ventana	OptiView Detection system	
CD68	PGM1	Prof. Falini (Perugia)	1:5	PT-link Flex	EnVision	Dako Real	Detection system	
CD163	10D6	Leica	1:100	PT-link Flex	EnVision	Dako Real	Detection system	

A semi-quantitative score from 0 to 3 was assigned to immune infiltrates: 0 = "none": no immune infiltrates; 1 = "focal": mostly perivascular in tumor with some intra-tumoral extension; 2 =

"moderate": prominent extension of immune infiltrates away from perivascular areas and amongst tumor cells); 3 = "strong" (immune infiltrates obscuring tumor) (148). Pathologists were blinded to clinical information.

Only cores with tumoral component were included in the analysis. The immunohistochemical scores were generally concordant among cores of the same patient, in case of heterogeneity the highest score was considered for the analysis.

For survival analysis samples were classified as negative (immunostaining = 0) or positive (immunostaining = 1 to 3) for all markers except: CD68+ cases that were classified in high expressing (severe and moderate expression) and low expressing (focal expression). Score for PD-L1 expression in TC: specimens with >5% membranous expression were considered positive.

4.1.1.2 - Post-induction chemotherapy (surgical samples)

In 86/129 patients, FFPE from tumoral masses surgically resected, after neoadjuvant chemotherapy, were collected. The full slides sections from FFPA were investigated by immunohistochemistry for CD8+ and Tia1 expression.

4.1.1.3 - Statistical analysis

The following factors were correlated with overall survival (OS) in all samples obtained at diagnosis: age (pediatric < 18 years vs. adult \geq 18 years), gender, LDH and phosphatase alkaline (PA) levels at baseline (normal vs. high), pathologic response (good: chemotherapy-induced tumor necrosis \geq 90%; poor: chemotherapy-induced tumor necrosis < 90%) (147), tumoral microenvironment components, PD-1 expression on IC, and PD-L1 both on TC and IC.

In the analysis on post-induction chemotherapy changes, CD8 and Tia1 expression were with

correlated with OS. OS was estimated according to the Kaplan and Meier method with their respective 95% confidence intervals (CI) and calculated from the first day of chemotherapy administration to death or last follow-up visit.

4.1.2 - - Synovial sarcoma

4.1.2.1 - Design and patients

This study is a systematic mono institutional retrospective analysis. From the previous series of 250 patients (149) referred to our Institute from 1976 to 2008, we selected patients admitted for first diagnosis; therefore, metastatic and recurrent patients at presentation were excluded. All patients with incomplete clinical and follow-up data were also excluded. General informed consent to the use of material was obtained from all adult patients or from parents/guardians for minors from 2004. The research protocol was approved by Rizzoli Orthopedic Institute ethics committee.

4.1.2.2 - Data collection

Demographic data (age at onset, gender, follow-up duration), clinical-histological presentation (biphasic, monophasic/poorly differentiated, tumor size, site), treatment (R0/R1 resection, adjuvant chemotherapy, adjuvant radiotherapy), and outcome (overall survival (OS)), were collected. Follow-up was obtained from hospital charts, or if necessary, by a phone call.

4.1.2.3 - Histology and molecular studies

The diagnosis was confirmed by pathologists with expertise in soft tissue and bone tumors, after revision of histological slides according to histopathological and immunohistochemical criteria (150). The presence of SS18 (SYT) gene rearrangement and fusion transcripts was assessed by Fluorescence in situ hybridization (FISH) and Reverse Transcriptase-Polymerase Chain Reaction (RT-

PCR) analysis for diagnosis confirmation.

4.1.2.4 - FISH analysis

FISH was performed using the SS18(SYT) (18q11.2) VYsis LSI Dual Color Break-apart DNA probes (Abbott Molecular, Des Plaines, IL, USA) according to the manufacturer's protocol. A minimum of 100 tumor cell nuclei with intact morphology as determined by DAPI counterstaining were counted in the previously marked neoplastic area. A positive result was defined as the presence of a visible translocation (separation of red and green signals > 3 signal diameters) in more than 10% of the cells (151).

4.1.2.5 - RT-PCR analysis

RNA was extracted from fresh tissue using a modified method including Trizol Reagent (Invitrogen, Carlsbad, CA) and the column of RNeasy Mini Kit (Qiagen GmbH, Hilden Germany). 2 µg of RNA was reverse transcribed using High Capacity cDNA Archive Kit (Applied Biosystems, Foster City, CA). The primers used for detection of t(X;18) SS18(SYT)-SSX1 and t(X;18) SS18(SYT)-SSX2 by PCR amplification was: forward SS18 5'GGA CAA GGT CAG CAG TAT GGA3'; reverse primers for SSX1 5'TTG GGT CCA GAT CTC TTA TT3'; and reverse for SSX2 5'TTGGGTCCAGATCTCTCGTG3' (152).

4.1.2.6 - Immunohistochemistry staining

The immunohistochemistry staining for synovial sarcoma are the same of osteosarcoma (see paragraph. 4.1.1.1).

This histological sections were coloured with haematoxylin eosin and the tumor microenvironment was characterized by applying antibodies directed against fixation resistant epitopes of CD3, CD8 (T tumor infiltrating lymphocytes: TILs), FOXP3 (T regulatory lymphocytes: T-regs), PD-1 expression on

immune-cells (IC), and PD-L1 on both tumour cells (TC) and IC was also investigated.

4.1.2.7 - Statistical analysis

The following parameters were examined for statistical prognostic correlations: total expression of PD-L1 (IC), PD-L1 (TC), CD8, CD3. The following categories were compared: patients age (adolescent and young adults (AYA) with < 30 years versus adults with ≥30 years); tumor size (≤5 cm versus >5 cm); surgical margins (adequate including wide or radical versus inadequate including intralesional, marginal or contaminated margins, according to Enneking's classification) (153); histology (biphasic versus other histotypes); adjuvant treatments (chemotherapy or radiotherapy performed within 3 months after tumor excision). Chi-square (χ^2) test with Fisher's exact p value was used to correlate protein expression with clinical parameters. Overall survival (OS) time was calculated from the time of admission at our Institute to death or last follow-up visit. All time-to-event end points were modelled using the method of Kaplan and Meier and analysed by the log-rank test. The results of the Cox model analysis were reported as relative risks (RRs) and 95% confidence intervals (CIs).

4.2 - Aim 2: Anti-VEGFR and anti-PD-1 activity in osteosarcoma and synovial sarcoma

4.2.1 - Human Cells

Peripheral blood mononuclear cells (PBMCs) were isolated from buffy coats of healthy donors by Ficoll-Hypaque centrifugation (Amersham, USA). CD3⁺ and CD14⁺ cells were purified by magnetic separation (MiltenyiBiotec, Germany), according to manufacturer's instructions. Purity of cell

populations was always > 90%.

4.2.1- Cell lines

Human osteosarcoma cell line SaOS-2 and MG-63 were obtained by Dr Massimo Serra Laboratory (Istituto Ortopedico Rizzoli, Bologna, Italy) and cultured in Dulbecco's modified Eagle's medium (DMEM) supplemented with 10% Fetal Bovin Serum (FBS) and antibiotics in 37 C° humidified atmosphere with 5% CO₂. Synovial sarcoma cell lines SYO-1, bearing the pathogenetic translocation (X;18)(p11.2;q11.2), was obtained by Dr Akira Kawai (National Cancer Center, Tokyo, Japan) and Dr. Aki Yoshida Laboratories (Okayama University, Tokyo, Japan) and cultured in alphaMEM supplemented with 10% FBS, or 10% fetal calf serum (FCS) and antibiotics in 37 C° humidified atmosphere with 5% CO₂. ATCC synovial sarcoma cell line SW982 was purchased from by American type Culture Collection and grown in alphaMEM 10% FBS, 100 U/ml penicillin and 100 µg/ml streptomycin. The cells were maintained in a humidified incubator in 5% CO₂ at 37 °C.

4.2.3 - Chemicals and Reagents

Sunitinib/SUTENT/PF-00262192 is an oral multitargeted tyrosine-kinase inhibitor (including VEGFR, kit and PDGFR) and it was provided by Pfizer Inc, NJ, USA. Axitinib/PF-01367866 is an oral multitargeted tyrosine-kinase inhibitor (including VEGFR, kit and PDGFR) and it was provided by Pfizer Inc., NJ, USA. Nivolumab/Opodo ia a umanized monoclonal, immunoglobulin G4 antibody to PD-1 and it was provided by Bristol Myers Squibb (NYC, NY, USA).

4.2.4 - Cell proliferation assay

The effects of Sunitinib on sarcoma cell lines were assessed using a CellTiter 96® AQueous One Solution Cell Proliferation Assay (MTS) – PROMEGA) (154). Cells at exponential phase were seeded in 96-well plates at a density of 5000 cells/well in 50 µl of the appropriate culture medium and incubated for 1 hour at 37°C to guarantee adherence. Each well plate was then added with

medium containing sunitinib (50 μ l) at different concentrations (drug final concentrations: 0 μ M, 0.5 μ M, 1 μ M, 3 μ M, 5 μ M, 7 μ M, 10 μ M) and for a total volume of 100 μ l. Each condition was repeated in 3 subsequent well plates (1 well plate for 24 hours, 1 for 48 hours, and 1 for 72 hours). After 24 h, 48 h, 72 h growth, the cells were treated with 20 μ l di CellTiter 96[®] AQueous One Solution Reagent. Following 3 h incubation (dark condition) the absorbance at 490 nm by a 96-well plate reader (Multiskan EX Thermo Fisher Scientific) was recorded. Each day a standard curve if untreated cells was seeded and the absorbance was measured in order to calculate cell number for each well plate.

4.2.5 - PD-L1 expression on sarcoma cell lines by flow cytometry

Flow cytometry was used to evaluate PD-L1 expression on sarcoma cell lines. Each osteosarcoma and synovial sarcoma cell line was harvested with brief Trypsin-EDTA treatment, washed in and centrifuged (5 min/2000 rpm). After counting the cells number, cell lines were washed and resuspended in phosphate-buffered saline (PBS) solution. For PD-L1 staining, the mAb anti-human CD274 (B7-H1) APC-conjugated (clone MIH1. Lot. E12159-1634; from eBiosciences, San Diego, CA) was used. (155). 100.000 cells were supplemented with 3 μ l Anti-Human PD-L1 antibody and re-suspended in PBS 50 μ l. Cell were incubated at 4 °C for 20 minutes, washed and resuspended in PBS. At least 10,000 events were collected from each sample at FACS Canto II cytofluorimeter. For each cell line, 100.000 unstained cells (autofluorescence) were used as a control. The number of replicates (cell lines at subsequent passages) was 4.

4.2.6 - Mixed lymphocyte reaction (MLR)

Human monocyte-derived immature dendritic cells (DCs) were generated by a 6-day culture of CD14⁺ cells in complete RPMI in presence of granulocyte-macrophage colony-stimulation factor (50 ng/mL; GM-CSF Endogen, USA) and IL-4 (800 U/mL; Miltenyi), as previously described (156, 157).

For DC pulsing, tumor cell lysate, obtained after three cycles of cells freeze-thawing and filtering through an insulin syringe, or Sunitinib-treated tumor cells (15 m5) were cultured for 24 hours with immature DCs (2:1 ratio) in RPMI medium. After culture, 15 000 tumor cells-loaded DCs were co-cultured with 150 000 CFSE-labeled allogeneic CD3⁺ T cells in presence or absence of Nivolumab (20 mg/ml). Briefly, allogeneic CD3⁺ T cells were labeled by CFSE (CellTrace™ CFSE Cell Proliferation Kit, Thermofisher, USA) at the concentration of 5 μM for 20 minutes at 37°C. After incubation, the cells were washed with PBS and seeded in flat-bottom 96-well microplates (150 000/well). At same cases, MLR was performed by co-culture of 150 000 CFSE-labeled CD3⁺ T cells with irradiated tumor cell line (3000 cGy) at ratio of 1:10. After 5 days, T cells were harvested, washed with PBS and T-cell proliferation by flow cytometry was evaluated. As negative control, 150 000 unstimulated CD3⁺ T cells were used. Proliferation index was calculated using FCS Express 4 Research Edition software.

4.2.7 - Flow cytometry immunophenotyping

In addition to proliferation, after 5 days of MLR, immunophenotype of stimulated CD3⁺ T cells were also characterized using following mAbs, according to manufacturer's instructions: CD3 APC-H7 (SK7, BD Biosciences, USA), CD4 Pe-Cy7(clone SK-3, Thermofisher, USA), CD8 PE (SK1, BD Biosciences) and PD-1 APC (EH12.2H7, Biolegend, USA). Briefly, 150 000 T cells were resuspended in 80 ml of PBS and stained with 3 ml of directly conjugated monoclonal antibodies. After incubation for 15 min at room temperature, the samples were washed with PBS. As positive control, CD3⁺ T cells stimulated for 3 days with phytohemagglutinin (PHA) (20 ug/ml) were used.

As negative control, 150 000 unstimulated CD3⁺ T cells were used, whereas 150 000 unstained CD3⁺ T cells were used as negative fluorescence control. For each sample, at least 10,000 events were collected at BD FACS Canto II (BD Biosciences) and analysed by using FCS Express 4 Research Edition software.

4.2.8 - Cell apoptosis assay

The effects of Sunitinib on the osteosarcoma and synovial sarcoma cell lines, apoptosis were measured using flow cytometry assay. After cultured in IMDM (or DMEM for Syo cell line), the adherent cells (150 000/well) were cultured in the presence of 0.5, 1, 3, 5, 7, 10, 12, 15, 20 and 30 mM Sunitinib for 24 hours in 24-well plate, removed from culture flasks using 0,05% trypsin-ethylenediamine tetraacetic acid (EDTA) (Life Technologies, USA) and washed in PBS. After 15 min of staining with 5 ml of APC Annexin V (BD Pharmingen, USA) in the dark at room temperature, the percentage of apoptotic cells were determined using Accuri C6 (BD Biosciences) flow cytometer and FCS Express 4 Research Edition software.

4.2.9 - Statistical analysis

Data were expressed as mean \pm standard error of mean (SEM) of values obtained in the experiments. Statistical analyses were performed with GraphPad Prism 6 software (GraphPad Software, Inc., La Jolla, USA), using ANOVA or unpaired t-test. P values < 0.05 were considered statistically significant.

4.3 - Aim 3: Anti-CXCR4 activity in osteosarcoma and synovial sarcoma

4.3.1 - Cell lines and chemicals

Cell lines

Human osteosarcoma cell line U2OS was obtained from American type Culture Collection and cultured in α MEM supplemented with 10% Fetal Bovine Serum (FBS) and antibiotics in 37 C humidified atmosphere with 5% CO₂.

Synovial sarcoma cell lines SYO-1 bearing the pathogenetic translocation (X;18)(p11.2;q11.2), were obtained by Dr Akira Kawai (National Cancer Center, Tokyo, Japan) and Dr. Aki Yoshida Laboratories (Okayama University, Tokyo, Japan) and cultured in α MEM supplemented with 10% FBS, or 10% fetal calf serum (FCS) and antibiotics in 37 C humidified atmosphere with 5% CO₂. Synovial sarcoma cell line SW982 were purchased by American type Culture Collection and grown in α MEM 10% FBS, 100 U/ml penicillin and 100 μ g/ml streptomycin. The cells were maintained in a humidified incubator in 5% CO₂ at 37 °C.

Bone Marrow Mesenchymal Stem Cells (BM-MSCs) have o been identified as pro-active tumor stroma- associated cells that are implicated in promoting cell survival, angiogenesis, invasion, and metastasis in addition to the evasion of the immune system (113). Osteosarcoma and synovial cells were then cultured in BM-MSCs conditioned medium (BM-MSC–CM), containing a higher concentration of CXCL12 (SDF-1) as compared to α MEM 10%FBS, and treated with CXCR4 inhibitors
Chemicals

MDX-1338/ BMS-936564/ Ulocuplumab s a fully human monoclonal antibody specific for human CXCR4Kuhne MR and it was provided by Bristol Myers Squibb (NYC, NY, USA) (158).

AMD3100 (Plerixafor), an FDA-EMA approved CXCR4 inhibitor to enhance mobilisation of haematopoietic stem cells for autologous transplantation, was purchased by Sigma (St Louis, MO, USA).

4.3.2 - Isolation and culture of human bone-marrow mesenchymal stem cells (BM-MSC)

Bone marrow (BM) sample was obtained from one male patient who underwent surgery at the Rizzoli Orthopaedic Institute after informed consent .The isolation of mononuclear cells and the expansion of cultures of human BM-MSCs *in vitro* were performed as previously described,

using gradient separation and plastic adherence methods (159). BM-MSCs were characterized by their ability to proliferate in culture, their adherent, spindle-shape morphology, their ability to differentiate toward osteoblastic, cartilage and adipogenic lineages and for the expression of CD 105, CD73 and lack of CD45 expression. BM-MSCs, after isolation and characterization, were seeded at 2000 cells/cm² and grown until 40-50% confluence in a-MEM supplemented with 20% FBS. Thereafter, cells were cultured in a-MEM supplemented with FBS 1% for 72 h in order to obtain conditioned medium (BM-MSC-CM), cells were then cultured in a-MEM supplemented with FBS 1% for 72 h. BM-MSC-CM were collected and stored at -80°C until use. BM-MSC-CM presented a high concentration of CXCR4 ligand SDF-1 as shown using ELISA kit (R&D Systems, USA), according to the directions of the manufacturer.

The BM-MSC-CM, after thawing at RT, was centrifuged at 1000 × g for 10 min, and filtered through 0.22-µm filters (Millipore, Billerica, MA) before being added to tumor cells. The BM-MSCs were used at passage 3–4 in this study.

4.3.3 - CXCR4 and SDF1 expression in sarcoma cell lines

RNA extraction

Total RNA was extracted from U2OS, SW982 and SYO-I cell lines using TRizol reagent (Invitrogen, Carlsbad, CA, USA), following the manufacturer's instructions. The concentrations of the total RNAs were measured using a spectrophotometer, and their purity and quality were checked through denatured gel electrophoresis.

CXCR4 mRNA expression analysis by Real Time PCR

mRNA levels of CXCR4, were determined in osteosarcoma cell line U2-OS and synovial sarcomas cells SYO-I and SW982 following TaqMan Reverse Transcription Protocol (Applied Biosystems, Life Technologies, CA, USA). Quantitative RT-PCR was performed using Viia7 sequence detection system (Applied Biosystems, Life Technologies, CA, USA).

CXCR4 expression was quantified by TaqMan Expression Assays (Hs00607978_s1); Applied Biosystems, Life Technologies, CA, USA) according to manufacturer's protocol. Expression of target genes was calculated by $2^{-\Delta\Delta CT}$ comparative method (Applied Biosystems, User Bulletin No. 2, P/N 4303859) and normalized to ACTB housekeeping gene (Hs99999903_m1 gene; TaqMan Expression Assays-Applied Biosystems).

Normal osteoblast and mesenchymal stem cells were used as calibrator for U2-OS and for synovial cell lines respectively.

CXCR4 and SDF1 (CXCL12) protein expression by FACS analysis

Cells were then stained with anti-CXCR4 antibody (ab2074 AbCam) (1:100 dilution in PBS) and with SDF1a antibody (FL-93- Sc-28876) (1:100 dilution in PBS). Following washes with wash buffer, cells were incubated with a goat-anti-rabbit secondary antibody FITCH conjugated (1:80 dilution in PBS) for 1 h in the dark. After two additional washes in wash buffer, flow cytometry were done by FACS Calibur Flow Cytometer (Becton Dickinson).

SDF1 (CXCL12) expression in culture medium by ELISA

Osteosarcoma and synovial sarcomas cells were incubated in a humidified incubator at 37 C. When the cells had reached confluence, the media were collected. After centrifugation, the supernatant was obtained for the detection of SDF-1 levels using an ELISA kit (R&D Systems, USA), according to the directions of the manufacturer.

4.3.4 - t(X;18) SS18(SYT)-SSX1 in synovial sarcoma by RT-PCR

2 µg of RNA from synovial cell lines was reverse transcribed using High Capacity cDNA Archive Kit (Applied Biosystems, Foster City, CA). The primers used for detection of t(X;18) SS18(SYT)-SSX1 and t(X;18) SS18(SYT)-SSX2 by PCR amplification was: forward SS18 5'GGA CAA GGT CAG CAG TAT GGA3'; reverse primers for SSX1 5'TTG GGT CCA GAT CTC TTA TT3'; and reverse for SSX2 5'TTGGGTCCAGATCTCTCGTG3'

4.3.5 - Cell viability and sensitivity

The cell viability was performed before and after MDX1338 (0.001 µg/ml, 0.005 µg/ml, 0.05 µg/ml), AMD3100 (5µg/ml, 20 µg/ml, 30 µg/ml). 200,000 cells were seeded in 6-well plate in αMEM 1% FBS, 25% BM-MS-CM. The cell suspension was carried out during the normal process of cell detachment from flask, which involves several steps including: the removal of medium, the addition of 4-5 ml of 1 X PBS to wash cell monolayer, the addition of 1 ml of trypsin-EDTA, which acts at an optimal temperature of 37 °C, and finally the addition of 4 ml of αMEM 10% FBS to inactivate the trypsin. The suspension obtained was inserted into a 15 ml tube and centrifuged at 1000 rpm for 5 minutes at room temperature to allow the removal of the supernatant and the pellet obtained was suspended in a known volume of αMEM.

The number of adherent, viable cells was assessed after 48h and 72h microscopically using an improved Neubauer haemocytometer and proliferation was assessed as the percentage of cells that excluded 0.2% trypan blue.

Living cells were counted and the number of cell/ml calculated by multiplying the average number of cells for 10,000, chamber conversion factor, and then for the volume of the flask, 5ml.

For combined treatments, cells were treated at the same time in combination with AMD3100 (30µg/ml) or MDX1338 (0.005µg/ml) and doxorubicin at different concentrations for 48h and 72h.

4.3.6 - Cell apoptosis assay

OS cells were seeded at 100,000/well in 6-well plates, allowed to attach overnight, and incubated with or without MDX1338 (0.005 µg/ml) or AMD3100 (30 µg/ml) for 48 and 72 h. According to the protocol kit (MEBCYTO Apoptosis kit; MBL International, Woburn, MA, USA), the adherent cells were trypsinized, detached, and combined with floating cells from the original growth medium, centrifuged and washed twice with PBS 1X. Cells were re-suspended in 500 µl of staining solution

containing FITC-conjugated Annexin V antibody and propidium iodide (PI) for 30 min and analyzed by flow cytometry.

The number of viable (Annexin⁻/PI⁻), apoptotic (Annexin⁺/PI⁻) and necrotic (Annexin⁺/PI⁺) cells were determined with the Cell Quest Software (BD Biosciences, San Jose, CA, USA), using a peak fluorescence gate to exclude cell aggregates during cell cycle analysis in a FACS Calibur flow cytometer (Becton-Dickinson, San Jose, CA, USA).

4.3.7 - Wound healing assays

Migration assay was performed on human U2OS and SW982. The cells were incubated at 37 °C in 5% CO₂ for 24 h, then incubated in 100% BM-MSC-CM supplemented or not with CXCR4 antagonists, AMD3100 (30µg/ml) and MDX1338 (0.005µg/ml).

A sterile 10µl pipette tip was used to make a wound across a cell culture monolayer. To investigate cell migration the plate was photographed at different time points after wounding (0h, 4h, 8h, 12h, 18h) and the area of wound was measured by ImageJv.1.45r software (160). The experiment was repeated three times. The extent of wound closure was determined as follows: wound closure (%) = $1 - (\text{wound width tx} / \text{wound width t0}) \times 100$. All experiments were performed at least three times.

4.3.8 - Statistical analysis

All data were presented as mean ± SE from three independent experiments. Statistical significance was analysed by the Student's t-test and a probability value of p<0.05 was considered to indicate a statistically significant difference.

5 - RESULTS

5.1 - Aim 1: Immune context in osteosarcoma and synovial sarcoma

5.1.1 - Osteosarcoma

5.1.1 - Tumoral microenvironment components prior chemotherapy (bioptic samples)

Eighty-six out of 129 patients with localized osteosarcoma analysed had evaluable results for at least 7 markers and were included in the present study.

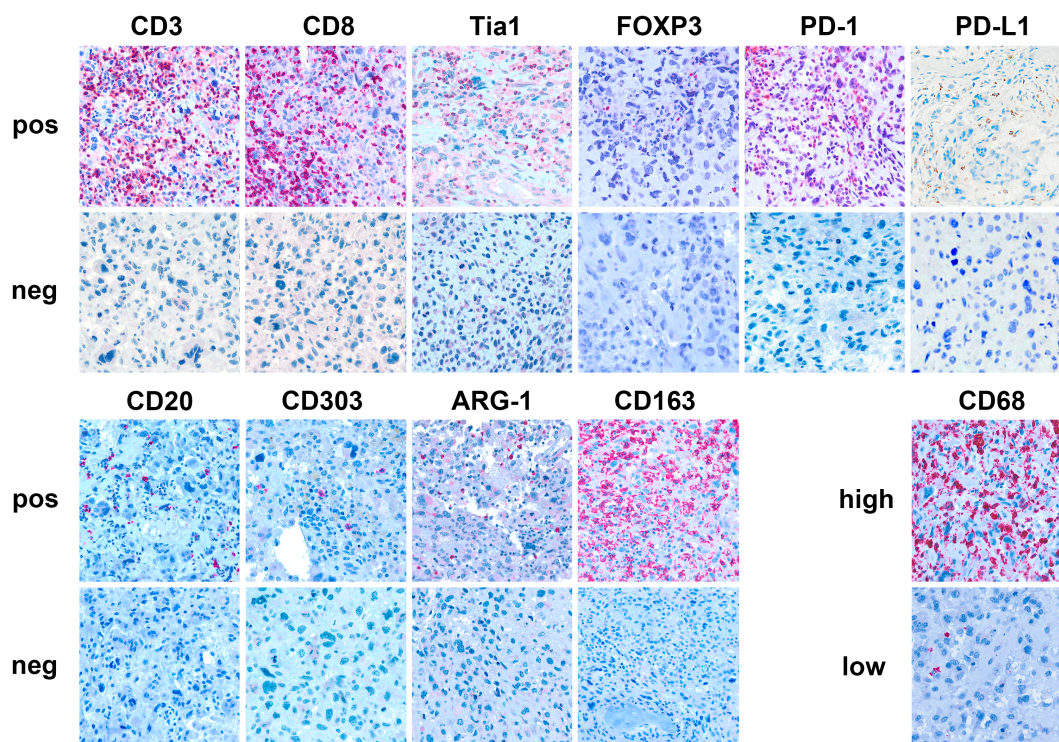
Most of the cases presented TILs (CD3+ 77/86, 90%; CD8+ 74/86, 86%, CD20+ 25/86, 29%) and FOXP3+ population (Treg) were detected in 28/86 (33%). Tia-1 was detected in 57/78 (73%) of the samples. TAMs (CD163 positive) were observed in the microenvironment in 47/70 (67%) of the patients, while 31/74 (37%) patients presented also high levels of CD68 positivity. Only 3/78 (4%) and 16/78 (21%) cases presented CD303+ and Arginase-1+ cells. PD-L1 expression was found in 12/86 (14%) patients in IC and 0/86 (0%) in TC; 19/86 (22%) showed PD-1 expression in IC (Table 1; Figure 1).

Table 1. Immunological characterization of tumor microenvironment in 86 patients with localized osteosarcoma.

	CD3 n (%)	CD8 n (%)	CD20 n (%)	FOXP3 n (%)	Tia1 n (%)	CD68* n (%)	CD163 n (%)	CD303 n (%)	Arg-1 n (%)	PD-L1 (TC) n (%)	PD-1 (IC) n (%)	PD-L1 (IC) n (%)
Pos	77 (90)	74 (86)	25 (29)	28 (33)	57 (73)	31 (37)	47 (67)	3 (4)	16 (21)	0 (0)	19 (22)	12 (14)
Neg	9 (10)	12 (14)	61 (71)	58 (67)	21 (27)	53 (63)	23 (33)	75 (96)	62 (79)	86 (100)	67 (78)	74 (86)

Arg-1: Arginase-1; TC: tumor cells; IC: immune cells; * CD-68: Pos: high level expression; neg: low level expression.

Figure 1. Tumor microenvironment components



Immunohistochemical expression in tumor microenvironment of CD3, CD8, CD20 (T tumor infiltrating lymphocytes: TILs), Tia-1 (cytotoxic T cell), FOXP3 (T regulatory lymphocytes: T-regs), PD-1, PD-L1, CD68 (tumor associated macrophages: TAM), BDCA-2/CD303 (plasmacytoid dendritic cells: pDC), Arginase-1 (myeloid derived suppressor cells: MDSC) proteins.

Survival analysis

With a median follow-up of 8 years (range 1-13), the 5-year OS was 74% (95% CI 64-85).

Univariate analysis showed better 5-year OS for good responders (good 89% vs. poor 57%, $p = 0.0001$), for cases with patients with CD8/Tia1 tumoral infiltrates ($CD8^+/Tia1^+$ 81% vs $CD8^+/Tia1^-$ 60% vs $CD8^-/Tia1^-$ 45%, $p = 0.002$) and patients with normal AP at baseline (AP normal 85% vs AP high 44%, $p = 0.04$) (Table 2, Figure 2).

Figure 2. a) 5-year overall survival according to CD8/Tia1 expression at diagnosis in localized osteosarcoma; b) 5-year overall survival according to PD-L1 expression at diagnosis in patients with CD8+ localized osteosarcoma.

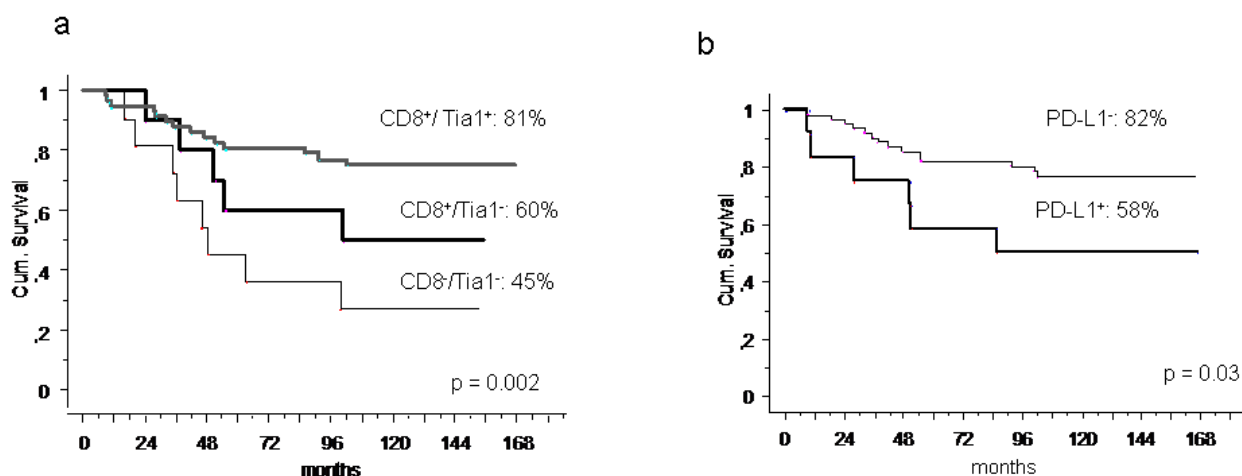


Table 2. Univariate Analysis for Overall Survival (OS) in localized osteosarcoma

	Pts N.	% 5-year OS	95% CI	P-value
Overall	86	74.5	65-84	
Age				0.9
≥ 18 years	27	74	57-90	
< 18 years	59	75	63-86	
Sex				0.8
Female	33	76	61-90	
Male	53	74	61-89	
Histologic Response^o				0.0001
Good	45	89	80-98	
Poor	40	57	42-73	
CD8				0.003
Positive	74	78	69-88	
Negative	12	50	22-78	
TIA-1^{oo}		70		0.008

Moderate	14	86	67-100	
Focal	43	79	67-91	
None	21	52	31-74	
CD8/ Tia1 °°				0.002
Positive / Positive	57	81	70-91	
Positive / Negative	10	60	30-90	
Negative / Negative	11	45	16-75	
CD3				0.07
Positive	77	78	69-87	
Negative	9	44	12-77	
FOXP3 *				0.13
Positive	28	75	54-93	
Negative	56	73	64-85	
PD-1 (IC)				0.6
Positive	19	74	54-93	
Negative	67	74	64-85	
PD-L1 (IC)				0.14
Positive	12	58	30-86	
Negative	74	77	67-87	
LDH °°				0.15
Normal	60	78	68-89	
High	18	61	39-84	
sAP				0.04
Normal	48	85	75-95	
High	38	64	48-80	
Arginase-1 **				0.3
Positive	16	81	62-100	
Negative	61	70	59-82	
CD303 °°				0.9
Positive	3	67	13-100	
Negative	75	73	63-83	
CD68 *				0.1
High	31	84	71-99	
Low	53	67	54-80	
CD163 ***				0.17
Positive	47	81	70-92	
Negative	23	56	36-77	

Not available in 1 patient; °° non available in 8 patients; * not available in 2 patients; ** not available in 7 patients; ***not available in 16 patients

No statistically significant difference was observed in 5-year OS according to PD-1, FOXP3, CD68, CD20, Arginase-1, CD303, CD163 expression in microenvironment, and age, gender or LDH, while PD-L1 (IC) positive cases had a non-significant inferior 5-year OS (PD-L1⁺ 58% vs PD-L1⁻ 77%, $p =$

0.14) (Table 2).

After multivariate analysis, good histologic response ($p = 0.007$) and a $CD8^+/Tia1^+$ lymphocytic infiltrate (0.05) were independently associated with better survival (Table 3).

Table 3. Multivariate Analysis for Overall Survival (OS) in patients with localized osteosarcoma

Variable	RR	95% CI	P
CD8/Tia1			
Positive/Positive	reference		0.05
Positive/Negative	1.8	0.7-5.2	0.2
Negative/Negative	3.1	1.2-7.8	0.01
Histologic Response			
Poor	reference		0.007
Good	0.27	0.1-0.7	
sPA			
Normal	reference		0.2
High	1.75	0.8-3.9	

Since PD-L1(IC) is a marker of cytotoxic function exhaustion, we investigated if PD-L1 expression could influence survival in the subgroup of patient with $CD8^+$ lymphocytes: at univariate analysis the 5-year OS was 82% (95%CI 73%-92%) in case of PD-L1 negative and 58% (95% CI 34%-78%) in positive PD-L1 ($p = 0.03$) (Figure 2).

At the multivariate analysis in this subgroup, lack of PD-L1 was and independent prognostic factor for longer survival ($p = 0.04$) (Table 4).

Table 4. Multivariate Analysis for Overall Survival in patients with $CD8^+$ localized osteosarcoma

Variable	RR	95% CI	P
PD-L1			

Negative	reference		0.04
Positive	2.8	1-7.4	
Histologic Response			
Poor	reference		0.02
Good	0.3	0.1-0.9	
sPA			
Normal	reference		0.5
High	1.4	0.5-3.8	

5.1.2 - Tumoral microenvironment post-induction chemotherapy (surgical samples)

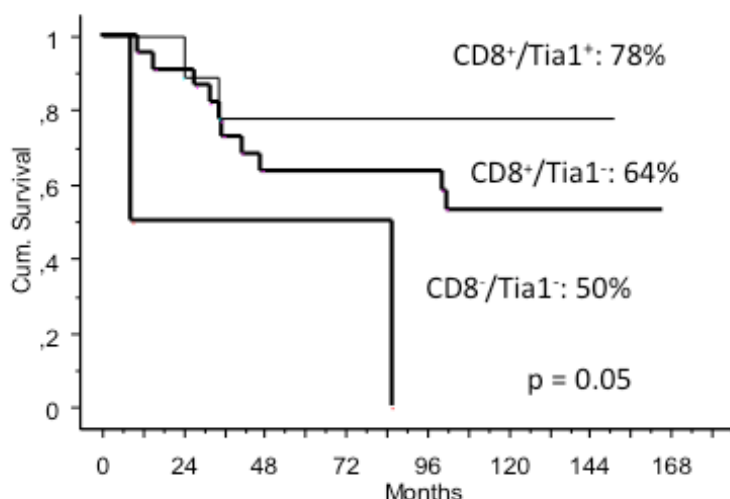
Based on multivariate analysis results on pre-treatment samples, a post-hoc analysis on CD8 and Tia1 was performed. Due to post-treatment changes 33/86 patients were assessable after treatment (excluding 53 patients with massive necrosis and no tumor).

Chemotherapy-induced changes of CD8+ TILs were as follow: all patients with score 0 (5 cases) were unchanged, the proportion of patients with score 1 decreased: 19/33 (58%) pre-chemotherapy, 14/33 (42%) post-treatment; and the proportion of patients with a score 2/3 increased: 9/33 (27%) to 12/33 (36%) ($p = 0.5$).

A survival analysis according to presence of CD8+/Tia1+ infiltrates presence in the surgical samples after induction-chemotherapy, confirmed their prognostic role: 5- year OS was 78% (CI% 51-100) for CD8+ /Tia1+ (22 patients), 64% (CI%43-84) for CD8+/Tia1- (9 patients) and none was alive with CD8- /Tia1- (2 patients) ($p = 0.05$) (Figure 3).

Figure 3. 5-year overall survival according to CD8/Tia1 expression

after induction chemotherapy in localized osteosarcoma



5.1.2 - Synovial Sarcoma

A total of 88 consecutive patients were selected. Forty-five patients were female and 43 male; median age was 37 years (range 11–63); 14 were adolescents and young adults (AYA) (<30 years) and 74 were adults (≥ 30 years). Size of the lesion was > 5 cm in 60 patients (68%), ≤ 5 cm in 24 (27%) and unknown in 4 patients. The tumor site was trunk in 13 cases (15%), lower extremity in 64 cases (73%), upper extremity in 11 cases (12%). Histotypes: 30 patients (34%) had biphasic synovial sarcoma, 51 (58%) monophasic synovial sarcoma and 7 (8%) poorly differentiated synovial sarcoma. All patients underwent surgery with adequate surgical margins in 68 cases, inadequate in 18 and in 2 cases surgical margins were unknown. Amputation was performed in 24 patients (27%). Forty-seven patients (53%) underwent adjuvant radiotherapy (RT) and 57 (65%) received chemotherapy: 27 of them (47%) preoperatively (epirubicin/adrymicin and ifosfamide combination in 49 cases,

non-ifosfamide containing regimen in 8 cases and in 1 case the treatment was unknown).

FISH and RT-PCR Analysis

By FISH analysis, all 88 SS presented SS18 (SYT) gene rearrangement resulting in (X;18)(p11.2;q11.2) translocation, thus confirming the histological diagnosis. The presence of SSX fusion transcripts was assessed on 46 frozen tissues by RT-PCR: 28 cases presented SSX1 variant, 18 had SSX2 variant.

Immunohistochemistry

Most of the cases presented TILs (CD3⁺ 79/82, 96%; CD8⁺ 73/84, 87%), while FOXP3⁺ population (Treg) were detected in 9/84 (11%). PD-L1 expression was found in 10/82 (12%) patients in IC and in 2/82 patients (2%) in TC. In 16/85 (19%) cases PD-1 expression in IC was demonstrated (Table 1).

Table 1. Immunological characterization of tumor microenvironment in 86 patients with localized synovial sarcoma

	CD3 n (%)	CD8 n (%)	FOXP3 n (%)	PD-L1 (TC) n (%)	PD-1 (IC) n (%)	PD-L1 (IC) n (%)
Pos	79 (96)	73 (87)	9 (11)	2 (2)	16 (19)	10 (12)
Neg	3 (4)	11 (13)	75 (89)	80 (98)	69 (81)	72 (88)

Outcome and statistical correlations

With a median follow-up of 6 years (1–30 years), the 5-year overall survival (OS) was 70% (95% CI 60-81%). The 5-year OS was significantly better for young patients (100% for AYA and 65% for adult patients, p = 0.003). The 5-year OS was not significantly different for patients CD8⁺ TILs.

Since patients were not homogenous for treatment we also performed the analysis in the sub-group of patients undergoing surgery without adjuvant chemotherapy.

Interestling, while patients CD8⁺ had a 5 and 10-year-OS of 62% and 50% respectively, all patients with no CD8 were long survivors (all alive after 10-years). After adjuvant chemotherapy 5-year

OS for CD8⁺ and CD8⁻ was 67% and 60% respectively ($p = 0.9$).

Table 2. Univariate Analysis for Overall Survival (OS) in localized synovial sarcoma

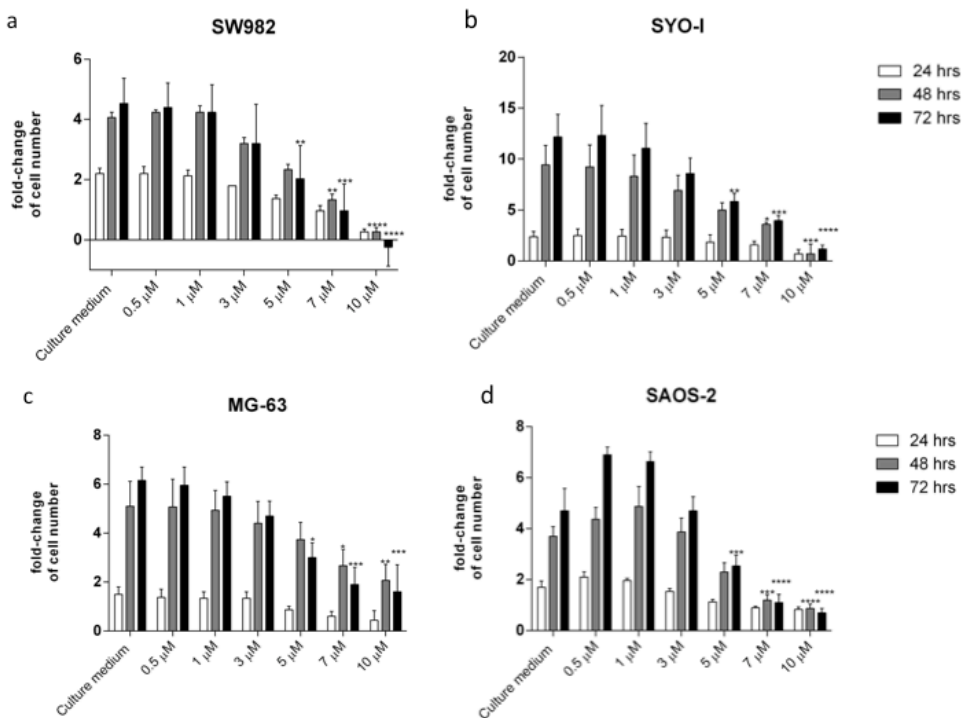
	Pts N.	% 5-year OS	95% CI	P-value
Overall	88	68	57-70	
Age				0.003
≥ 30 years (adult)	74	65	50-78	
< 30 years (AYA)	14	100		
Size (uk in 4)				0.4
< 5 cm	24	82	66-98	
≥ 5 cm	60	67	53-80	
Histology				0.5
Biphasic	30	67	53-80	
Other	58	76	59-93	
Chemotherapy				0.5
Yes	60	68	54-81	
No	38	73	67-85	
CD8 (uk in 4)				0.4
Positive	73	66	53-78	
Negative	11	72	44-99	
CD3 (uk in 4)				0.5
Positive	79	67	55-78	
Negative	3	33	0-87	
FOXP3 (uk in 4)				0.9
Positive	9	76	47-100	
Negative	75	65	53-77	
PD-1 (IC)				0.7
Positive	16	63	37-89	
Negative	69	68	56-80	
PD-L1 (IC)				0.8
Positive	10	66	33-100	
Negative	72	66	53-78	
PD-L1 (TC)				NV
Positive	2	100		
Negative	80	65	53-66	

5.2 - Aim 2: Anti-VEGFR and anti-PD-1 activity in osteosarcoma and synovial sarcoma

5.2.1 - Sunitinib malate inhibit proliferation in sarcomas

The sunitinib effect on proliferation was studied in synovial sarcoma cell lines (SYO-1 and SW982) and in 2 osteosarcoma cell lines (MG-63 and osteoblastic SaOS-2). Treatment of synovial sarcoma cell line SW982 for 24 h, 48 h, 72 h with 0.5 μ M, 1 μ M, 3 μ M, 5 μ M, 7 μ M an 10 μ M sunitinib inhibited proliferation in a dose-dependent manner as assessed by cell proliferation-assay (Figure 1a), with best result obtained after 72 h with 10 μ M sunitinib. The effect on synovial cell line SYO-1 was very similar (Figure 1b), but the greater inhibition of proliferation was reached at 48 h with 10 μ M sunitinib. Treatment of osteosarcoma cell lines MG-63 and SaOS-2 for 24 h, 48 h, 72 h at increasing sunitinib concentration was also able to inhibit proliferation in a dose-dependent manner (Figure 1c, 1d), with best result obtained after 72 h with 10 μ M sunitinib.

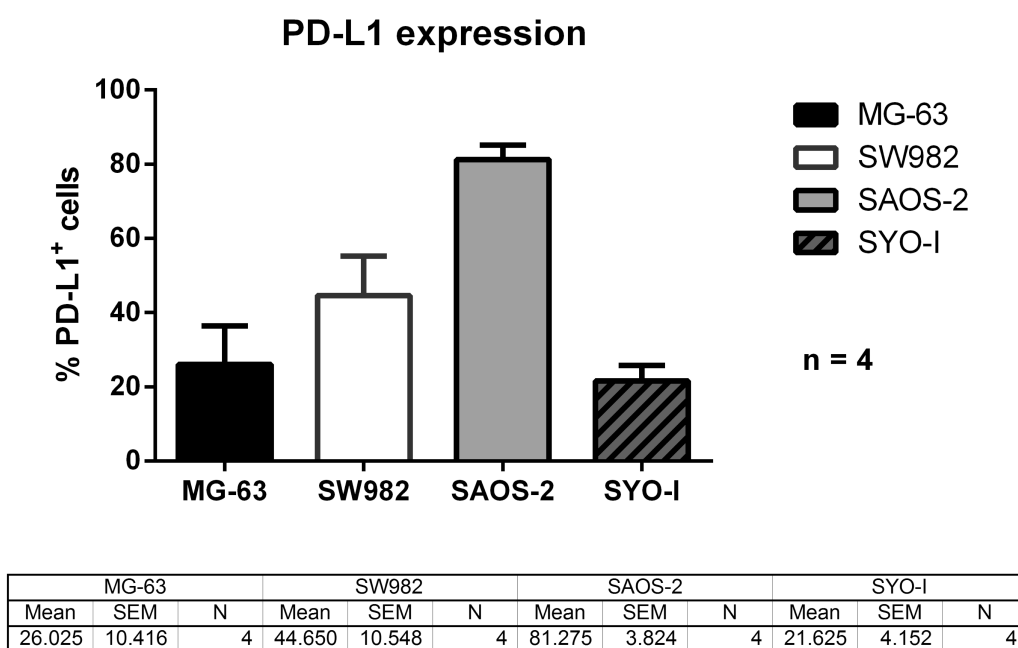
Figure 1. Sunitinib significantly reduce proliferation in sarcomas



5.2.2 - Sarcoma cell lines express PD-L1

PD-L1 expression was detected in all cell lines tested, with a median expression (in 4 experiments) ranging from 21.6% (SYO-1) al' 81.3% (SaOS-2) (Figure 2)

Figure 2. Express of PD-L1 in osteosarcoma and synovial sarcoma



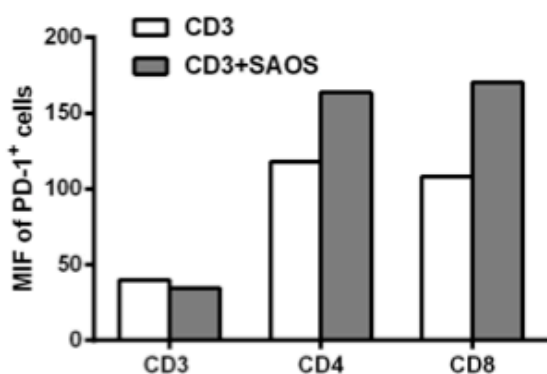
5.2.3 - PD-1 blockade hamper sarcoma-induced-PD1 expression on lymphocytes

Lymphocytes – sarcoma co-culture

We hypothesized that sarcoma cell lines were tolerogenic by increasing PD-1 expression on

lymphocytes. We demonstrated that mean intensity of fluorescence (MIF) for PD-1 was increased by osteosarcoma cell line SaOS-2 (Figure 3).

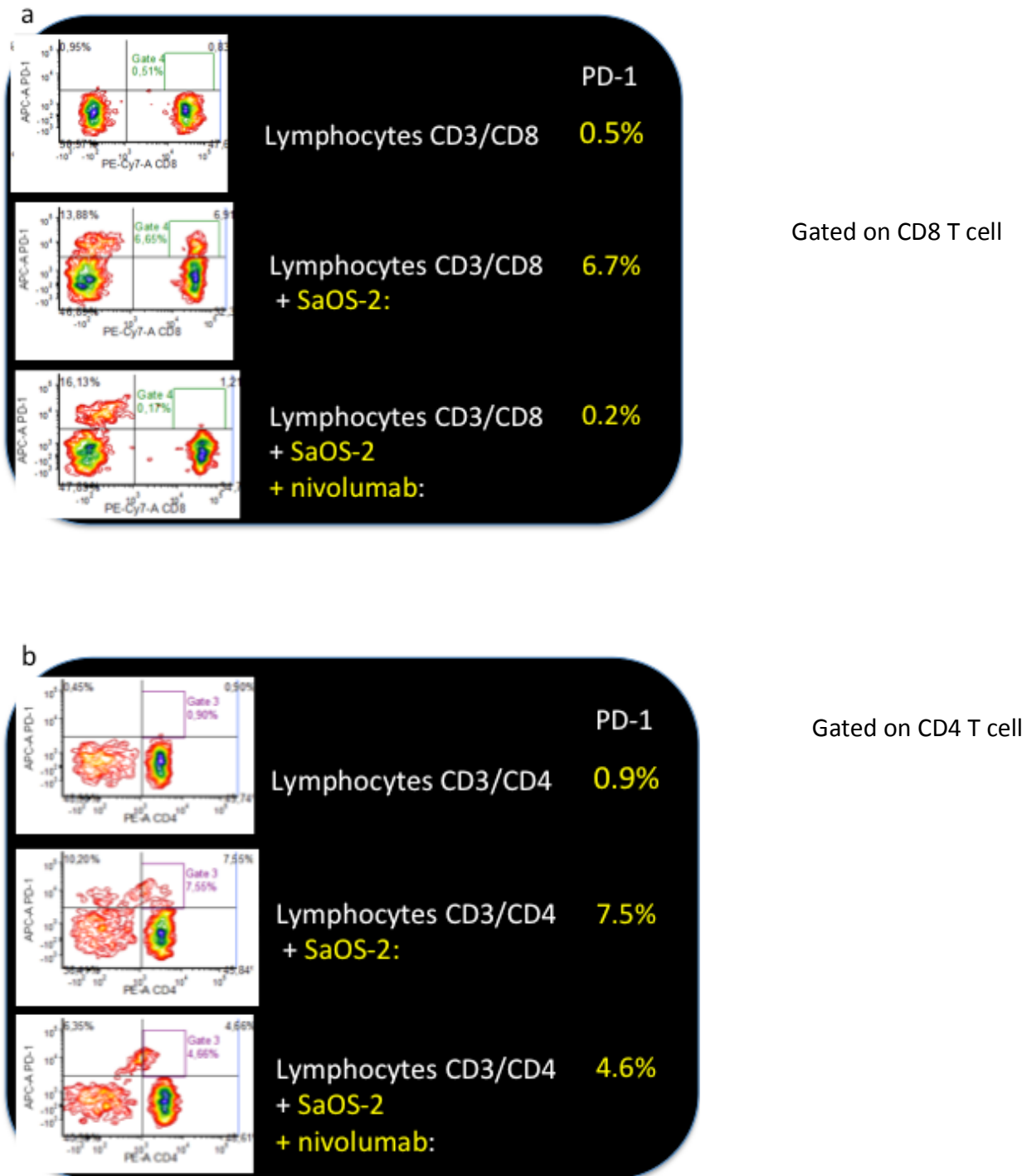
Figure 3. Osteosarcoma cell line SaOS-2 induced increase of PD-1 MIF (mean intensity of fluorescence) in CD4 and CD8 lymphocytes.

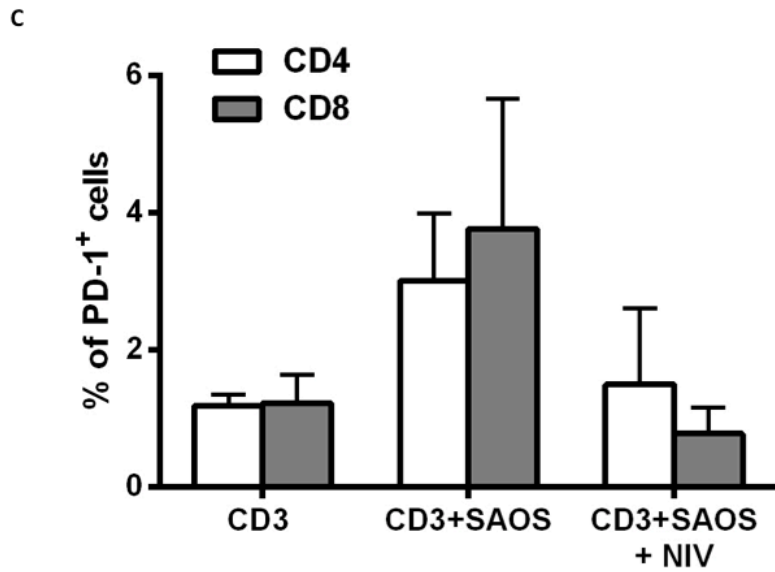


We also assumed that nivolumab /PD-1 blockade might hamper sarcoma tolerance, by decreasing PD-1 expression.

As said, adding osteosarcoma cell line SaOS-2 prior to the functional assays significantly increased PD-1 expression on lymphocytes (CD3+/CD8+), and nivolumab, was able to decrease PD-1 expression (Figure 4 a, c); similar effects were observed on CD4+ gated lymphocytes (Figure 4 b,c).

Figure 4. Osteosarcoma cell line SaOS-2 co-cultured with lymphocytes induced PD-1 up-regulation both on CD3/CD8 lymphocytes (from 0.5% to 6.7%) (a, c) and on CD3/CD4 lymphocytes (from 0.9% to 7.5%) (b, c); nivolumab counteracts PD-1 up-regulation, 0% expression after nivolumab exposure, on CD3/CD8 lymphocytes (a, c), and reduction on CD3/CD4 lymphocytes, (b, c).



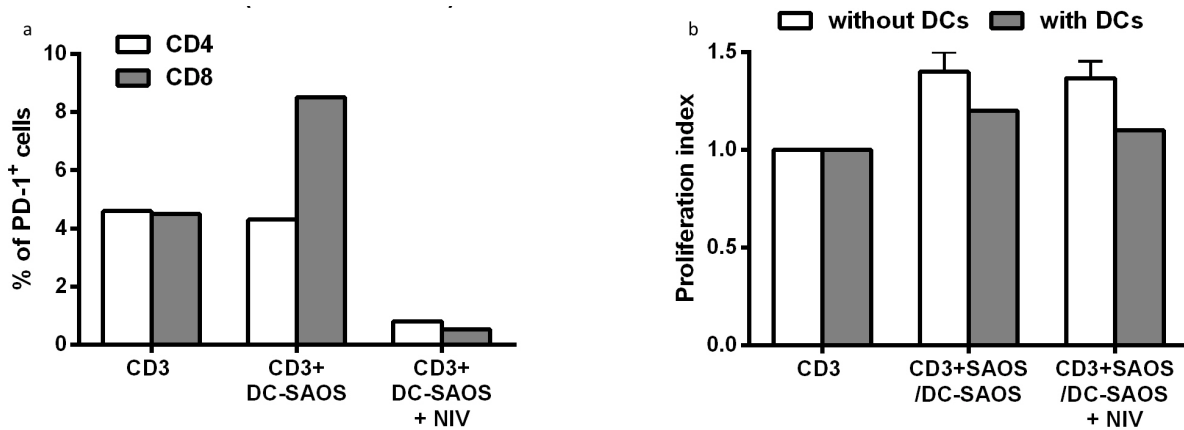


Lymphocytes - Dendritic cell (DCs) coculture (allogeneic mixed lymphocyte reaction - MLR)

The ability of nivolumab to promote T-cell response was also evaluated in vitro using allogeneic MLR.

In an allogeneic MLR, human monocyte-derived immature dendritic cells (DCs) pulsed with SaOS-2 cell line lysate were co-cultured with lymphocytes: PD-1 blockade with nivolumab systematically resulted in a dramatic decrease of PD-1 expression on lymphocytes, while their proliferation was unchanged (Figure 5).

Figure 5. PD-1 up-regulation induced by dendritic cells (DCs) pulsed with osteosarcoma cell line SaOS; nivolumab counteracts PD-1 up-regulation both on CD3/CD8 and CD3/CD4 lymphocytes (a), while the proliferation is not affected with a proliferation index only slightly increase after SaOS-2 co-culture (both in presence of lymphocytes only or lymphocytes and DCs co-culture) and almost unchanged after nivolumab supplementation (b).

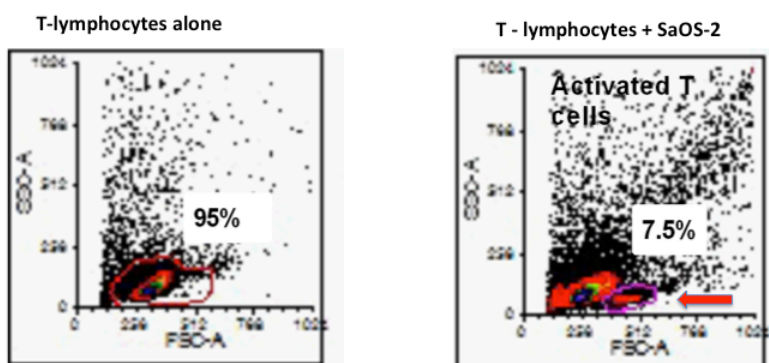


5.2.4 - Nivolumab activity on *activated* T-lymphocytes

Lymphocytes – sarcoma co-culture

After exposure of T lymphocytes to osteosarcoma cell line SaOS-2, we observed the induction of a new subset of *activated* T-lymphocytes, distinguished by a morphological shift on forward scatter (Figure 6)

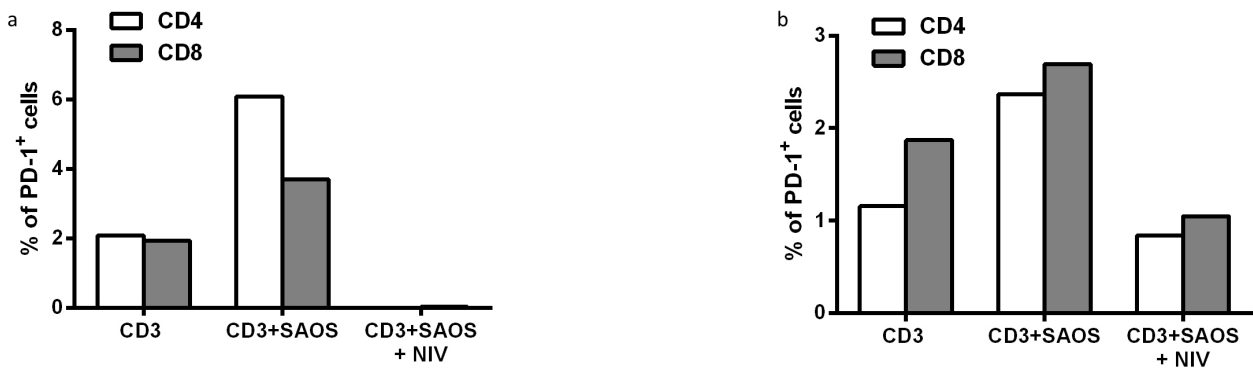
Figure 6. Induction of a new subset of activated T-lymphocytes, distinguished by a morphological shift on forward scatter (red arrow)



The effect of nivolumab in the sub group of *activated* T-lymphocytes was more pronounced, if compared with *inactivated* lymphocytes as shown in Figure 7.

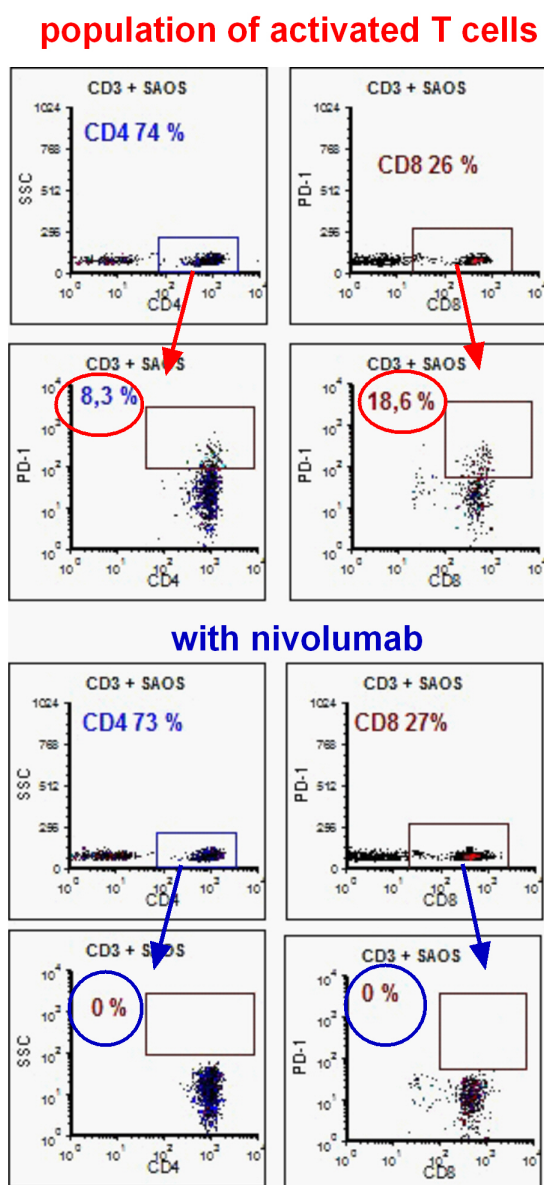
Figure 7. PD-1 up-regulation induced by osteosarcoma cell line SaOS-2;

no PD-1 expression can be detected after nivolumab both on CD4 and CD8 on *activated* T-cells (a), while on *non-activated* lymphocytes PD-1 expression is similar to baseline levels for CD4 (b), and reduced but still expressed on CD8 (a).



After performing the same analysis in the subset of CD8 or CD4 *activated* lymphocytes, we observed the ability of nivolumab to reduce/abort PD-L1 up-regulation is increased, as compared to the entire group of CD8/CD4 lymphocytes (Figure 8).

Figure 8. PD-1 up-regulation induced by osteosarcoma cell line SaOS-2 in the subset of *activated* CD4 and CD8 lymphocytes; after nivolumab PD-1 expression is abrogated both on CD4⁺ *activated* lymphocytes (PD-1 positivity from 8.62% to 0%) (*left panel*) and CD8⁺ *activated* lymphocytes (PD-1 positivity from 19.63% to 0%) (*right panel*)

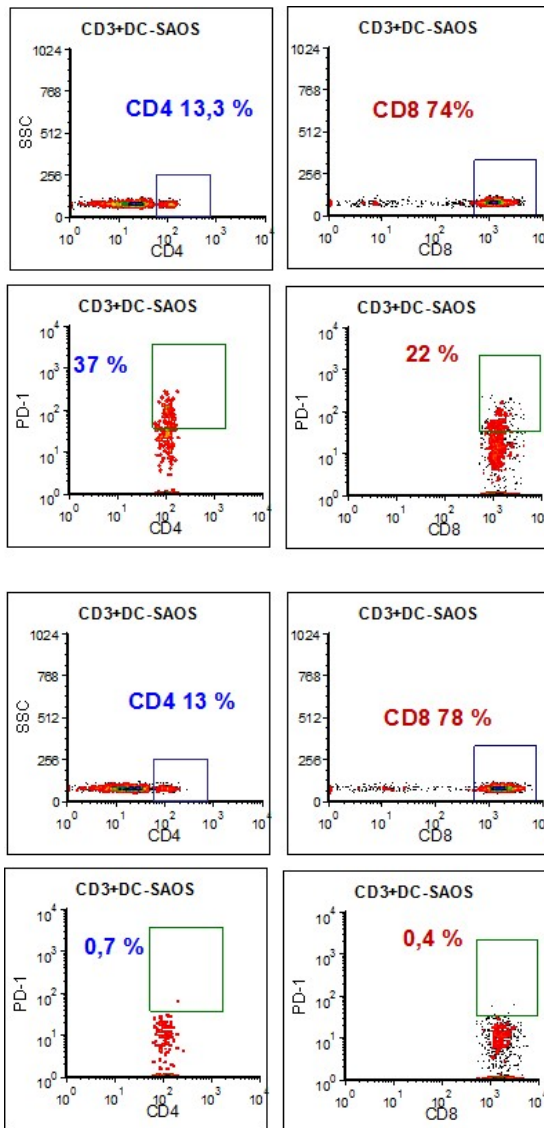


Lymphocytes - Dendritic cell (DCs) co-culture (allogeneic mixed lymphocyte reaction - MLR)

Similarly, in allogeneic MLR, when lymphocytes were co-cultured with DCs pulsed with osteosarcoma, PD-1 blockade with nivolumab systematically resulted in a dramatic decrease of PD-

1 expression on the subset of CD4⁺ and CD8⁺ *activated* lymphocytes (Figure 9).

Figure 9. PD-1 up-regulation induced by dendritic cells (CDs) pulsed with osteosarcoma cell line SaOS-2; nivolumab counteracts PD-1 up-regulation on CD4⁺ *activated* lymphocytes (PD-1 positivity from 35.29% to 0.76%) (*left panel*) and on CD8⁺ *activated* lymphocytes (PD-1 positivity from 21.66% to 0.49%) (*right panel*)

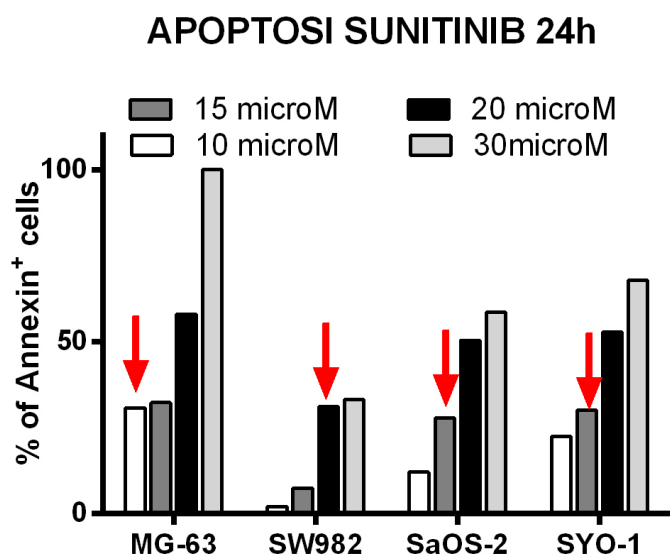


5.2.5 - Sunitinib induce apoptosis in sarcoma

We used sunitinib at 4 different concentrations (10 μ M, 15 μ M, 20 μ M and 30 μ M). Sunitinib induced dose-dependent cell death as demonstrated with Annexin test in osteosarcoma (MG-63

and SaOS-2), in synovial sarcoma (SYO-1 and SW982) (Figure 10).

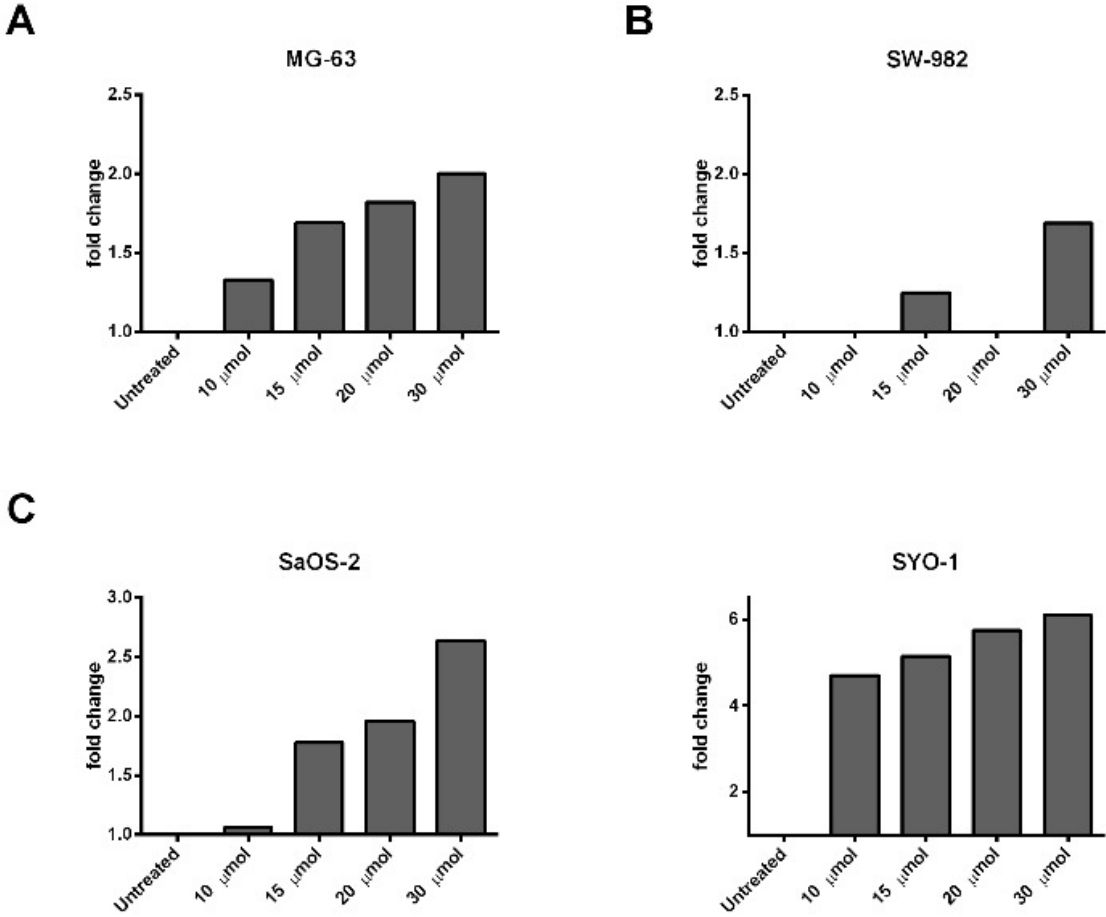
Figure 10. Dose-dependent apoptosis in osteosarcoma (SaOS-2 and MG-63) and synovial sarcoma (SW982 and SYO-1) cell lines, with red arrow showing for each cell line a concentration of sunitinib sufficient to obtain at least 30% of apoptotic cells, after 24 hours exposure to different concentration of sunitinib



5.2.6 – Sunitinib and PD-L1 expression in sarcoma

Sunitinib was able to immunomodulate the expression of PD-L1 in synovial sarcoma and SaOS-2 osteosarcoma cell lines assessed, while MG-63, an osteosarcoma cell line, showed constant levels of PL-L1 expression after sunitinib 5, 7 e 10 μ M (Figure 11).

Figure 11. A dose-dependent PD-L1 up-regulation was demonstrated in osteosarcoma cell lines SaOS-2 and MG-63 and in synovial sarcoma cell line SYO-1 (A, C and D), while an up-regulation of PD-L1 expression was shown at concentration of 30 μ M in SW982 cell line with no changes with lower doses (B).



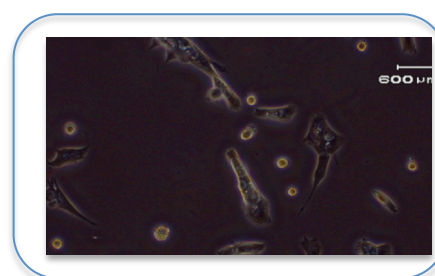
5.3 - Aim 3: Anti-CXCR4 activity in osteosarcoma and synovial sarcoma

5.3.1 - SYT-SSX translocation in synovial sarcoma cell lines

Before all the experiments, we tested our synovial sarcoma cell lines for the presence of the pathognomonic translocation: the commercial sarcoma cell line SW982 lacked SYT-SSX translocation, as expected, while SYO-1 carried the SYT-SSX translocation.

Table 1. t(X;18) SS18(SYT)-SSX1 in synovial sarcoma by RT-PCR

Cell lines	SYT-SSX translocation
SYO-1	Positive (SYT-SSX1, SYT-SSX2)
SW982	Negative



5.3.2 - CXCR4 and SDF-1 (CXCL12) expression in sarcoma cell lines

To evaluate whether CXCR4 and its corresponding ligands SDF-1 (CXCL12) contributed to sarcoma progression, we first determined the mRNA and protein expression of CXCR4 in 3 cell lines (SW982, SYO-1, U2OS) using qRT-PCR (TaqMan gene expression assay) and by FACS analysis, respectively.

CXCR4 mRNA was expressed in all 3 cell lines and the highest expression level was found in SYO-1 as compared with both commercial sarcoma cell line SW982 (using mesenchymal cells as calibrator) and osteosarcoma cell lines U2OS (using osteoblast as calibrator) (Table 2).

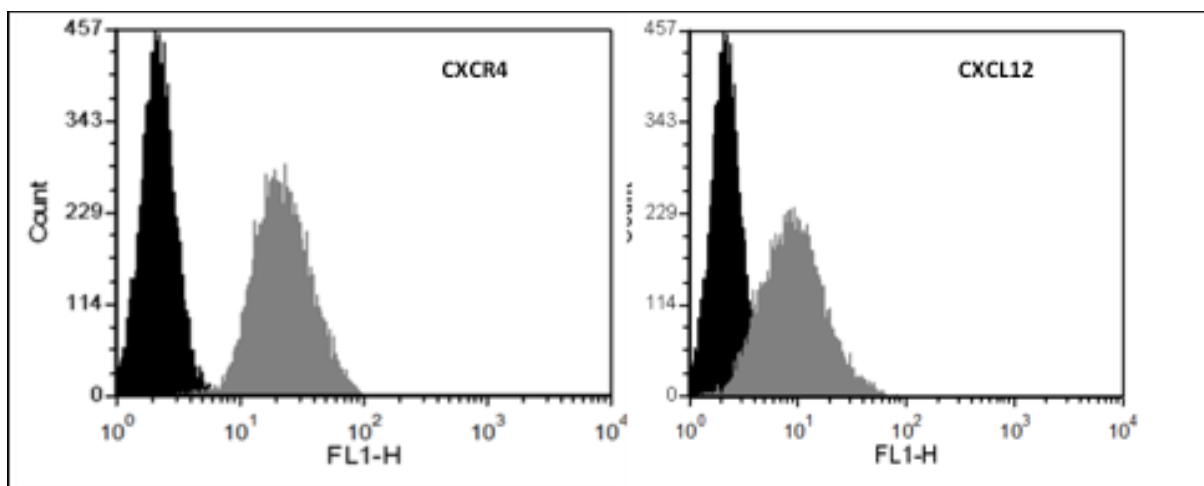
Table 2. CXCR4 (mRNA) expression in sarcoma cell lines

Cell lines	CXCR4 expression (2_DDCT)
SW982 (synovial sarcoma)	4482
SYO-1 (synovial sarcoma)	50012
U2OS (osteosarcoma)	131

Then we evaluated protein expression of CXCR4 and SDF-1 (CXCR12) by immunofluorescence analysis. The three cell lines showed a different distribution of expression (Figure 1-3):

- Osteosarcoma U2OS cell line expressed CXCR4 and SDF-1 (CXCR12) in 98% and 80% of cells, respectively

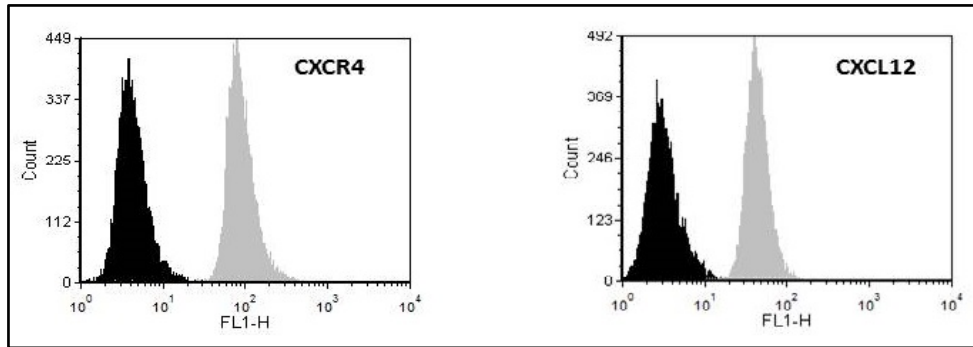
Figure 1. CXCR4 and SDF-1 (CXCR12) in osteosarcoma U2OS cell line



- synovial sarcoma SW982 cells expressed CXCR4 (left panel, grey spike) and SDF-1 (CXCL12)

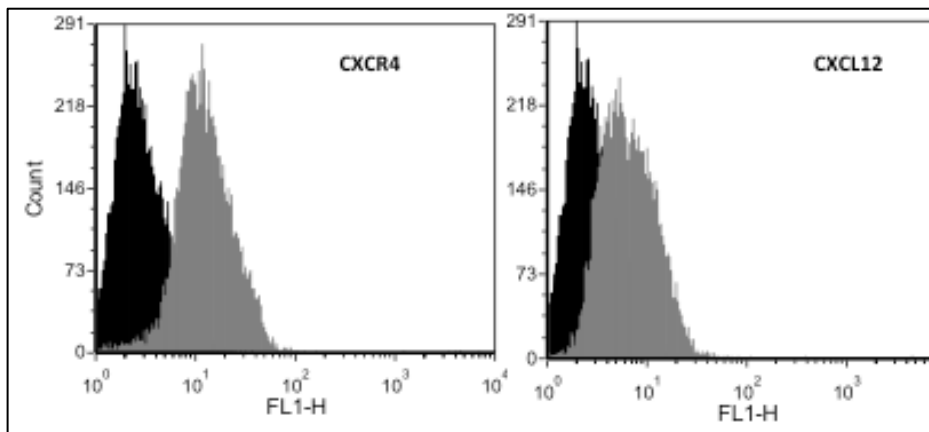
(right panel, grey spike) in 83.5 and 41% respectively, as compared with control (black spike)

Figure 2. CXCR4 and SDF-1 (CXCL12) in SW982 cell line



- Synovial sarcoma SYO-I cell line expressed CXCR4 and SDF-1 (CXCL12) in 12.0% and 6.0%, respectively.

Figure 3 CXCR4 and SDF-1 (CXCL12) in synovial sarcoma SYO-I cell line



5.3.3 - SDF-1 (CXCL12) expression in different media

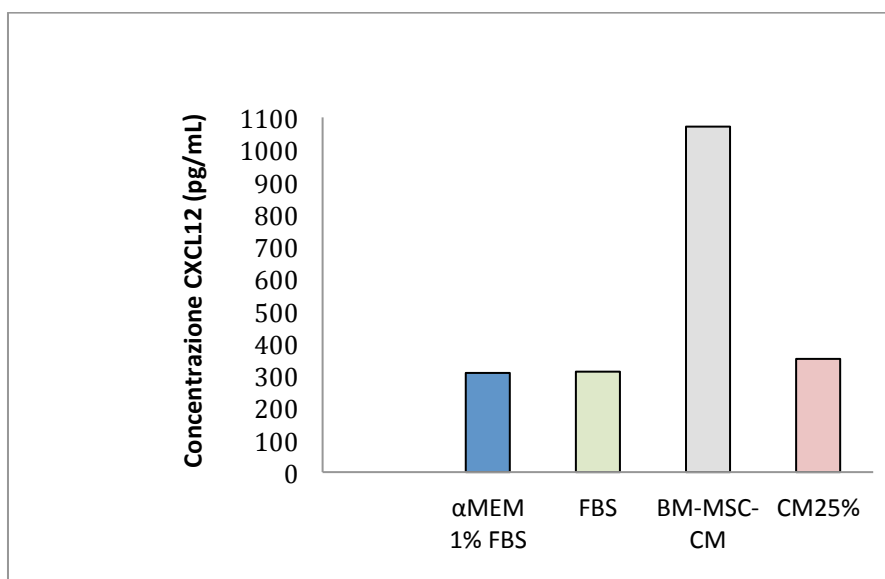
By Elisa analysis the levels of SDF-1 (CXCL12) was higher in in BM-MSC-CM, when compared to

αMEM alone, or αMEM supplemented with 25% BM-MSC (Table 3).

Table 3. SDF1 (CXCL12) expression in αMEM

Conditions	SDF-1α/CXCL12 (pg/mL)
αMEM 1% FBS	307,5616
αMEM 1% FBS +25% BM-MSC	351.09
BM-MSC –CM (100% BM.MSC)	1071,369

Figure 4. SDF-1 (CXCL12) concentration in different media



5.3.4 - Treatment with MDX1338 and AMD3100 reduce SW983 and U2OS proliferation

MDX and AMD3100, specific chemical inhibitor for CXCR4, can block SDF-1/CXCR4 signalling pathway. Our goal was to investigate whether MDX1338/AMD3100 treatment can reduce osteosarcoma (U2OS) and synovial sarcoma (SW982) cell viability (experiments on SYO-1 synovial sarcoma cell line are ongoing). Secondly, we evaluated if the combined use of doxorubicin and CXCR4 inhibitors could result in additive or synergistic inhibition effect.

Synovial sarcoma (SW982) cell viability after CXCR4 inhibitor treatment

SW982 cells responded to different MDX1338 concentrations (0.001 µg/ml, 0.005 µg/ml, 0.05 µg/ml), with a small reduction of cell viability, reaching a cell death rate at 72h of 22% with 0.005 µg/ml drug concentration (Figure 5).

Similarly, AMD3100 treatment (5 µg/ml, 20 µg/ml, 30 µg/ml) caused a cell viability reduction of 30% after 72 h using a drug concentration of 30 µg/ml (Figure 6).

Figure 5. SW982 proliferation after treatment with MDX1338

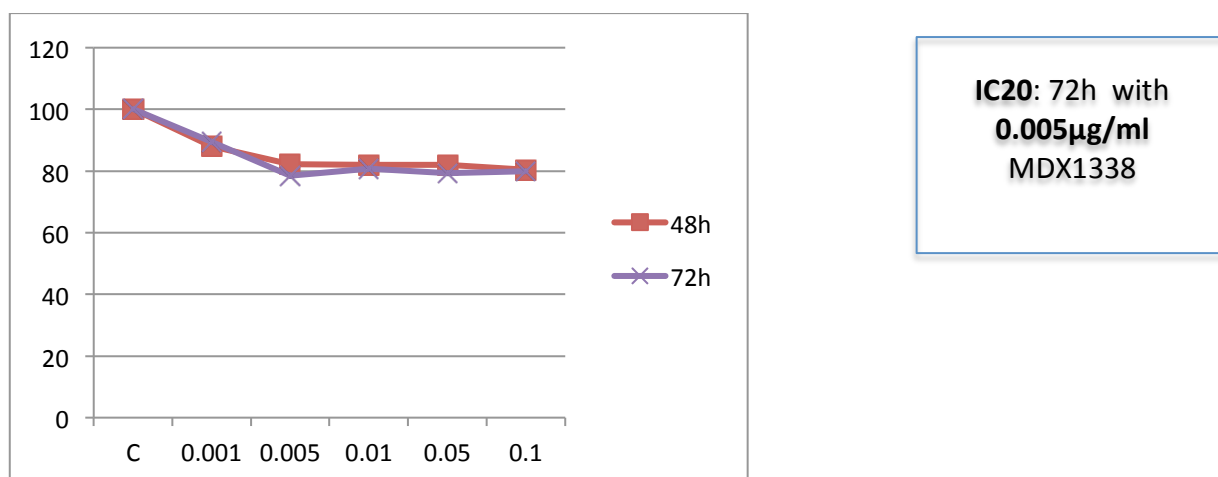
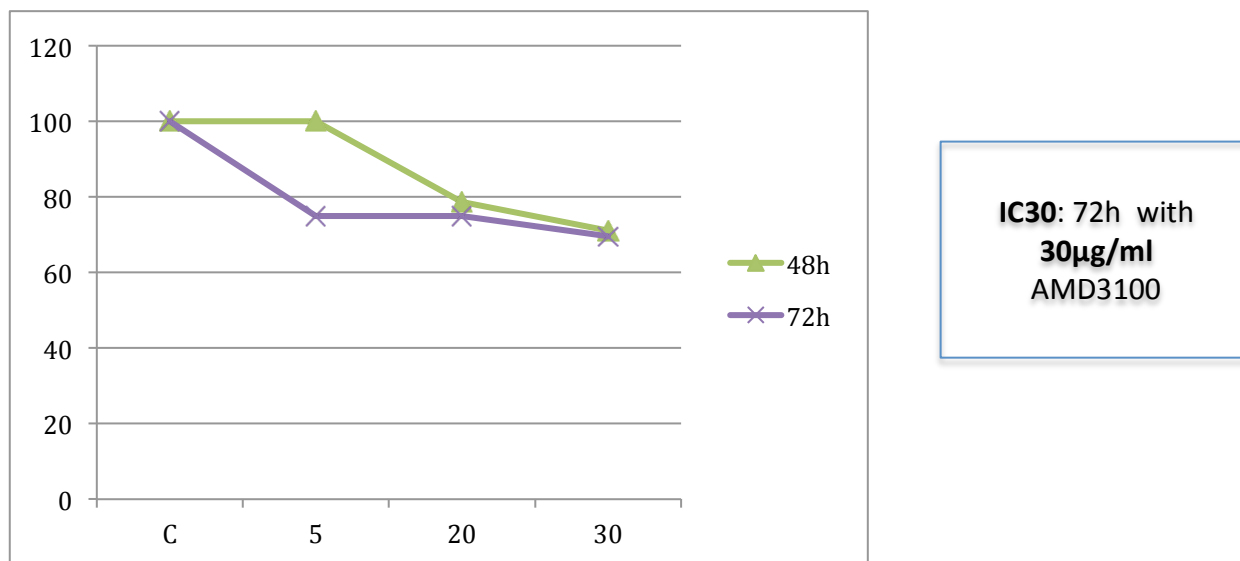


Figure 6. SW982 proliferation after treatment with AMD3100



Osteosarcoma cell viability (U2OS) after CXCR4 inhibitor treatment

Several MDX1338 concentrations were tested (0.001 µg/ml, 0.005 µg/ml, 0.05 µg/ml), at 48h. We observed the best results at using a drug concentration of 0.005 µg/ml, with a cell viability decrease of about 30% (Figure 7).

Similarly, for AMD3100 we assessed different concentrations (5 µg/ml, 20µg/ml, 30 µg/ml) at 48h, and obtained a 40% of reduction in cell viability with a drug concentration of 30 µg/ml (Figure 8).

Figure 7. U2OS-2 proliferation after treatment with MDX1338

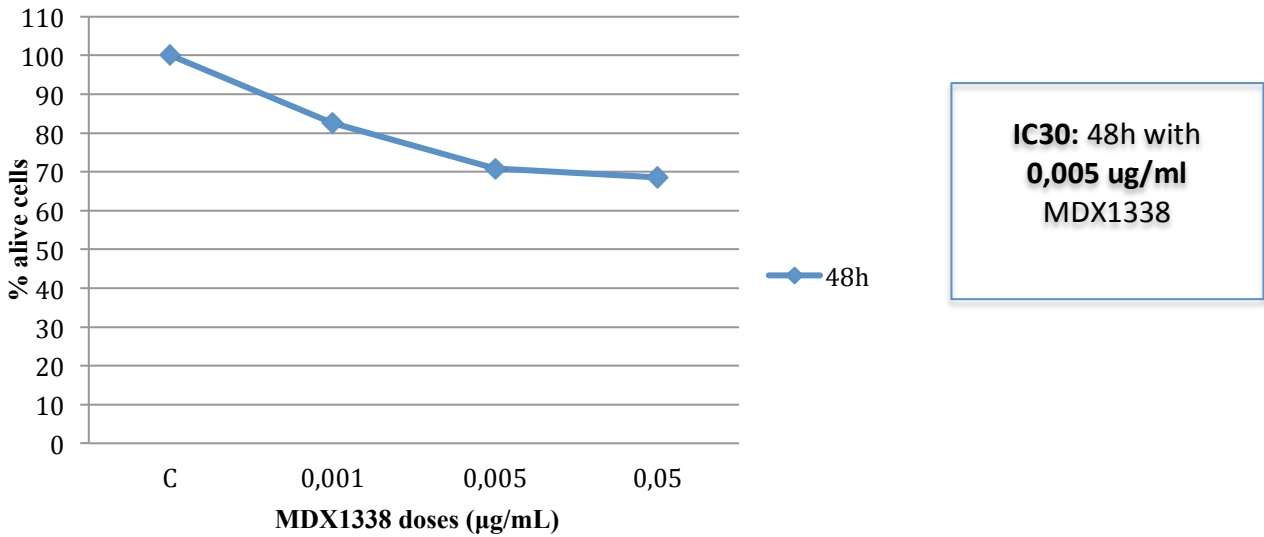
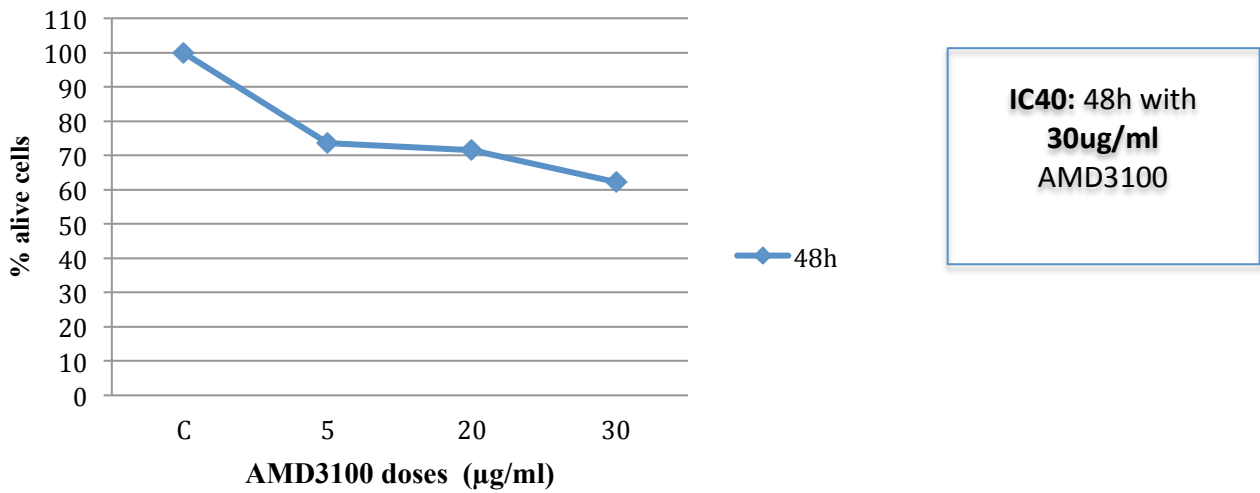


Figure 8. U2OS proliferation after treatment with AM3100



5.3.5 - Treatment with MDX1338 and AMD3100 does not change CXCR4 expression

We wanted to verify whether the treatment with CXCR4 inhibitors might be able to change (induce/reduce) the expression of CXCR4 protein. FACS analysis demonstrated that CXCR4

expression in SW982 (Figure 9) and U2OS (Figure 10) was almost unchanged after 72h of MDX1338 (0.005 µg/ml) and AMD3100 (30 µg/ml treatment) (2.93% and 0.78% reduction respectively)

Figure 9. CXCR4 expression in SW982 changes after treatment with CXCR4 inhibitors

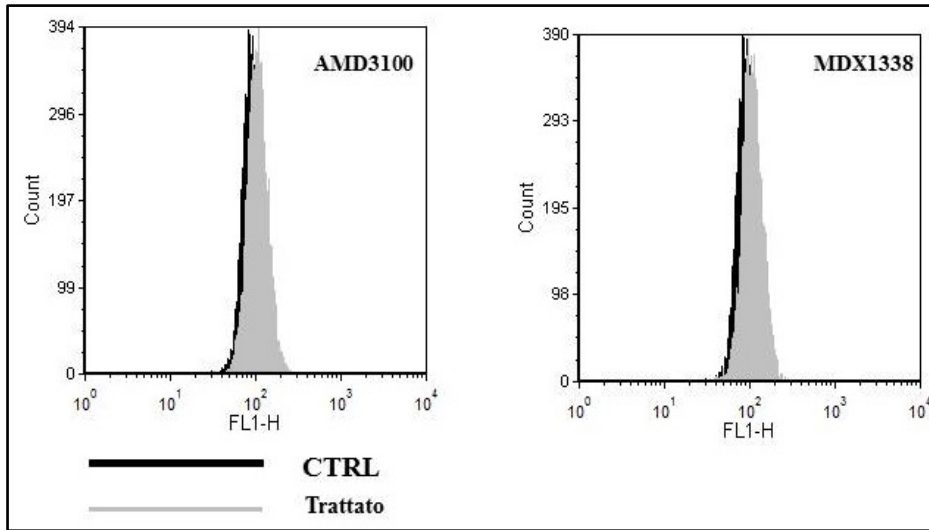
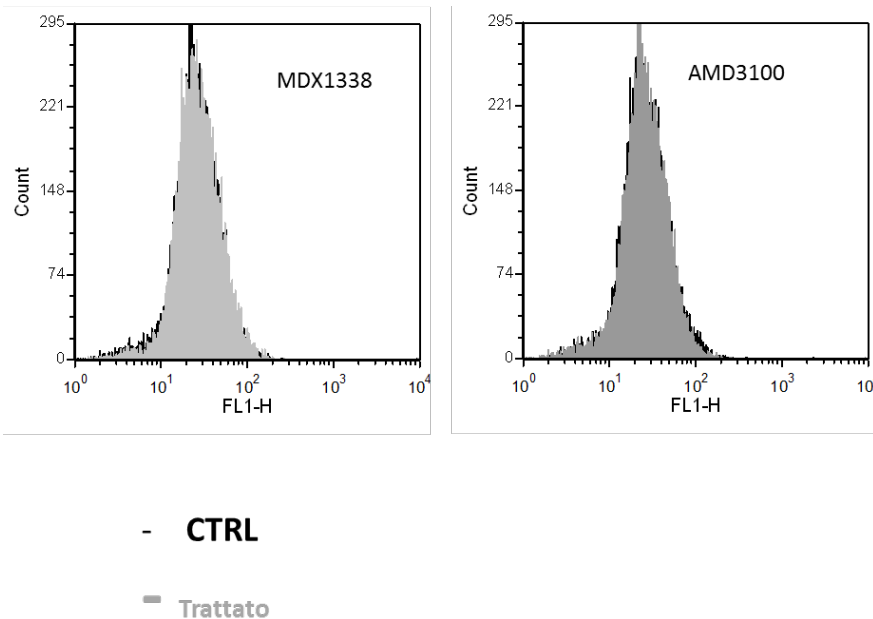


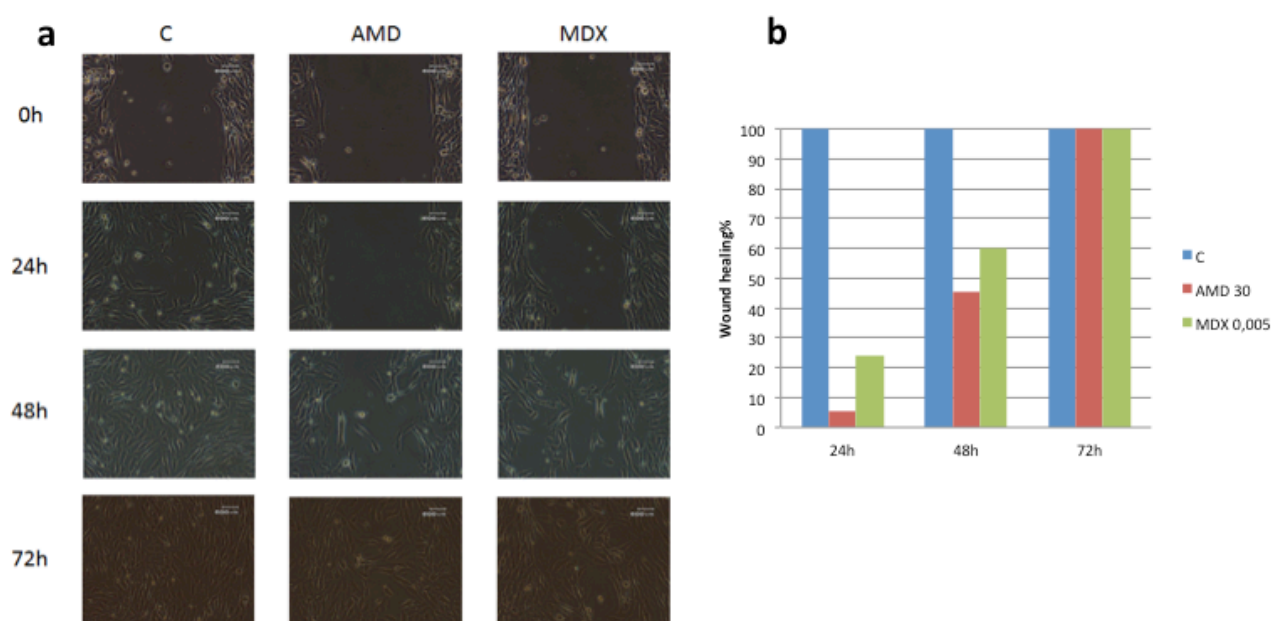
Figure 10. CXCR4 expression in U2OS changes after treatment with CXCR4 inhibitor



5.3.6 - Treatment with MDX1338 and AMD3100 reduces SW982 and U2OS cells migration

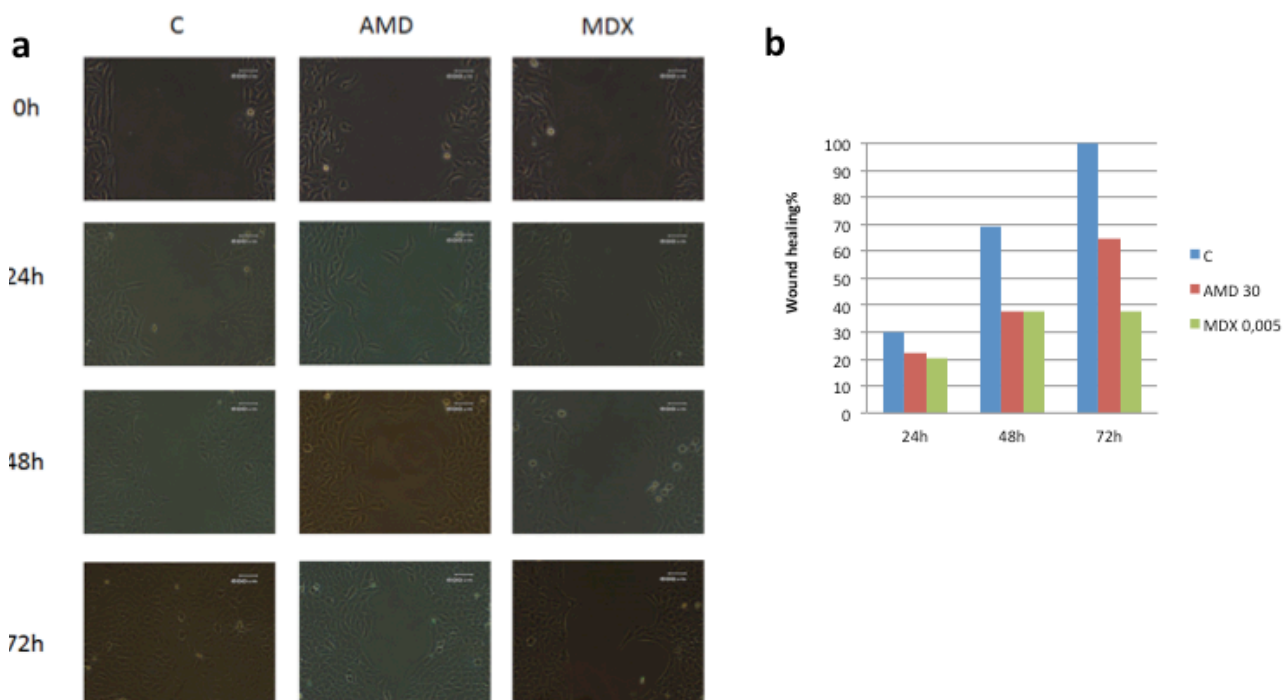
We explored whether MDX1338 and AMD3100 could decrease migration of SW982 cells. CXCL12 is a potent chemotactic factor and can induce directional migration of hematopoietic and non-hematopoietic cells. Wound healing assay at different time points (24h, 48h, 72h) reached the complete wound closure after 24 hours of treatment, with a short-term slowing down up to 48h with both AMD3100 and MDX1338, when compared to control (Figure 11)

Figure 11. SW982 migration after treatment with CXCR4 inhibitors: a) Image-based monitoring; b) Wound closure expressed as a percentage of the initial wound area that has healed.



In contrast, U2OS responded to MDX1338 and AMD3100 treatment with an evident decrease of cell motility up to 72h compared to control (Figure 12).

Figure 12. U2OS migration after CXCR4 inhibitor treatment: a) Image-based monitoring; b) Wound closure expressed as a percentage of the initial wound area that has healed.

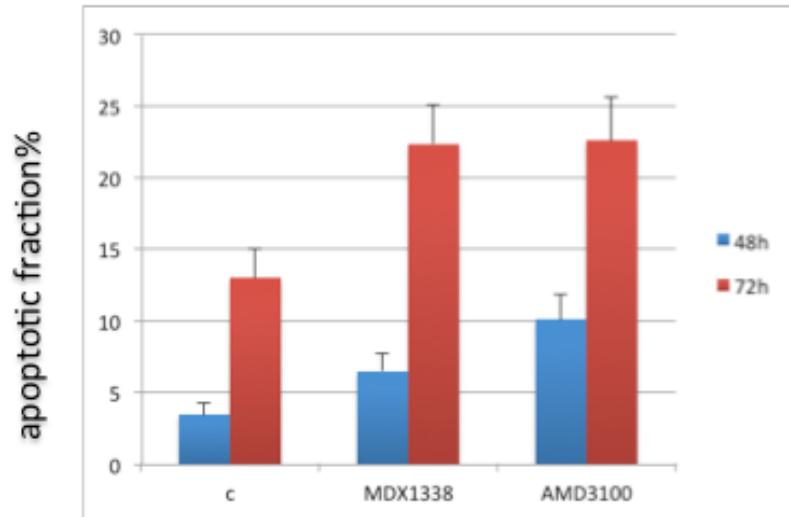


5.3.7 -Treatment with MDX1338 and AMD3100 promote SW982 and U2OS cells apoptosis

The effects of MDX1338 (0.005 $\mu\text{g} / \text{ml}$) and AMD3100 (30 $\mu\text{g} / \text{ml}$) on SW982 cell apoptosis was analyzed by flow cytometry. Experimental results showed a significant increase of apoptotic cells after CXCR4 inhibitors treatments compared with the untreated cells. The percentage of apoptotic cells was 3.42% and 12.9% at 48h and 72h respectively in untreated cells versus 6.4% ($p=0.006$) and 22.3% ($p= 0.002$) respectively for MDX1338, and 10.0% ($p=0.003$) and 23% ($p=0.004$) for AMD 3100

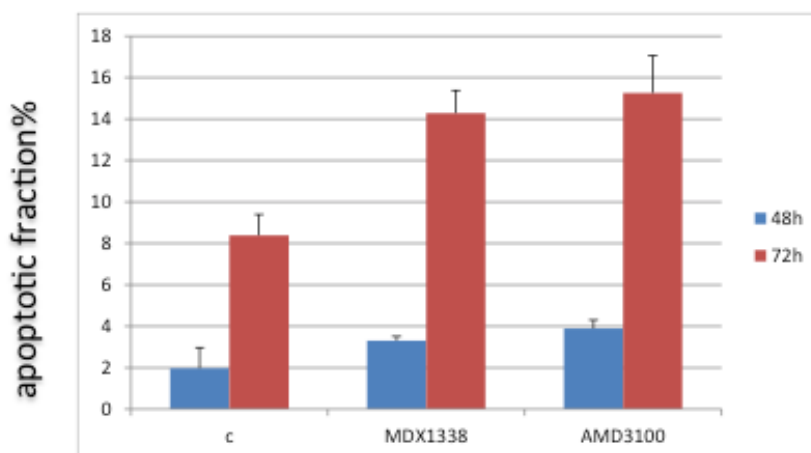
(Figure 13).

Figure 13. SW982 apoptosis after treatment with CXCR4 inhibitors



U2OS cells responded similarly to CXCR4 inhibitors, with an increase of the apoptotic rate 1.9% and 8.3% at 48h and 72h in untreated cells, versus 3.3% ($p= 0.013$) and 14.2% ($p= 0.011$) after treatment with MDX1338 and 3.9% ($p=0.019$) and 15.2% ($p=0.022$) after AMD3100 administration (Figure 14).

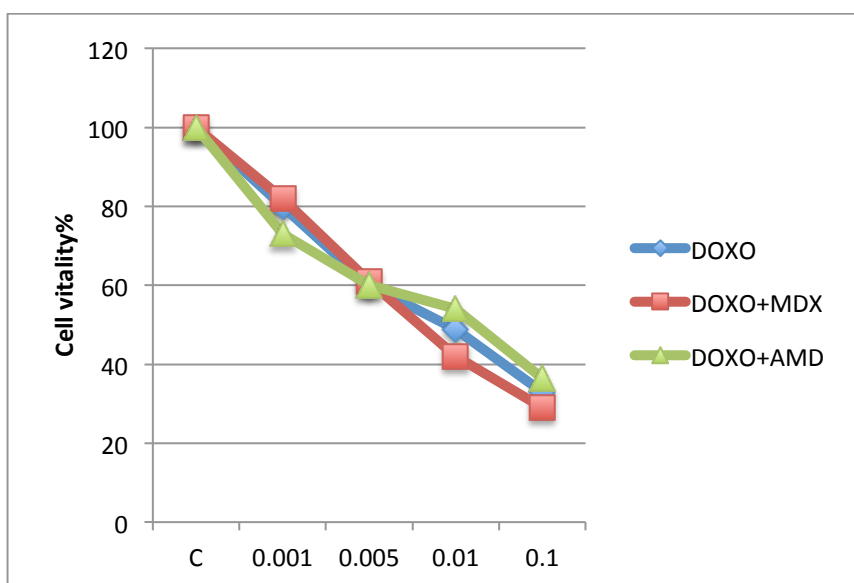
Figure 14. U2OS apoptosis after treatment with CXCR4 inhibitors



5.2.8 - Doxorubicin – CXCR4 inhibitor combined treatments

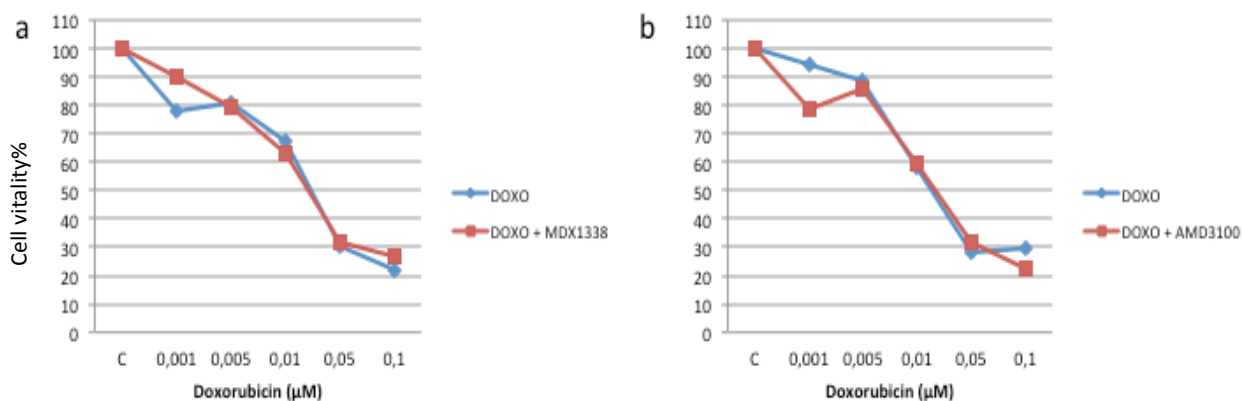
Finally, SW982 and U2OS were exposed to increasing doses of doxorubicin (0.001, 0.005, 0.01, 0.1 $\mu\text{g/ml}$) alone and combined with sub-toxic doses of MDX1338 (0.005 $\mu\text{g/ml}$) and AMD3100 (30 $\mu\text{g/ml}$) for 72h. Data demonstrated that both CXCR4 inhibitors didn't change doxorubicin activity in terms of cell vitality on SW982 cells, with overlapping IC₅₀ values of doxorubicin (0.01 $\mu\text{g/ml}$, 0.0075 $\mu\text{g/ml}$, 0.018 $\mu\text{g/ml}$ respectively), combined with either MDX1338 or AMD3100 (Figure 15).

Fig 15. Cell vitality with combined treatment of doxorubicin and MDX1338 / AMD3100 on SW982 cells



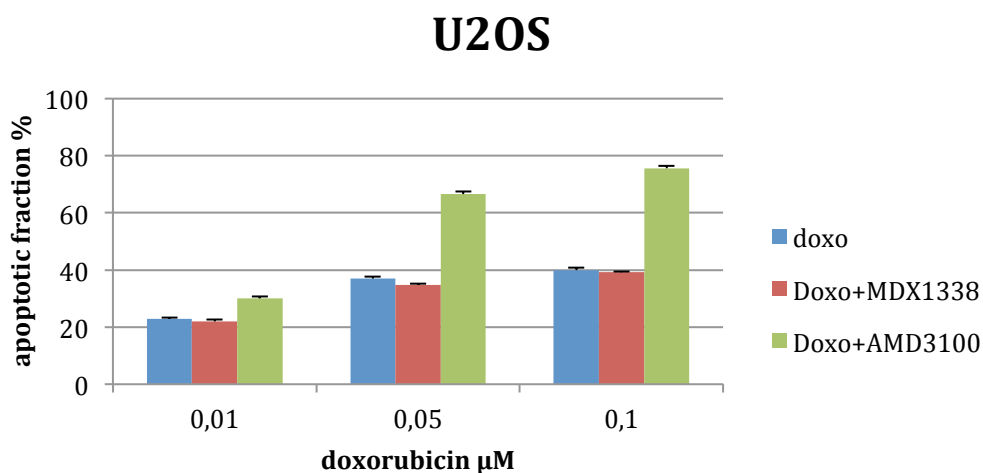
Similarly, U2OS showed similar IC₅₀ values to doxorubicin alone (IC₅₀=0.04), as compared with doxorubicin (Figure 16).

Fig 16. Cell vitality with combined treatment of doxorubicin and a) MDX1338 or b) AMD3100 on U2OS cells



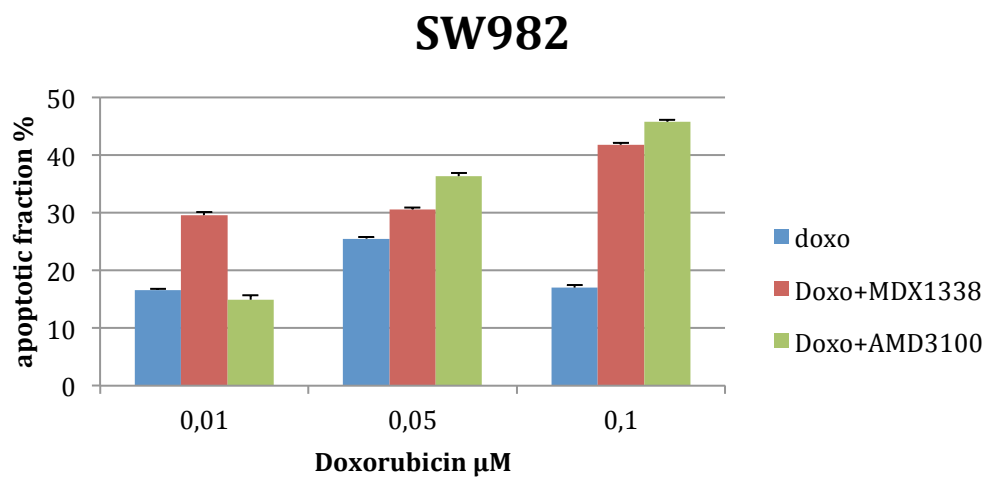
We then assessed if there was synergy between doxorubicin and CXCR4 inhibitors in terms of apoptosis. No significant differences were found in U2OS after 72h of combined treatments with respect to doxorubicin alone at a dose of 0.01 μM, while when the dose of doxorubicin was increased at 0.05 or 0.1 μM, a significant increase of apoptosis was observed with 30 μM of AMD3100 ($p = 0.0005$), but no significant change was observed after combined treatment with MDX1338 (Figure 17).

Figure 17. Percentage of apoptotic cells in U2OS after combined treatment of doxorubicin (blue bar) and MDX1338 (brown) or AMD3100 (green) as compared to doxorubicin alone



On the other hand, when synovial sarcoma SW982 cell lines were exposed to doxorubicin associated with either MDX1338 or AMD3100, the apoptotic fraction increased as compared to apoptosis after doxorubicin alone (Figure 18) ($p=0.0005$).

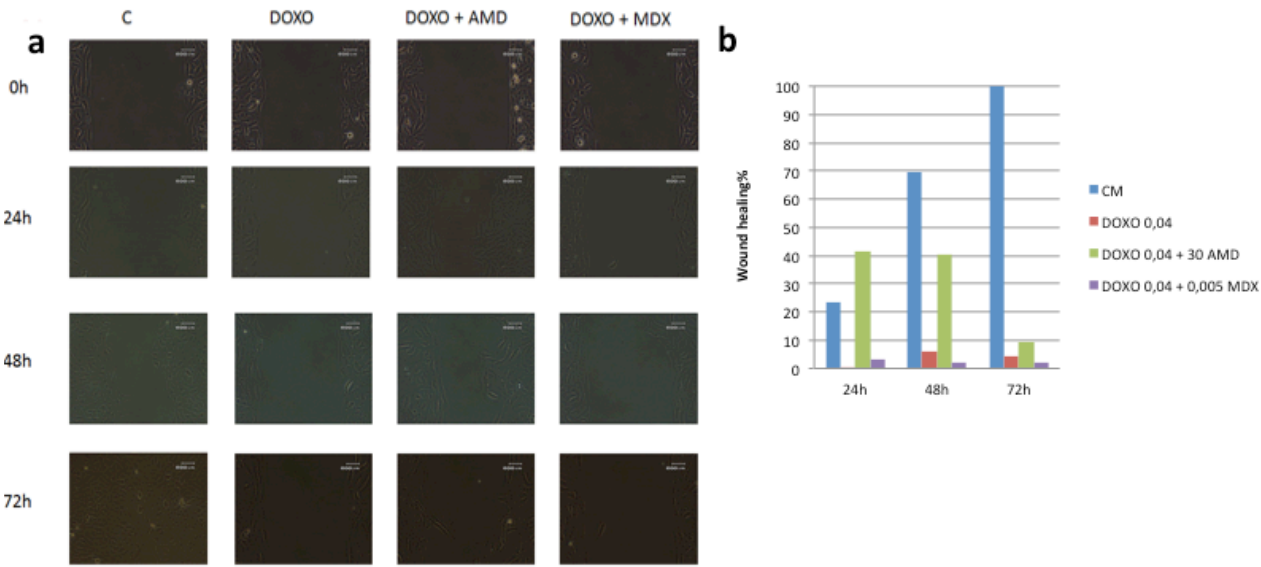
Figure 18. Percentage of apoptotic cells in SW982 after combined treatments



Finally, we assessed the synergy of doxorubicin and CXCR4 inhibitors on migration.

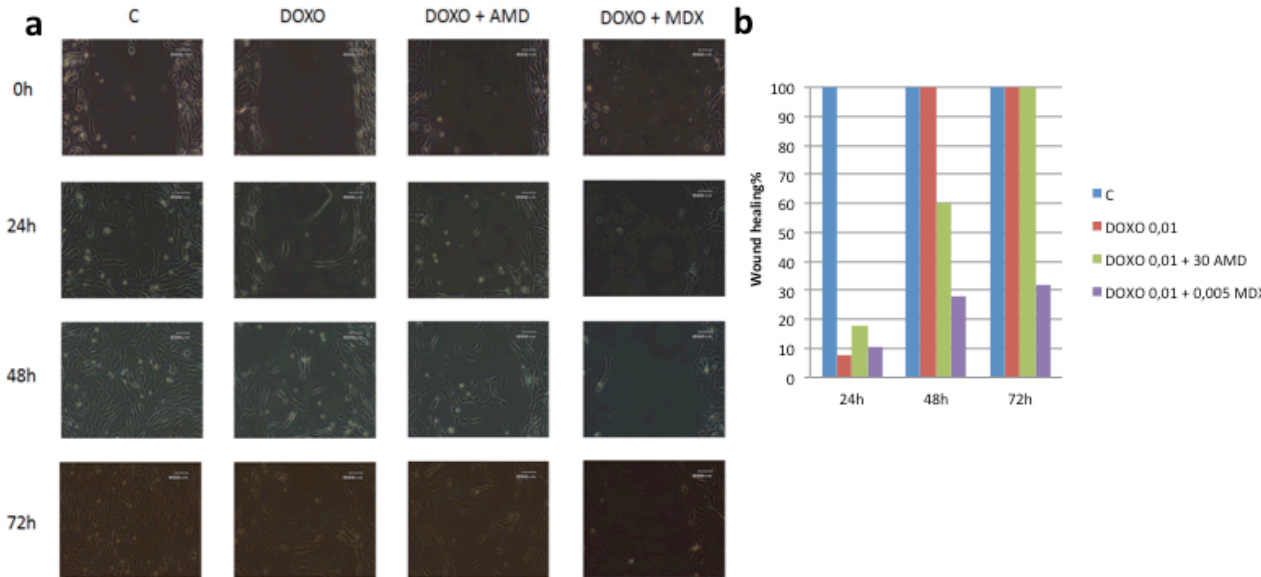
In osteosarcoma, wound healing assay at different time points (24h, 48h, 72h) demonstrated a complete wound closure after 72 hours in osteosarcoma, with similar inhibition with doxorubicin alone or combined treatment with CXCR-4 inhibitors (Figure 19).

Figure 19. U2OS migration after treatment with CXCR4 inhibitors and doxorubicin: a) Image-based monitoring; b) Wound closure expressed as a percentage of the initial wound area that has healed.



On the other hand, wound healing assay at different time points (24h, 48h, 72h) demonstrated a complete wound closure after 24 hours in synovial sarcoma, with synergic inhibition with doxorubicin or CXCR-4 inhibitors at 48 hours, limited to MDX1338 after 72h (Figure 19).

Figure 20. SW982 migration after combined treatment with CXCR4 inhibitors and doxorubicin: a) Image-based monitoring; b) Wound closure expressed as a percentage of the initial wound area that has healed.



6 - DISCUSSION

During the past decade, work that began with the mouse studies by Robert Schreiber, Lloyd Old and colleagues (161-164), and that culminated with the demonstration that infiltrating T cells have a major effect on the clinical attributes of human cancer (165, 166), has changed the field of tumour immunology. Indeed, a recent review by Hanahan and Weinberg included “avoiding immune destruction” as a hallmark of cancer, in addition to the previously established hallmark of tumour-promoting inflammation (113). The potential effect of a patient’s immune system on clinical outcome is not only of academic interest but it also has important implications for the identification of prognostic markers, and markers that predict responses to chemotherapy and radiotherapy.

A demonstration of the effect of the host immune response on tumour invasion, recurrence and metastasis has come from analyses of the in situ immune components and how these are organized within human tumours (25, 27, 29, 30, 33, 34, 37, 39, 42, 44, 46). Indeed, immune infiltrates are heterogeneous between tumour types, and are very diverse from patient to patient.

The aim of this project was to characterize osteosarcoma and synovial sarcoma tumor microenvironment, to assess how the infiltrating immune cells can affect the prognosis of patients and to assess the activity of immune modulating (anti-PD-1), antiangiogenic (anti-VEGFRs, anti-PDGFRs) compounds and migration inhibitors (anti-CXCR4) in a in vitro model of sarcomas.

The role of microenvironment in tumor immune escape is well recognized. Several studies addressed the role of tumor microenvironment in pathobiology and its impact on survival of osteosarcoma (52, 53, 167 – 170), however none is specific for osteosarcoma in the localized stage, nor compared the prognostic power of immune-infiltrate with the other validate prognostic factor routinely used in clinical practice (147).

The present study, including patients with osteosarcoma in a localized stage, and treated within the same protocol (146) demonstrated an independent prognostic role of CD8+ and Tia1 lymphocytes.

The first study demonstrating the association between CD8 infiltrate and cancer specific survival was published in 2001 (39) and similar findings were subsequently confirmed among many histotypes (see paragraph 2.2.2.1, Table 1, ref 25, 27, 29, 30, 33, 34, 37, 39, 42, 44, 46).

In the sarcoma field both a series of 33 osteosarcoma, including metastatic and localised patients (52) and a large soft tissue sarcoma French study, including several histotypes and also low grades lesions, failed to demonstrate a prognostic role for CD8+ lymphocytes (51). The results of our study are in contrast with those data (51, 52); in fact a strong advantage in terms of survival has been observed in patients with CD8+ infiltrate.

To investigate the differentiation state of tumor-infiltrating T cells, tissues were analysed for Tia1 expression, which is a marker of cytotoxic function: the prognostic significance of CD8+ cells was even more relevant when the tumor infiltrate was characterized by the concomitant presence of Tia1+ lymphocytes. Tia1+ lymphocytes might represent a more efficient subset of CD8+ effector cells, playing an important role in immune-surveillance of osteosarcoma (67).

The prognostic role of cytotoxic TILs CD8/Tia1 was also confirmed after induction chemotherapy, while chemotherapy does not seem to induce significant changes in CD8+ TILs: all cases with no CD8+ TILs prior chemotherapy, were confirmed negative after chemotherapy, while a slight increase on score severity (1 to 2/3) was observed.

In our study, the rate of PD-L1 expression in IC was 14%. Previous studies on osteosarcoma samples reported a higher rate of positive expression of PD-L1(IC) ranging from 25% (49) to 74% (70). This difference might be related to the heterogeneity of the cases examined, being many of them metastatic, while our patients all had localized disease. In fact, it is well known that PD-L1 expression increases in advanced stages of the diseases as reported by Sundara Y et al: 13% in primary tumours, 25% in local relapses tissue and 48% in metastatic ($p = 0.002$) (167).

In our study a trend towards an inferior survival for positive PD-L1(IC) patients was observed. Other reports were able to demonstrate a significantly inferior event-free-survival (EFS) for osteosarcoma patients with positive PD-L1(IC) (52). A prognostic role for PD-L1 was also confirmed by Kim et al, at RNA level (67). Interestingly, in our series, the PD-L1(IC) expression has a prognostic significance at multivariate analysis in the subgroup of patients with CD8+ immune-infiltrate. It might be hypothesised that “PD-L1”-mediated immune-suppression negatively influences CD8+ lymphocytes function (see in paragraph 2.2.1 Figure 1). In addition, it was shown that tumor response to PD-L1/PD-1 inhibition is directly related to both the level of PD-L1 expression and lymphocytic infiltration of the tumor (148, 171 – 173).

None of the patients had PD-L1 on tumor cells, as shown for other histotypes, such as colon rectal and gastric carcinoma (174, 175). About 7% of osteosarcoma presented PD-L1 in the neoplastic clone in the study by Koirala et al (52), while head and neck squamous cell carcinoma, melanoma, breast and kidney cancer frequently express PD-L1 on the surface of tumour (148, 176). Such variable expression among different studies may reflect the variable susceptibility of tumour cells and infiltrating immune cells to cytokines and other stromal factors in the tumour milieu (59). In fact there are two distinct type of PD-L1 expression: the first is a *constitutive (innate)* expression on

tumoral cells membranes, with an homogenous patter; the second is *adaptative*, and can be found both on tumoral cells or in macrophage (59).

In 67% of the cases we found CD163+ macrophages in microenvironment. CD163 was shown to be a useful marker for M2-like macrophages, which have a “pro-tumoral” activity, in contrast with M1-like macrophages characterized by a “tumoricidal” activity (26)

In our series no difference in survival according with presence of TAMs, characterized by both CD163 and CD68 expression, was observed (CD163+ 81% vs. CD163- 56%, $p = 0.17$), while in other osteosarcoma series a prognostic role of TAMs was suggested (168, 169). This might be explained by different statistical analysis design and different stages of patients included (168, 169).

Our data suggest a role of immune-infiltrate in progression of localized osteosarcoma, and might support the use of immune-modulating agents in the treatment of this tumor. Of interest, mifamurtide, a modulator of innate immunity, which increases a wide variety of immunomodulatory molecules (177) and favours CD8 and NK cell activation (178), has been approved by EMA for the treatment of patients with localized high-grade osteosarcoma based on the results of a randomized trial (179).

Specific data on immune infiltrate and synovial sarcoma were lacking till recently (180, 181), and the number of patient with synovial sarcoma included, 22 (180) and 29 cases (181), is relatively small. Our series, including 88 patients with localized synovial sarcoma, demonstrated low proportion of cases with PD-1 and PD-L1 expression, both on tumor and on immune cells, and high CD3/CD8 expression, similarly to D’ Angelo et al. CD8 TILs had not prognostic impact in our series, while in the sub-group of patients treated with surgery and no adjuvant chemotherapy, cases CD8⁺ had best

outcome (all alive at 10-years). While we have no reason for this, similar findings on synovial sarcoma were recently published (180, 181). The presence of high levels of CD8⁺ lymphocytes in the tumor correlated with a worse metastases-free survival (MFS) and showed a trend towards worse EFS in a report on 22 cases by van Erp AEM et al. (180). Furthermore, Nowicki et al. showed an association for CD8 with worse progression-free survival (PFS), in addition to worse PFS for PD-1 expression in the tumor-invasive margins, in 29 patients with synovial sarcoma (181).

Overall, expression of immune checkpoint could be a positive prognostic marker in osteosarcoma, and a negative prognostic marker in synovial sarcoma. Further research into the synovial sarcoma immune context might help in immunotherapeutic approach to this histotype.

Immunotherapy for treatment of cancer has been always a fascinating topic. Immune cells are initially attracted to tumor cells by the presence of tumor specific antigens. Cancers with higher mutational loads present greater numbers of tumor specific neoantigens and are frequently associated with robust immune infiltration (182)

Osteosarcoma demonstrates significant genetic complexity, with the majority of tumors displaying loss of both p53 and RB (183), In addition, 33% of primary osteosarcoma shows evidence of chromothripsis, or chromosome shattering (184) and over 50% exhibit kataegis, or localized areas of hypermutation (185). The high mutational load in osteosarcoma, along with the regular interaction between immune cells and bone cells in normal tissue, suggests that osteosarcoma may be an immunogenic tumor and evasion of the immune response may be an important component of its pathogenesis.

Several studies addressed the role of NY-ESO-1 in synovial sarcoma and recently, in a panel of 108 synovial sarcoma positivity for NY-ESO-1, PRAME, MAGEA4 was confirmed in the majority of the cases (186).

Although previous studies have suggested a potential role for immune cells in osteosarcoma, to date no study has provided an in vitro model to assess checkpoint inhibitors in sarcoma.

Vascular endothelial growth factor (VEGF), v-akt murine thymoma viral oncogene homolog (AKT), platelet-derived growth factor (PDGF), mitogen-activated protein kinase (MAPK), are variably expressed in osteogenic sarcoma, and were found to be a critical signalling pathway for osteosarcoma growth (187,188). In vitro and in vivo preclinical activity of multi-TKI such as sunitinib and sorafenib was demonstrated (189,190).

Sunitinib might exert its immunostimulatory activity through the modulation of the ratio of immunostimulatory versus immunoregulatory cells. In fact, In addition to its pro-angiogenic function, VEGF has immunomodulating properties, which include increasing the influx of lymphocytes and DCs into the tumour, while decreasing the intratumoural frequencies of TReg cells and myeloid-derived suppressor cells (MDSCs) (191,192).

We sought to analyse the combined effect of sunitinib and nivolumab in sarcoma cell lines. Sunitinib was able to inhibit proliferation in synovial sarcoma and osteosarcoma cell lines, with best result obtained after 72 h with 10 μ M sunitinib. These results are similar to those observed in other studies with gliomas (193) and osteosarcomas (194).

We addressed the expression rate of PD-L1 in sarcomas cell lines: the range of expression was wide, from 20% to 40% for synovial sarcoma, and from 20 to 80% for osteosarcoma. It was recently reported that the expression of programmed PD-L1 in the immune component increased with pazopanib therapy, while CD8 expression decreased (195).

It is unclear if the same happens with sunitinib (196,197), but at least in one case report PD-L1 tumor expression by immunohistochemistry was higher in the post- sunitinib tumor tissue sample, as compared with pre-sunitinib tumor tissue sample, the number of stained tumor cells (198).

We showed that sunitinib was able to immunomodulate the expression of PD-L1 in 3 out of 4 cell lines assessed, with a dose-dependent up-regulation for the osteosarcoma cell line SaOS-2. We also demonstrate dose-dependent cell death in osteosarcoma cells and synovial sarcoma cell lines treated with sunitinib, with a significant increase observed with lower concentration (10 μ M) for osteosarcoma MG-63 cell line and 100% apoptotic rate at 30 μ M; on the other hand synovial sarcoma required higher concentration (20 μ M) and were only partially sensitive to sunitinib treatment.

We then assessed the effect of nivolumab and we were able to demonstrate that nivolumab /PD-1 blockade might hamper sarcoma tolerance, by decreasing PD-1 expression: in fact, coculturing PD-L1-positive sarcoma cell lines and lymphocyte we induced PD-1 expression on lymphocyte; after nivolumab PD-1 was reduced. Notably, we identified a subgroup of *activated* lymphocytes and found that this sub-population of lymphocytes was specifically sensitive to nivolumab PD-1 induced immune-modulation, with PD-1 expression completely abolished after treatment with nivolumab. We are planning to further characterize these activated lymphocytes to assess their potential role in

predicting response to nivolumab treatment.

Trial addressing the immune-modulator effect of sunitinib combined with nivolumab in metastatic renal cell carcinoma (mRCC) were performed, and compared to pazopanib combination (199) mRCC patients (≥ 1 prior systemic therapy) received nivolumab in combination with sunitinib (50 mg, 4 weeks on, 2 weeks off) or pazopanib (800 mg daily), until progression or unacceptable toxicity.

Responses were seen, by first assessment (6 weeks), in 56% and 41% of pazopanib/nivolumab and sunitinib/nivolumab respectively (199). PFS rate at 24 weeks was 78% for sunitinib arm and 55% for pazopanib arm, while in a non-inferiority phase II trial in renal carcinoma (200) response rates of 31% and 24% for pazopanib and sunitinib respectively, were reported, suggesting that nivolumab might be synergic with TKI in the context of kidney cancer. Only recently, a phase I-II trial addressing the impact of immune modulation on the efficacy of sunitinib via its potential synergy with anti PD-1 in the context of sarcomas (<https://clinicaltrials.gov/ct2/show/NCT03277924>) and will enrol soft tissue sarcoma and bone sarcomas. In particular, high grade soft tissue sarcoma will be included. It might be anticipated that some histotypes such as undifferentiated pleomorphic sarcoma (UPS) and synovial sarcoma might be more sensitive to this approach, being more frequently diagnosed in patients immune-suppressed due to transplant (201) and proven sensitive to pazopanib in the PALETTE phase III trial (202).

The rationale of using nivolumab in bone sarcoma includes anecdotal report of spontaneous regression in osteosarcoma (203) and genomic instability described for both osteosarcoma (204) and Ewing sarcoma (205, 206). It is in fact well known that numeric alterations of the PD-1 ligand loci (207), higher neoantigen burden, and DNA repair pathway mutations (208) might increase sensitivity to immune-treatment. Nevertheless, data of the SARC28 trial, on the use of

pembrolizumab monotherapy both in bone and in soft tissue sarcoma are disappointing, with the exception of specific histotypes such as undifferentiated pleomorphic sarcoma or dedifferentiated liposarcoma (105). Enrolment to expanded cohorts of those subtypes is ongoing to confirm and characterize the activity of pembrolizumab in sarcoma.

Therefore it is important to find way to enhance response to immune-modulator and to identify predictive factors of response. For example, it was demonstrated that melanoma patients express higher levels of PD-L1 on circulating T cells than healthy volunteers, and higher PD-L1 expression together with CD137 expression on blood CD8+ T cells predicts sensitivity to the combination of anti-CTLA-4+ anti-PD-1 treatment (209).

Characterize peripheral blood lymphocytes changes over sunitinb and nivolumab treatment and studying CD8/PD-L1 co-expression might help to guide treatment in this difficult setting. In this contest, the Immune Biomarkers Task Force of the Society for Immunotherapy of Cancer (SITC), an international multidisciplinary panel of experts, proposed guidelines on predictors of response to immunotherapy, focusing on the complexity of the tumor microenvironment, with its diversity of immune genes, proteins, and pathways naturally present at baseline and in circulation (210).

In the last experiment of our project, ongoing, DCs pulsed with synovial sarcoma and osteosarcoma cell lines *pre-treated* with sunitinib will be cocultured with lymphocytes and ability of nivolumab to ambrogate PD-1 expression will be compared to that of nivolumab on lymphocytes cocultured with DCs pulsed with untreated cell lines.

Last, we addressed the role of stromal cell-derived factor 1 (SDF-1 or CXCL12) and its receptor chemokine receptor 4 (CXCR4) in sarcoma progression. Metastasis is in fact a highly organized

process and various molecular families are involved in cancer metastases and with tumor-stroma interactions, or tumor microenvironment interaction. The tumor microenvironment consists of resident non-cancerous cells (stromal fibroblasts, endothelial cells and immune cells), connective tissue and extracellular matrix, altogether supporting tumor structure, angiogenesis and growth.

Mounting evidence indicates that chemokines and their specific receptors play a vital role in organ-specific metastasis. SDF-1 or CXCL12 and its receptor CXCR4 have been extensively studied and are involved in tumorigenicity, proliferation, metastasis and angiogenesis in multiple human cancers (211-215).

CXCR4 antagonist can block CXCR4/ SDF-1 interaction and has been shown effective in inhibiting tumor cell metastasis by targeting various pathways (140-145,216). But there are few studies about the combined effect of CXCR4 antagonist and chemotherapy on sarcoma cells survival and growth.

To confirm the positive effect of SDF-1-CXCR4 axis on sarcoma survival and metastasis, we first measured the expression of CXCR4 and SDF-1 in several osteosarcoma and synovial sarcoma cell lines. We showed that the expression of CXCR4 and SDF-1 were varying in different cell lines and no obvious correlation was found between the expression of CXCR4 and SDF-1 (CXCL12).

This is in contrast with other studies on chronic lymphocytic leukemia (CLL), showing no expression of CXCL12 by flow cytometry and CXCL12 gene expression by RT-PCR was also negative in the large majority of samples (216), while it confirmed other recent findings on osteosarcoma (217). This difference might reflect histotype-specific homing pathway and suggests that, unlike in sarcomas, in CLL the activation of CXCR4 induced by CXCL12 occurs either by cell-cell interactions with non-leukemia CXCL12 expressing cells, likely located in lymphatic tissues, or mediated by soluble CXCL12. Also, inverse correlation for CXCR4 expression at gene and protein level was noted,

with osteosarcoma cell line U2OS presenting low expression of CXCR4 m-RNA and 98% positivity for protein FACS analysis, while synovial sarcoma (SYO-1 cell line) presented high levels of CXCR-4 mRNA and only 12% protein expression.

Several studies have reported that BM-MSCs, which are known to be involved in tissue homeostasis and regeneration can be recruited into primary tumors and become active components of the tumor microenvironment, such as cancer-associated fibroblasts (CAFs) (218,219) BM-MSCs contribute to tumor cell growth and metastatic behavior in a variety of cancers, including breast (220), colon cancer (221) and osteosarcoma (222-225).

In a study by Fontanella et al, the role of BM-MSCs in promoting growth, migration and invasion was addressed in osteosarcoma and hepatocellular carcinoma cell lines demonstrating that when these cell lines were treated for 24h with conditioned medium from BM-MSCs, a significant increase was observed in CXCR4 mRNA and protein levels was observed (226). We demonstrated that levels of SDF-1 (CXCL12) protein was higher in BM-MSC-CM, when compared to α MEM alone, or α MEM supplemented with 25% BM-MSC (see in paragraph 5.3.2 Table 3). Therefore we used BM-MSC-CM to test the activity of CXCR4 inhibitors.

As a noncompetitive CXCR4 inhibitor, AMD3100 can block the SDF-1-CXCR4 axis. The inhibition effect of AMD3100 on migration, invasion and metastasis of various cancer cells has been confirmed by a large amount of experimental researches (227).

Ulocuplumab (BMS-936564)/MDX1338 is a first in class, fully human IgG4 monoclonal antibody that has been engineered to specifically bind to CXCR4 (228). In vitro studies have shown that Ulocuplumab (BMS-936564) has a potent anti-tumor activity in established tumor including AML, NHL, and multiple myeloma xenograft models (228).

However, researches focused on the effect of AMD3100 and MDX1338 on migration, and data on proliferation and apoptosis are scarce.

Furthermore, CXCR4 expression seems to play a role in resistance to chemotherapy in synovial sarcoma (124) and this is the first study addressing SDF1-CXCR4 axis role in this histotypes.

We speculated that AMD3100 and MDX1338 may have strong activity in osteosarcoma and synovial sarcoma *in vitro* and that the activity was synergic with chemotherapy. The results of our *in vitro* experiments showed that treatment with MDX1338 and AMD3100 was able to reduce SW983 and U2OS proliferation, without changing CXCR4 expression in sarcoma cell lines.

Also, this study confirmed that both drug were able to reduce SW982 and U2OS cells migration. The ability to induce apoptosis was confirmed when drugs were employed alone (Figure 13), especially after 72 h.

Combined treatment with doxorubicin and MDX1338 /AMD3100 was not synergic, with over-imposable curves in terms of cell vitality.

The apoptotic rate was no significantly different after 72h of combined treatments doxorubicin + MDX1338, with respect to doxorubicin alone, while a slight increase only after doxorubicin with AMD3100 was observed, although this difference was not significant.

In conclusion, our results showed AMD3100/MDX1338 could effectively induce apoptosis and inhibition of proliferation and invasion of osteosarcoma and synovial sarcoma cells.

When combined with chemotherapy, CXCR4 inhibitors did not increase proliferation inhibition, while AM3100 combined with doxorubicin (not MDX1338) was able to increase apoptosis as compared to doxorubicin monotherapy in osteosarcoma cell lines. Also, both AM3100 and

MDX1338, demonstrated synergic activity in synovial sarcoma cell line SW982, when doxorubicin was employed at a dose of 0.1 µM.

Last, in synovial sarcoma, inhibition of migration was significantly increased when doxorubicin was combined with CXCR4 inhibitors, as compared to doxorubicin alone.

Among several CXCR4 inhibitors, Plerixafor (AMD3100), already approved for poor mobilizer patients in bone marrow transplant program, has reached clinical testing.

For instance, phase I-II trial with chemotherapy combined with Plerixafor, or other CXCR4 inhibitors are ongoing (Table 1), and will confirm the potential chemosensitizing effect of this approach in several hematologic and solid tumors, including Ewing sarcoma.

Table 1. Ongoing clinical trials with CXCR4 inhibitors in hematologic malignancies and in solid tumors

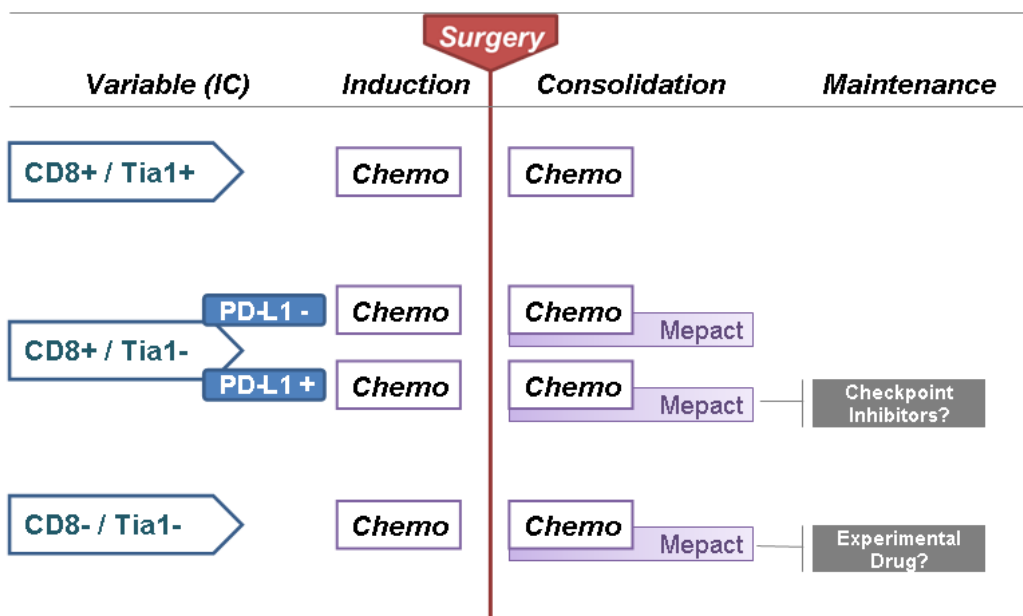
<i>Drug name</i>	<i>Mechanism of action</i>	<i>Indication</i>	<i>Phase</i>	
HEMATOLOGIC MALIGNANCIES				
AMD3100 + Cytarabine and Daunorubicin	CXCR4 inhibitor	Newly acute myeloid leukaemia	1	NCT00990054
AMD3100 + vinorelbine	CXCR4 inhibitor	Myeloma/leukaemia	2	NCT01220375
AMD3100 + azacitidine	CXCR4 inhibitor	Myelodysplastic syndrome	1	NCT01065129
AMD3100 + sorafenib	CXCR4 inhibitor	Acute myeloid leukaemia pt with FLT3 mutations	1	NCT00943943
AMD3100 + retuximab	CXCR4 inhibitor	CLL and small lymphocytic leukaemia; Lymphoma NHL/MM;	1,2 1,2	NCT00694590 NCT00444912
AMD3100 + bortezomib	CXCR4 inhibitor	Relapsed MM	1,2	NCT00903968
MDX-1338 + Cytarabine	CXCR4 inhibitor	Newly acute myeloid leukaemia	1,2	NCT02305563
SOLID TUMOURS				
MSX-122	CXCR4 inhibitor	Refractory metastatic or locally advanced solid tumours	1	NCT00591682
AMD3100	CXCR4 inhibitor	With bevacizumab in glioblastoma Ewing sarcoma, neuroblastoma, brain tumours	1 1,2	NCT01339039 NCT01288573
AMD3100	CXCR4 inhibitor	Advanced pancreatic, ovarian and clorectal Cancers	1,2	NCT02179970

Chronic lymphoid leukaemia; MM multiple myeloma, NHL Non Hodgkin lymphoma

7 - CONCLUSIONS

In conclusion, CD8/Tia1 cytotoxic T-lymphocytes emerge as an important mediator of the anti-tumor immune response. Also, this study highlights the prognostic role of tumor microenvironment in the setting of localized osteosarcoma. The data are intriguing, but a clinical application requires confirmations in other series in order to use immune-stratification to plan treatment strategy (Figure 4).

Figure 4. Proposal for ‘Immune-infiltrate based treatment algorithm’ for localized osteosarcoma.



Effort to standardize immune-infiltrate scoring system, including PD-L1 thresholds, CD8 density and location (invasive margin versus central tumor) are ongoing, and an international consortium has been initiated to validate and promote the *Immunoscore* in routine clinical settings (229). The results of this international consortium may result in the implementation of the *Immunoscore* as a prognostic tool, designated TNM-I (TNM-Immune), and might also serve to guide design predictive study to immunotherapeutics.

In the era of immunotherapy, modulation of immune response with chemotherapy or anti-VEGF

targeted compound represent an important area of research.

Tumor - stroma interaction has emerged as an important player of chemotherapy resistance and possibly with immune-resistance, since the administration of a CXCR4 inhibitor was synergic with α -PD-L1 antibody in a mice model of pancreatic cancer (230).

Effort to better combine tumor-targeted agent with microenvironment target drugs might represent the key to increase the survival plateau reached for many aggressive solid tumors, including sarcomas.

8 – BIBLIOGRAPHY

1. Marina N, Smeland S, Bielak SS et al. Comparison of MAPIE versus MAP in patients with a poor response to preoperative chemotherapy for newly diagnosed high-grade osteosarcoma (EURAMOS-1): an open-label, international, randomised controlled trial. *Lancet Oncol.* 2016;17(10):1396-1408.
2. Picci P, Manfrini M, Fabbri N, et al. Atlas of musculoskeletal tumors and tumorlike lesions. The Rizzoli Case Archive. Eds. 2014. Springer International Publishing
3. Klein MJ, Siegal GP. Osteosarcoma: anatomic and histologic variants. *Am J Clin Pathol.* 2006 Apr;125(4):555-81.
4. Raymond AK, Jaffe N. Osteosarcoma multidisciplinary approach to the management from the pathologist's perspective. *Cancer Treat Res.* 2009;152:63-84.
5. Raymond AK, Jaffe N. Conditions that mimic osteosarcoma. *Cancer Treat Res.* 2009;152:85-121.
6. Picci P. Osteosarcoma (osteogenic sarcoma). *Orphanet J Rare Dis.* 2007 Jan 23;2:6.
7. Patel SR, Vadhan-Raj S, Papadopolous N, et al. High-dose ifosfamide in bone and soft tissue sarcomas: results of phase II and pilot studies--dose-response and schedule dependence. *J Clin Oncol.* 1997;15:2378-2384.
8. Palmerini E, Jones RL, Marchesi E, et al. Gemcitabine and docetaxel in relapsed and unresectable high-grade osteosarcoma and spindle cell sarcoma of bone. *BMC Cancer.* 2016;16:280
9. Duffaud F, Egerer G, Ferrari S, et al. A phase II trial of second-line pemetrexed in adults with advanced/metastatic osteosarcoma. *Eur J Cancer.* 2012;48:564-570.

10. Grignani G, Palmerini E, Dileo P, et al. A phase II trial of sorafenib in relapsed and unresectable high-grade osteosarcoma after failure of standard multimodal therapy: an Italian Sarcoma Group study. *Ann Oncol.* 2012;23:508-516.
11. Grignani G, Palmerini E, Ferraresi V, et al. Italian Sarcoma Group. Sorafenib and everolimus for patients with unresectable high-grade osteosarcoma progressing after standard treatment: a non-randomised phase 2 clinical trial. *Lancet Oncol.* 2015;16:98-107.
12. Picci P, Mercuri M, Ferrari S, et al. Survival in high-grade osteosarcoma: improvement over 21 years at a single institution. *Ann Oncol.* 2010 Jun;21(6):1366-73.
13. Bixby SD, Hettmer S, Taylor GA, Voss SD.: Synovial sarcoma in children: imaging features and common benign mimics. *AJR Am J Roentgenol.* 2010 Oct;195(4):1026-32.
14. O'Sullivan PJ, Harris AC, Munk PL.: Radiological features of synovial cell sarcoma. *Br J Radiol.* 2008 Apr;81(964):346-56.
15. Cai W, Sun Y, Wang W, Han C, Ouchida M, Xia W, Zhao X, Sun B.: The Effect of SYT-SSX and Extracellular Signal-Regulated Kinase (ERK) on Cell Proliferation in Synovial Sarcoma. *Pathol Oncol Res.* 2011, 17: 357-367.
16. Palmerini E, Staals EL, Alberghini M, et al. Synovial sarcoma: retrospective analysis of 250 patients treated at a single institution. *Cancer.* 2009 Jul 1;115(13):2988-98.
17. Palmerini E, Paioli A, Ferrari S. Emerging therapeutic targets for synovial sarcoma. *Expert Rev Anticancer Ther.* 2014
18. Kkravasilis V, Seddon BM, Ashley S, et al. Significant clinical benefit of first-line 16. palliative chemotherapy in advanced soft-tissue sarcoma: retrospective analysis and

- identification of prognostic factors in 488 patients. *Cancer* 2008;112:1585-91
19. van der Graaf WT, Blay JY, Chawla SP, et al. Pazopanib for metastatic soft-tissue sarcoma (PALETTE): a randomised, double-blind, placebo-controlled phase 3 trial. *Lancet*. 2012 19;379(9829):1879-86.
 20. de Visser KE, Eichten A, Coussens LM. Paradoxical roles of the immune system during cancer development. *Nature Reviews Cancer*, vol. 6, no. 1, pp. 24–37, 2006.
 21. Medzhitov R, Janeway Jr CA. Innate immunity: the virtues of a nonclonal system of recognition. *Cell*, vol. 91, no. 3, pp. 295–298, 1997.
 22. Kaech SM, Hemby A, Kersh E, et al. Molecular and functional profiling of memory CD8 T cell differentiation. *Cell*, vol. 111, no. 6, pp. 837–851, 2002.
 23. Galon J, Fridman WH, Pages F. The adaptive immunologic microenvironment in colorectal cancer: a novel perspective. *Cancer Res* 2007; 67:1883–1886.
 24. Mantovani A, Allavena P, Sica, et al. Cancer-related inflammation. *Nature* 2008;454:436–444.
 25. Dieu-Nosjean, M. C. et al. Long-term survival for patients with non-small-cell lung cancer with intratumoral lymphoid structures. *J. Clin. Oncol* 2008;26:4410–4417.
 26. Balkwill F, Mantovani A. Inflammation and cancer: back to Virchow? *Lancet* 2001;357:539–545.
 27. Galon J et al. Type, density, and location of immune cells within human colorectal tumors predict clinical outcome. *Science* 2006;313:1960–1964.
 28. Fridman WH, Pagès F, Sautès-Fridman C, Galon, J. The immune contexture in human tumours: impact on clinical outcome. *Nat. Rev. Cancer* 2012;12:298–306.
 29. Clark, W. H. Jr. et al. Model predicting survival in stage I melanoma based on tumor progression. *J. Natl Cancer Inst.* 81, 1893–1904 (1989).

30. Tefany, F. J., Barnetson, R. S., Halliday, G. M., McCarthy, S. W. & McCarthy, W. H. Immunocytochemical analysis of the cellular infiltrate in primary regressing and non-regressing malignant melanoma. *J. Invest. Dermatol.* 97, 197–202 (1991).
31. Ladanyi, A. et al. FOXP3+ cell density in primary tumor has no prognostic impact in patients with cutaneous malignant melanoma. *Pathol. Oncol. Res.* 16, 303–309 (2010).
32. Miracco, C. et al. Utility of tumour-infiltrating CD25+FOXP3+ regulatory T cell evaluation in predicting local recurrence in vertical growth phase cutaneous melanoma. *Oncol. Rep.* 18, 1115–1122 (2007).
33. Badoual, C. et al. Prognostic value of tumor-infiltrating CD4+ T-cell subpopulations in head and neck cancers. *Clin. Cancer Res.* 12, 465–472 (2006).
34. Mahmoud, S. M. et al. Tumor-infiltrating CD8+ lymphocytes predict clinical outcome in breast cancer. *J. Clin. Oncol.* 29, 1949–1955 (2011).
35. Mahmoud, S. M. et al. An evaluation of the clinical significance of FOXP3+ infiltrating cells in human breast cancer. *Breast Cancer Res. Treat.* 127, 99–108 (2011).
36. Bates, G. J. et al. Quantification of regulatory T cells enables the identification of high-risk breast cancer patients and those at risk of late relapse. *J. Clin. Oncol.* 24, 5373–5380 (2006).
37. Nakakubo, Y. et al. Clinical significance of immune cell infiltration within gallbladder cancer. *Br. J. Cancer* 89, 1736–1742 (2003).
38. Winerdal, M. E. et al. FOXP3 and survival in urinary bladder cancer. *BJU Int.* 108, 1672–1678 (2011).
39. Zhang L, Conejo-Garcia JR, Katsaros D, et al. Intratumoral T cells, recurrence, and survival in epithelial ovarian cancer. *N Engl J Med* 2003; 348:203–213.
40. Leffers, N. et al. Prognostic significance of tumor-infiltrating T-lymphocytes

- in primary and metastatic lesions of advanced stage ovarian cancer. *Cancer Immunol. Immunother.* 58, 449–459 (2009).
41. Curiel, T. J. et al. Specific recruitment of regulatory-T cells in ovarian carcinoma fosters immune privilege and predicts reduced survival. *Nature Med.* 10, 942–949 (2004).
 42. Schumacher, K., Haensch, W., Roefzaad, C. & Schlag, P. M. Prognostic significance of activated CD8+ T cell infiltrations within esophageal carcinomas. *Cancer Res.* 61, 3932–3936 (2001).
 43. Frey, D. M. et al. High frequency of tumor-infiltrating + FOXP3 regulatory T cells predicts improved survival in mismatch repair-proficient colorectal cancer patients. *Int. J. Cancer* 126, 2635–2643 (2010).
 44. Nakano, O. et al. Proliferative activity of intratumoral CD8+ T-lymphocytes as a prognostic factor in human renal cell carcinoma: clinicopathologic demonstration of antitumor immunity. *Cancer Res.* 61, 5132–5136 (2001).
 45. Jensen, H. K., Donskov, F., Nordmark, M., et al. Increased intratumoral FOXP3-positive regulatory immune cells during interleukin-2 treatment in metastatic renal cell carcinoma. *Clin. Cancer Res.* 15, 1052–1058 (2009).
 46. Karja, V. et al. Tumour-infiltrating lymphocytes: a prognostic factor of PSA-free survival in patients with local prostate carcinoma treated by radical prostatectomy. *Anticancer Res.* 25, 4435–4438 (2005).
 47. Petersen, R. P. et al. Tumor infiltrating Foxp3+ regulatory T-cells are associated with recurrence in pathologic stage I NSCLC patients. *Cancer* 107, 866–2872 (2006).
 48. Fukunaga, A. et al. CD8+ tumor-infiltrating lymphocytes together with CD4+ tumor-infiltrating lymphocytes and dendritic cells improve the prognosis of patients with pancreatic adenocarcinoma. *Pancreas* 28, e26–e31 (2004).

49. Hiraoka, N., Onozato, K., Kosuge, T., Hirohashi, S. Prevalence of FOXP3+ regulatory T cells increases during the progression of pancreatic ductal adenocarcinoma and its premalignant lesions. *Clin. Cancer Res.* 12, 5423–5434 (2006).
50. Heimberger, A. B. et al. Incidence and prognostic impact of FoxP3+ regulatory T cells in human gliomas. *Clin. Cancer Res.* 14, 5166–5172 (2008).
51. Toulmonde M, Adam J, Bessedé A et al. Integrative assessment of expression and prognostic value of PDL1, IDO, and kynurenine in 371 primary soft tissue sarcomas with genomic complexity. *J Clin Oncol* 2016; 34: (suppl; abstr 11008).
52. Koirala P, Roth ME, Gill J et al. Immune infiltration and PD-L1 expression in the tumor microenvironment are prognostic in osteosarcoma. *Sci Rep* 2016; 6:30093.
53. Gomez-Brouchet A, Illac C, Gilhodes, et al. CD163-positive tumor-associated macrophages and CD8-positive cytotoxic lymphocytes are powerful diagnostic markers for the therapeutic stratification of osteosarcoma patients: An immunohistochemical analysis of the biopsies from the French OS2006 phase 3 trial. *Oncoimmunology* 2017;6(9).
54. Tumeh PC, Harview CL, Yearley JH, et al. PD-1 blockade induces responses by inhibiting adaptive immune resistance. *Nature*. 2014;515(7528):568-571.
55. Dong, H., Zhu, G., Tamada, K. & Chen, L. B7-H1, a third member of the B7 family, co-stimulates T-cell proliferation and interleukin-10 secretion. *Nat. Med.* 5, 1365–1369 (1999).
56. Dong, H. et al. Tumor-associated B7-H1 promotes T-cell apoptosis: a potential mechanism of immune evasion. *Nat. Med.* 8, 793–800 (2002).
57. Mazanet, M. M. & Hughes, C. C. B7-H1 is expressed by human endothelial cells and suppresses T cell cytokine synthesis. *J. Immunol.* 169, 3581–3588 (2002).

58. Parsa, A. T. et al. Loss of tumor suppressor PTEN function increases B7-H1 expression and immunoresistance in glioma. *Nat. Med.* 13, 84–88 (2007).
59. Topalian SL, Taube JM, Anders RA, et al. Mechanism-driven biomarkers to guide immune checkpoint blockade in cancer therapy. *Nat Rev Cancer.* 2016 May;16(5):275-87.
60. Taube, J. M. et al. Colocalization of inflammatory response with B7-H1 expression in human melanocytic lesions supports an adaptive resistance mechanism of immune escape. *Sci. Transl Med.* 4, 127ra37 (2012).
61. Cimino-Mathews, A. et al. PD-L1 (B7-H1) expression and the immune tumor microenvironment in primary and metastatic breast carcinomas. *Hum. Pathol.* 47, 52–63 (2016).
62. Lyford-Pike, S. et al. Evidence for a role of the PD-1:PD-L1 pathway in immune resistance of HPV-associated head and neck squamous cell carcinoma. *Cancer Res.* 73, 1733–1741 (2013).
63. Llosa, N. J. et al. The vigorous immune microenvironment of microsatellite instable colon cancer is balanced by multiple counter-inhibitory checkpoints. *Cancer Discov.* 5, 43–51 (2015).
64. Lipson, E. J. et al. Durable cancer regression off-treatment and effective reinduction therapy with an anti-PD-1 antibody. *Clin. Cancer Res.* 19, 462–468 (2013).
65. Thompson, E. D. et al. Patterns of PD-L1 expression and CD8 T cell infiltration in gastric adenocarcinomas and associated immune stroma. *Gut.* 2017 May;66(5):794-801.
66. Taube JM et al. Differential expression of immune-regulatory genes associated with PD-L1 display in melanoma: implications for PD-1 pathway blockade. *Clin. Cancer Res.* 21, 3969–3976 (2015).
67. Kim JR, Moon YJ, Kwon KS, et al. Tumor infiltrating PD1-positive lymphocytes and

- the expression of PD-L1 predict poor prognosis of soft tissue sarcomas. PLoS One 8:e82870, 2013.
68. D'Angelo SP, Shoushtari AN, Agaram NP, et al: Prevalence of tumor-infiltrating lymphocytes and PD- L1 expression in the soft tissue sarcoma microenvironment. Hum Pathol 2015;46:357-65.
69. Movva S, Wen W, Chen W, et al: Multi-platform profiling of over 2000 sarcomas: identification of biomarkers and novel therapeutic targets. Oncotarget 6:12234-47, 2015.
70. Shen JK et al, Programmed Cell Death Ligand 1 Expression in Osteosarcoma. Cancer Immunol Res. 2014;2:690-8.
71. Kostine M, Cleven AH, de Miranda NF, et al, Analysis of PD-L1, T-cell infiltrate and HLA expression in chondrosarcoma indicates potential for response to immunotherapy specifically in the dedifferentiated subtype. Mod Pathol. 2016 Sep;29(9):1028-37
72. Poon RT, Fan ST, Wong J. Clinical implications of circulating angiogenic factors in cancer patients. J Clin Oncol. 2001;19(4):1207-25.
73. Chen D, Mellman I. Oncology meets immunology: the cancer-immunity cycle Immunity 2013;39:1-10
74. Abdeen A, Chou AJ, Healey JH, et al. Correlation between clinical outcome and growth factor pathway expression in osteogenic sarcoma. Cancer. 2009 Nov 15;115(22):5243-50.
75. Mendel DB, Laird AD, Xin X, et al. In vivo antitumour activity of SU11248, a novel tyrosine kinase inhibitor targeting vascular endothelial growth factor and platelet-derived growth factor receptors: determination of a pharmacokinetic / pharmacodynamic relationship. Clin Cancer Res. 2003;9:327–37
76. <https://www.cancer.gov/about-cancer/treatment/drugs/fda-sunitinib-malate>

77. Eberst L, Cropet C, Le Cesne A, et al. The off-label use of targeted therapies in sarcomas: the OUTC'S program. *BMC Cancer*. 2014; 14:870.
78. Mucha P, Świtaj T, Kozak K, et al. Long-term results of therapy with sunitinib in metastatic alveolar soft part sarcoma. *Tumori*. 2017 May 12;103(3):231-235.
79. Italiano A, Kind M, Cioffi A, et al. Clinical activity of sunitinib in patients with advanced desmoplastic round cell tumor: a case series. *Target Oncol*. 2013 Sep;8(3):211-213
80. Stacchiotti S, Pantaleo MA, Astolfi A, et al. Activity of sunitinib in extraskeletal myxoid chondrosarcoma. *Eur J Cancer*. 2014 Jun;50(9):1657-64
81. Kumar RM, Arlt MJ, Kuzmanov A, et al. Sunitinib malate (SU-11248) reduces tumour burden and lung metastasis in an intratibial human xenograft osteosarcoma mouse model. *Am J Cancer Res*. 2015 Jun 15;5(7):2156-68.
82. Farsaci B, Higgins JP, and Hodge JW. Consequence of Dose Scheduling of Sunitinib on Host Immune Response Elements and Vaccine Combination Therapy. *Int J Cancer*. 2012; 130(8): 1948–1959.
83. Yang Z, Zhang B, Li D, et al. Mast cells mobilize myeloid- derived suppressor cells and Treg cells in tumor microenvironment via IL-17 pathway in murine hepatocarcinoma model. *PLoSOne*. 2010; 5:e8922.
84. Finke JH, Rini B, Ireland J, Rayman P, et al. Sunitinib reverses type-1 immune suppression and decreases T-regulatory cells in renal cell carcinoma patients. *Clin Cancer Res*. 2008; 14:6674–82.
85. . Camus, M. et al. Coordination of intratumoral immune reaction and human colorectal cancer recurrence. *Cancer Res*. 69, 2685–2693 (2009).
86. Gabrilovich D I, Ishida T, Nadaf S, et al. Antibodies to vascular endothelial growth factor enhance the efficacy of cancer immunotherapy by improving endogenous

- dendritic cell function. *Clin. Cancer Res.* 5, 2963–2970 (1999).
87. . Adotevi, O. et al. A decrease of regulatory T cells correlates with overall survival after sunitinib-based antiangiogenic therapy in metastatic renal cancer patients. *J. Immunother.* 33, 991–998 (2010).
88. Ko, J. S. et al. Sunitinib mediates reversal of myeloid- derived suppressor cell accumulation in renal cell carcinoma patients. *Clin. Cancer Res.* 15, 2148–2157 (2009).
89. Yang, J. C. et al. A randomized trial of bevacizumab, an anti-vascular endothelial growth factor antibody, for metastatic renal cancer. *N. Engl. J. Med.* 349, 427–434 (2003)
90. Nardin, A. et al. Dacarbazine promotes stromal remodeling and lymphocyte infiltration in cutaneous melanoma lesions. *J. Invest. Dermatol.* 131, 1896–1905 (2011).
91. . Zitvogel, L., Apetoh, L., Ghiringhelli, F. & Kroemer, G. Immunological aspects of cancer chemotherapy. *Nature Rev. Immunol.* 8, 59–73 (2008)
92. Teng, M. W. et al. Conditional regulatory T-cell depletion releases adaptive immunity preventing carcinogenesis and suppressing established tumor growth. *Cancer Res.* 70, 7800–7809 (2010).
93. Hodi, F. S. et al. Improved survival with ipilimumab in patients with metastatic melanoma. *N. Engl. J. Med.* 363, 711–723 (2010).
94. . Waldmann, T. A. Effective cancer therapy through immunomodulation. *Annu. Rev. Med.* 57, 65–81 (2006)
95. Reck, M. et al. Ipilimumab in combination with paclitaxel and carboplatin as first-line therapy in extensive-disease-small-cell lung cancer: results from a randomized, double-blind, multicenter Phase 2 trial. *Ann Oncol* 2013;24:75–83.
96. Ignacio Melero, David M. Berman, M. Angela Aznar, et al. Evolving synergistic combinations of targeted immunotherapies to combat cancer. *Nat Rev*

- Cancer. 2015;15(8):457-72.
97. Coley WB II. Contribution to the knowledge of sarcoma. *Annals of Surgery*. 1891;14(3):199–220.
98. Kluwe J, Mencin A, Schwabe RF. Toll-like receptors, wound healing, and carcinogenesis. *Journal of Molecular Medicine*. 2009;87(2):125–138.
99. Balkwill F. Tumour necrosis factor and cancer. *Nature Reviews Cancer*. 2009;9(5):361–371.
100. Modlin RL. Innate immunity: ignored for decades, but not forgotten. *Journal of Investigative Dermatology*. 2012;132(3):882–886.
101. Chiriva-Internati M, Pandey A, Saba R et al. Cancer testis antigens: a novel target in lung cancer. *International Reviews of Immunology*, vol. 31, no. 5, pp. 321–343, 2012.
102. Robbins PF, Morgan RA, Feldman SA, et al. Tumor regression in patients with metastatic synovial cell sarcoma and melanoma using genetically engineered lymphocytes reactive with NY-ESO-1. *J Clin Oncol*. 2011 Mar 1;29(7):917-24.
103. Robbins PF, Kassim SH, Tran TL, et al. A pilot trial using lymphocytes genetically engineered with an NY-ESO-1-reactive T-cell receptor: long-term follow-up and correlates with response. *Clin Cancer Res*. 2015;21(5):1019-27.
104. Pardoll DM. The blockade of immune checkpoints in cancer immunotherapy. *Nat Rev Cancer*. 2012;12(4):252-64.
105. Tawbi HA, Burgess M, Bolejack V, et al. Safety and efficacy of PD-1 blockade using pembrolizumab in patients with advanced soft tissue (STS) and bone sarcomas. *Lancet Oncol*. 2017 Oct 4. pii: S1470-2045(17)30624-1
106. Paoluzzi L, Cacavio A, Ghesani M et al. Response to anti-PD1 therapy with

- nivolumab in sarcoma Clin Sarcoma Res. 2016;6:24.
107. Maki RG, Jungbluth AA, Gnjatic SA. Pilot Study of Anti-CTLA4 Antibody Ipilimumab in Patients with Synovial Sarcoma. Sarcoma. 2013;2013:168145.
108. S. Chawla, B.A. Van Tine, S. Pollack, et al. A phase 2 study of CMB305 and atezolizumab in NY-ESO-1+ soft tissue sarcoma: Interim analysis of immunogenicity, tumor control and survival. Annals of Oncology, 2017. Volume 28, Issue suppl_5, Abs 1480PD.
109. Bhowmick NA, Chytil A, Plieth D, et al. TGF-beta signaling in fibroblasts modulates the oncogenic potential of adjacent epithelia. Science 2004;303:848–51.
110. Gupta N, Duda DG. Role of stromal cell-derived factor 1 α pathway in bone metastatic prostate cancer. J Biomed Res. 2016;30(3):181-5.
111. Quail DF, Joyce JA. Microenvironmental regulation of tumor progression and metastasis. Nat Med. 2013;19(11):1423-37.
112. Barcellos-de-Souza P, Gori V, Bambi F, et al. Tumor microenvironment: bone marrow-mesenchymal stem cells as key players. Biochim Biophys Acta. 2013 Dec;1836(2):321-35.
113. Hanahan D, Weinberg RA. Hallmarks of cancer: the next generation. Cell 2011;144: 646–674.
114. Chaturvedi P, Gilkes DM, Wong CC, et al. Hypoxia-inducible factor-dependent breast cancer-mesenchymal stem cell bidirectional signaling promotes metastasis. J Clin Invest. 2013 Jan;123(1):189-205.
115. Halpern JL, Kilbarger A, Lynch CC, et al. Mesenchymal stem cells promote mammary cancer cell migration in vitro via the CXCR2 receptor. Cancer Lett 2011;308:91–99.
116. Teicher BA, Fricker SP. CXCL12 (SDF-1)/CXCR4 pathway in cancer. Clin. Cancer Res 2010;16: 2927–2931.

117. Furusato B, Mohamed A, Uhlén M, et al. CXCR4 and cancer. *Pathol Int.* 2010 Jul;60(7):497-505
118. Olumi AF, Grossfeld GD, Hayward SW, et al. Carcinoma-associated fibroblasts direct tumor progression of initiated human prostatic epithelium. *Cancer Res* 1999;59:5002–11.
119. Orimo A, Gupta PB, SgROI DC, et al. Stromal fibroblasts present in invasive human breast carcinomas promote tumor growth and angiogenesis through elevated SDF-1/CXCL12 secretion. *Cell* 2005;121:335–48.
120. Burger JA, Peled A. CXCR4 antagonists: targeting the microenvironment in leukemia and other cancers. *Leukemia* 2009;23: 43–52.
121. Zhang P, Dong L, Yan K, et al. CXCR4-mediated osteosarcoma growth and pulmonary metastasis is promoted by mesenchymal stem cells through VEGF. *Oncol Rep* 2013;30:1753–1761.
122. Yu FX, Hu WJ, He B, et al. Bone marrow mesenchymal stem cells promote osteosarcoma cell proliferation and invasion. *World J Surg Oncol* 2015;13:52.
123. Li YJ, Dai YL, Zhang WB, et al. Clinicopathological and prognostic significance of chemokine receptor CXCR4 in patients with bone and soft tissue sarcoma: a meta-analysis. *Clin Exp Med.* 2017 Feb;17(1):59-69.
124. Palmerini E, Benassi MS, Quattrini I, et al. Prognostic and predictive role of CXCR4, IGF-1R and Ezrin expression in localized synovial sarcoma: is chemotaxis important to tumor response? *Orphanet J Rare Dis.* 2015;10:6.
125. Lu Y, Guan GF, Chen J, et al. Aberrant CXCR4 and β -catenin expression in osteosarcoma correlates with patient survival. *Oncol Lett.* 2015;10(4):2123-9.
126. Guan G, Zhang Y, Lu Y, et al. The HIF-1 α /CXCR4 pathway supports hypoxia-

- induced metastasis of human osteosarcoma cells. *Cancer Lett.* 2015;357(1):254-64.
127. Miyoshi K, Kohashi K, Fushimi F, et al. Close correlation between CXCR4 and VEGF expression and frequent CXCR7 expression in rhabdomyosarcoma. *Hum Pathol.* 2014;45(9):1900-9.
128. Guo M, Cai C, Zhao G, et al. Hypoxia promotes migration and induces CXCR4 expression via HIF-1alpha activation in human osteosarcoma. *PloS one.* 2014;9(3):e90518.
129. Berghuis D, Schilham MW, Santos SJ, et al. The CXCR4-CXCL12 axis in Ewing sarcoma: promotion of tumor growth rather than metastatic disease. *Clin Sarcoma Res.* 2012;2(1):24.
130. Baumhoer D, Smida J, Zillmer S, et al. Strong expression of CXCL12 is associated with a favorable outcome in osteosarcoma. *Mod Pathol.* 2012;25(4):522-8.
131. Lin F, Zheng SE, Shen Z, et al. Relationships between levels of CXCR4 and VEGF and blood-borne metastasis and survival in patients with osteosarcoma. *Med Oncol.* 2011;28(2):649-53.
132. Oda Y, Tateishi N, Matono H, et al. Chemokine receptor CXCR4 expression is correlated with VEGF expression and poor survival in soft-tissue sarcoma. *Int J Cancer.* 2009;124(8):1852-9.
133. Oda Y, Yamamoto H, Tamiya S, et al. CXCR4 and VEGF expression in the primary site and the metastatic site of human osteosarcoma: analysis within a group of patients, all of whom developed lung metastasis. *Mod Pathol.* 2006;19(5):738-45.
134. Laverdiere C, Hoang BH, Yang R, et al. Messenger RNA expression levels of CXCR4 correlate with metastatic behavior and outcome in patients with osteosarcoma. *Clin Cancer Res.* 2005;11(7):2561-7.

135. Domanska UM, Kruizinga RC, Nagengast WB, et al. A review on CXCR4/CXCL12 axis in oncology: No place to hide. *European Journal of Cancer* 2013;49:219–230.
136. Meads MB, Hazlehurst LA, Dalton WS. The bone marrow microenvironment as a tumor sanctuary and contributor to drug resistance. *Clin Cancer Res* 2008;14:2519–26.
137. Konopleva MY, Jordan CT. Leukemia stem cells and microenvironment: biology and therapeutic targeting. *J Clin Oncol* 2011;29:591–9
138. Nefedova Y, Cheng P, Alsina M, et al. Involvement of Notch-1 signaling in bone marrow stroma-mediated de novo drug resistance of myeloma and other malignant lymphoid cell lines. *Blood* 2004;103:3503–10.
139. Lwin T, Hazlehurst LA, Dessureault S, et al. Cell adhesion induces p27Kip1-associated cell-cycle arrest through down-regulation of the SCFSkp2 ubiquitin ligase pathway in mantle-cell and other non-Hodgkin B-cell lymphomas. *Blood* 2007; 110:1631–8.
140. Nervi B, Ramirez P, Rettig MP, et al. Chemosensitization of acute myeloid leukemia (AML) following mobilization by the CXCR4 antagonist AMD3100. *Blood* 2009;113:6206–14.
141. Gilbert LA, Hemann MT. DNA damage-mediated induction of a chemoresistant niche. *Cell* 2010;143:355–66.
142. Dillmann F, Veldwijk MR, Laufs S, et al. Plerixafor inhibits chemotaxis toward SDF-1 and CXCR4-mediated stroma contact in a dose-dependent manner resulting in increased susceptibility of BCR–ABL+ cell to imatinib and nilotinib. *Leuk Lymphoma* 2009;50:1676–86.
143. Redjal N, Chan JA, Segal RA, et al. CXCR4 inhibition synergizes with cytotoxic chemotherapy in gliomas. *Clin Cancer Res* 2006;12:6765–71.
144. Lee CH, Kakinuma T, Wang J, et al. Sensitization of B16 tumor cells with a CXCR4

- antagonist increases the efficacy of immuno- therapy for established lung metastases. *Mol Cancer Ther* 2006;5:2592–9.
145. Kim M, Koh YJ, Kim KE, et al. CXCR4 signaling regulates metastasis of chemoresistant melanoma cells by a lymphatic metastatic niche. *Cancer Res* 2010;70:10411–21.
146. Ferrari S, Ruggieri P, Cefalo G et al. Neoadjuvant chemotherapy with methotrexate, cisplatin, and doxorubicin with or without ifosfamide in nonmetastatic osteosarcoma of the extremity: an Italian sarcoma group trial ISG/OS-1. *J Clin Oncol* 2012; 30:2112-2118.
147. Picci P, Bacci G, Campanacci M et al. Histologic evaluation of necrosis in osteosarcoma induced by chemotherapy. *Cancer* 1985; 56:1515–1521.
148. Taube JM, Klein A, Brahmer JR et al. Association of PD-1, PD-1 ligands, and other features of the tumor immune microenvironment with response to anti-PD-1 therapy. *Clin Cancer Res* 2014; 20: 5064-5074.
149. Palmerini E, Staals EL, Alberghini M et al. Synovial sarcoma: retrospective analysis of 250 patients treated at a single institution. *Cancer* 2009;115:2988-2998.
150. Fletcher CDM, Unni KK, Mertens F. Pathology and genetics of tumours of soft tissue and bone. Lyon, France: IARC Press; 2002.
151. Lu YJ, Birdsall S, Summersgill B, et al. Dual colour fluorescence in situ hybridization to paraffin-embedded samples to deduce the presence of the der(X)t(X;18)(p11.2;q11.2) and involvement of either the SSX1 or SSX2 gene: a diagnostic and prognostic aid for synovial sarcoma. *J Pathol.* 1999;187:490–6.
152. Sun Y, Gao D, Liu Y, Huang J, Lessnick S, Tanaka S. IGF2 is critical for tumorigenesis by synovial sarcoma oncoprotein SYT- SSX1. *Oncogene.* 2006;25(7):1042–52.

153. Enneking WF, Spanier SS, Goodman MA. Current concepts review. The surgical staging of musculoskeletal sarcoma. *J Bone Joint Surg.* 1980;62-A:1027–30.
154. https://ita.promega.com/products/cell-health-assays/cell-viability-and-cytotoxicity-assays/celltiter-96-aqueous-one-solution-cell-proliferation-assay-_mts_/?catNum=G3582
155. <http://www.ebioscience.com/human-cd274-antibody-apc-mih1.htm>
156. Trabanelli S, Lecciso M, Salvestrini V, et al. PGE2-induced IDO1 inhibits the capacity of fully mature DCs to elicit an in vitro antileukemic immune response. *J Immunol Res* 2015;2015:253191.
157. Curti A, Pandolfi S, Aluigi M, et al. Interleukin-12 production by leukemia-derived dendritic cells counteracts the inhibitory effect of leukemic microenvironment on T cells. *Exp Hematol* 2005;33:1521-30.
158. Kuhne MR, Mulvey T, Belanger B, et al. BMS-936564/MDX-1338: a fully human anti-CXCR4 antibody induces apoptosis in vitro and shows antitumor activity in vivo in hematologic malignancies. *Clin Cancer Res.* 2013 Jan 15;19(2):357-66.
159. Pierini, B. Dozza, E. Lucarelli, et al. Efficient isolation and enrichment of mesenchymal stem cells from bone marrow. *Cytotherapy* 2012;14:686–693.
160. <http://rsbweb.nih.gov/ij/>
161. Dunn, G. P., Old, L. J. & Schreiber, R. D. The three Es of cancer immunoediting. *Annu. Rev. Immunol.* 22, 329–360 (2004).
162. Koebel, C. M. et al. Adaptive immunity maintains occult cancer in an equilibrium state. *Nature* 450, 903–907 (2007).
163. Schreiber RD, Old LJ, Smyth MJ Cancer immunoediting: integrating immunity's

- roles in cancer suppression and promotion. *Science* 2011;331:1565-1570.
164. Shankaran V. et al. IFN γ and lymphocytes prevent primary tumour development and shape tumour immunogenicity. *Nature* 2001;410:1107-1111.
165. Galon J et al. Type, density, and location of immune cells within human colorectal tumors predict clinical outcome. *Science* 2006;313:1960-1964.
166. Mlecnik, B. et al. Histopathologic-based prognostic factors of colorectal cancers are associated with the state of the local immune reaction. *J Clin Oncol* 2011;29:610-618.
167. Sundara YT, Kostine M, Cleven AH et al. Increased PD-L1 and T-cell infiltration in the presence of HLA class I expression in metastatic high-grade osteosarcoma: a rationale for T-cell-based immunotherapy. *Cancer Immunol Immunother* 2017; 66: 119-128.
168. Dumars C, Ngyuen JM, Gaultier A et al. Dysregulation of macrophage polarization is associated with the metastatic process in osteosarcoma. *Oncotarget* 2016; 7: 78343-78354.
169. Buddingh EP, Kuijjer ML, Duim RA et al. Tumor-infiltrating macrophages are associated with metastasis suppression in high-grade osteosarcoma: a rationale for treatment with macrophage activating agents. *Clin Cancer Res* 2011; 17: 2110–2119.
170. Kleinerman ES, Jia SF, Griffin J et al. Phase II study of liposomal muramyl tripeptide in osteosarcoma: the cytokine cascade and monocyte activation following administration. *J Clin Oncol* 1992; 10: 1310–1316.
171. Afanasiev OK, Yelistratova L, Miller N et al. Merkel polyomavirus-specific T cells fluctuate with merkel cell carcinoma burden and express therapeutically targetable PD-1 and Tim-3 exhaustion markers. *Clin Cancer Res* 2013; 9: 5351-5360.
172. Herbst RS, Soria JC, Kowanetz M et al. Predictive correlates of response to the anti-PD-L1 antibody MPDL3280A in cancer patients. *Nature* 2014; 515: 563-567.

173. Tumeah PC, Harview CL, Yearley JH et al. PD-1 blockade induces responses by inhibiting adaptive immune resistance. *Nature* 2014; 515: 568–571.
174. Llosa NJ, Cruise M, Tam A et al. The vigorous immune microenvironment of microsatellite instable colon cancer is balanced by multiple counter-inhibitory checkpoints. *Cancer Discov* 2015; 5: 43-51.
175. Lipson EJ, Sharfman WH, Drake CG et al. Durable cancer regression off- treatment and effective reinduction therapy with an anti-PD-1 antibody. *Clin. Cancer Res* 2013; 19: 462-468.
176. Lyford-Pike S, Peng S, Young GD et al. Evidence for a role of the PD-1:PD-L1 pathway in immune resistance of HPV- associated head and neck squamous cell carcinoma. *Cancer Res* 2013; 73: 1733-1741.
177. Kleinerman ES, Jia SF, Griffin J, et al. Phase II study of liposomal muramyl tripeptide in osteosarcoma: the cytokine cascade and monocyte activation following administration. *J Clin Oncol* 1992;10(8):1310-6
178. ten Hagen TL, van Vianen W, Savelkoul HF et al. Involvement of T cells in enhanced resistance to *Klebsiella pneumoniae* septicemia in mice treated with liposome-encapsulated muramyl tripeptide phosphatidylethanolamine or gamma interferon. *Infect Immun* 1998; 66: 1962-1977.
179. Meyers PA, Schwartz CL, Krailo MD et al. Osteosarcoma: the addition of muramyl tripeptide to chemotherapy improves overall survival – a report from the Children’s Oncology Group. *J Clin Oncol* 2008; 26: 633-663.
180. van Erp AEM, Versleijen-Jonkers YMH, Hillebrandt-Roeffen MHS et al. Expression and clinical association of programmed cell death-1, programmed death-ligand-1 and CD8+ lymphocytes in primary sarcomas is subtype dependent.

- Oncotarget. 2017;8(41):71371-71384.
181. Nowicki TS, Akiyama R, Huang RR, et al. Infiltration of CD8 T Cells and Expression of PD-1 and PD-L1 in Synovial Sarcoma. *Cancer Immunol Res.* 2017; 5:118–26.
 182. Gajewski TF, Schreiber H, Fu YX. Innate and adaptive immune cells in the tumor microenvironment. *Nat Immunol.* 2013;14:1014–1022.
 183. Broadhead ML, Clark JC, Myers DE, et al. The molecular pathogenesis of osteosarcoma: a review. *Sarcoma* 2011, 959248, 10.1155/2011/959248 (2011).
 184. Jones MJ, Jallepalli PV. Chromothripsis: chromosomes in crisis. *Dev Cell* 2012;23:908–917.
 185. Chen X. et al. Recurrent somatic structural variations contribute to tumorigenesis in pediatric osteosarcoma. *Cell Rep.* 2014;7:104–11.
 186. Iura K, Maekawa A, Kohashi K, et al. Cancer-testis antigen expression in synovial sarcoma: NY-ESO-1, PRAME, MAGEA4, and MAGEA1. *Hum Pathol.* 2017 Mar;61:130-139.
 187. Abdeen A, Chou AJ, Healey JH, et al. Correlation between clinical outcome and growth factor pathway expression in osteogenic sarcoma. *Cancer.* 2009 Nov 15;115(22):5243-50.
 188. Kubo T, Piperdi S, Rosenblum J, et al. Platelet-derived growth factor receptor as a prognostic marker and a therapeutic target for imatinib mesylate therapy in osteosarcoma. *Cancer.* 2008 May 15;112(10):2119-29.
 189. Kumar RM, Arlt MJ, Kuzmanov A, Born W, Fuchs B. Sunitinib malate (SU-11248) reduces tumour burden and lung metastasis in an intratibial human xenograft osteosarcoma mouse model. *Am J Cancer Res.* 2015 Jun 15;5(7):2156-68.
 190. Y Pignochino, G Grignani, G Cavalloni, et al. Sorafenib blocks tumour growth,

- angiogenesis and metastatic potential in preclinical models of osteosarcoma through a mechanism potentially involving the inhibition of ERK1/2, MCL-1 and ezrin pathways. *Mol Cancer* 2009;8:118–130.
191. Farsaci B, Higgins JP, Hodge JW. Consequence of Dose Scheduling of Sunitinib on Host Immune Response Elements and Vaccine Combination Therapy. *Int J Cancer*. 2012;130(8):1948–1959.
192. Yang Z, Zhang B, Li D, et al. Mast cells mobilize myeloid-derived suppressor cells and Treg cells in tumor microenvironment via IL-17 pathway in murine hepatocarcinoma model. *PLoS One*. 2010; 5:e8922.
193. de Boüard S, Herlin P, Christensen J, et al. Antiangiogenic and anti-invasive effects of sunitinib on experimental human glioblastoma. *Neuro Oncol* 2007; 9: 412-42310.
194. Kumar RM, Arlt MJ, Kuzmanov A, et al. Sunitinib malate (SU-11248) reduces tumour burden and lung metastasis in an intratibial human xenograft osteosarcoma mouse model. *Am J Cancer Res*. 2015;5(7):2156-68.
195. Powles T, Sarwar N, Stockdale A, et al. Safety and efficacy of pazopanib therapy prior to planned nephrectomy in metastatic clear cell renal cancer. *JAMA Oncol* 2016; 2(10):1303–9.
196. Sharpe K, Stewart GD, Mackay A, et al. The effect of VEGF-targeted therapy on biomarker expression in sequential tissue from patients with metastatic clear cell renal cancer. *Clin Cancer Res* 2013;19(24):6924–34.
197. Liu XD, Hoang A, Zhou L, et al. Resistance to antiangiogenic therapy is associated with an immunosuppressive tumor microenvironment in metastatic renal cell carcinoma.

- Cancer Immunol Res (2015) 3(9):1017–29.
198. Ruiz-Bañobre J, Anido U, Abdulkader I, et al. Long-term Response to Nivolumab and Acute Renal Failure in a Patient with Metastatic Papillary Renal Cell Carcinoma and a PD-L1 Tumor Expression Increased with Sunitinib Therapy: A Case Report. *Front Oncol.* 2016;6:250. eCollection.
 199. Amin A et al. Nivolumab in combination with sunitinib or pazopanib in patients with metastatic renal cell carcinoma (mRCC). *J Clin Oncol* 2014;32:5s (suppl; abstr 5010).
 200. Motzer RJ, et al. Pazopanib versus sunitinib in metastatic renal-cell carcinoma. *N Engl J Med* 2013; 369:722-731.
 201. Penn I. Sarcomas in organ allograft recipients. *Transplantation.* 1995;60(12):1485-91.
 202. van der Graaf WT, et al. Pazopanib for metastatic soft-tissue sarcoma (PALETTE): a randomised, double-blind, placebo-controlled phase 3 trial. *Lancet.* 2012;379(9829):1879-86.
 203. Matsuo T, et al. Extraskelatal osteosarcoma with partial spontaneous regression. *Anticancer research.* 2009;29(12):5197-201.
 204. Stephens PJ, Greenman CD, Fu B, et al. Massive genomic rearrangement acquired in a single catastrophic event during cancer development. *Cell.* 2011;144: 27–4.
 205. Ohali A, Avigad S, Cohen IJ, et al. High frequency of genomic instability in Ewing family of tumors. *Cancer Genet Cytogenet.* 2004;150:50–6.
 206. Ferreira BI, Alonso J, Carrillo J, et al. Array CGH and gene-expression profiling reveals distinct genomic instability patterns associated with DNA repair and cell-cycle checkpoint pathways in Ewing’s sarcoma. *Oncogene.* 2008;27:2084–90.
 207. Rizvi NA et al. Mutational landscape determines sensitivity to PD-1 blockade in non-small cell lung cancer. *Science.* 2015;348(6230):124-8.

208. Sampson JN, et al. Analysis of Heritability and Shared Heritability Based on Genome-Wide Association Studies for Thirteen Cancer Types. *J Natl Cancer Inst.* 2015;107(12).
209. Jacquelot N, Roberti MP, Enot DP, et al. Predictors of responses to immune checkpoint blockade in advanced melanoma. *Nat Commun.* 2017;8(1):592.
210. Gnjatic S, Bronte V, Brunet LR, et al. Identifying baseline immune-related biomarkers to predict clinical outcome of immunotherapy. *J Immunother Cancer.* 2017;5:44
211. E. Perissinotto, G. Cavalloni, F. Leone, et al. Involvement of chemokine receptor 4/stromal cell-derived factor 1 system during osteosarcoma tumor progression. *Clin. Cancer Res.* 2005;11:490–97.
212. Bachelder RE, Wendt MA, Mercurio AM. Vascular endothelial growth factor promotes breast carcinoma invasion in an autocrine manner by regulating the chemokine receptor CXCR4. *Cancer Res.* 2002;62:7203-7206.
213. Barbero S, Bonavia R, Bajetto A, et al. Stromal cell-derived factor 1a stimulates human glioblastoma cell growth through the activation of both extracellular signal-regulated kinases 1/2 and Akt. *Cancer Res.* 2003;63:1969-1974.
214. Kijima T, Maulik G, Ma PC, et al. Regulation of cellular proliferation, cytoskeletal function, and signal transduction through CXCR4 and c-Kit in small cell lung cancer cells. *Cancer Res* 2002;62:6304- 6311.
215. Lai TH, Fong YC, Fu WM, et al. Stromal cell-derived factor-1 increase avb3 integrin expression and invasion in human chondrosarcoma cells. *J Cell Physiol* 2009;218:334–342.
216. Kashyap MK, Kumar D, Jones H, et al. Ulocuplumab (BMS-936564 / MDX1338):

- a fully human anti- CXCR4 antibody induces cell death in chronic lymphocytic leukemia mediated through a reactive oxygen species- dependent pathway. *Oncotarget*. 2016;7(3):2809-22.
217. Jiang C et al. AMD3100 combined with triptolide inhibit proliferation, invasion and metastasis and induce apoptosis of human U2OS osteosarcoma cells. *Biomedicine & Pharmacotherapy* 2017; 86:677–685.
218. Koh BI, Kang Y. The pro-metastatic role of bone marrow-derived cells: a focus on MSCs and regulatory T cells. *EMBO Rep*. 2012 13:412–422.
219. Bergfeld SA, DeClerck YA. Bone marrow-derived mesenchymal stem cells and the tumor microenvironment, *Cancer Metastasis Rev* 2010;29:249–261.
220. Karnoub AE, Dash AB, Vo AP, et al. Mesenchymal stem cells within tumour stroma promote breast cancer metastasis. *Nature* 2007;4:557–563.
221. Hogan NM, Joyce MR, Murphy JM, et al., 56 Impact of mesenchymal stem cell secreted PAI-1 on colon cancer cell migration 57 and proliferation, *Biochem. Biophys. Res. Commun*. 2013;14:574-579.
222. Tu B, Du L, Fan QM, et al. STAT3 activation by IL-6 from mesenchymal stem cells promotes the proliferation and metastasis of osteosarcoma. *Cancer Lett* 2012;325:80-88.
223. Xu WT, Bian WT, Fan QM, et al. Human mesenchymal stem cells (hMSCs) target osteosarcoma and promote its growth and pulmonary metastasis, *Cancer Lett*. 2009;281:32–41.
224. Zhang P, Dong L, Yan K, et al. CXCR4-mediated osteosarcoma growth and pulmonary metastasis is promoted by mesenchymal stem cells through VEGF. *Oncol Rep*. 2013;30:1753–1761.

225. Yu FX, Hu WJ, He B, et al. Bone marrow mesenchymal stem cells promote osteosarcoma cell proliferation and invasion. *World J Surg Oncol* 2015;13:52.
226. Fontanella R, Pelagalli A, Nardelli A, et al. A novel antagonist of CXCR4 prevents bone marrow-derived mesenchymal stem cell-mediated osteosarcoma and hepatocellular carcinoma cell migration and invasion. *Cancer Lett.* 2016;370(1):100-7.
227. Portella L, Vitale R, De LS, et al. Preclinical development of a novel class of CXCR4 antagonist impairing solid tumors growth and metastases. *PLoS One* 2012;8:758–767.
228. Kuhne MR, Mulvey T, Belanger B, et al. BMS-936564/MDX-1338: a fully human anti-CXCR4 antibody induces apoptosis in vitro and shows antitumor activity in vivo in hematologic malignancies. *Clin Cancer Res* 2013;19:357-366
229. Galon J, Mlecnik B, Bindea, G et al. Towards the introduction of the ‘Immunoscore’ in the classification of malignant tumours. *J Pathol* 2014; 232: 199–209.
230. Feig C, Jones JO, Kraman M, et al. Targeting CXCL12 from FAP-expressing carcinoma-associated fibroblasts synergizes with anti-PD-L1 immunotherapy in pancreatic cancer. *Proc Natl Acad Sci U S A.* 2013;110(50):20212-7.

9 – ACKNOWLEDGMENTS

I thank Prof Pierluigi Lollini, both tutor and PhD chair, extremely supportive in either role

I thank Dr Stefano Ferrari and Dr Piero Picci, my mentors and guide for over 10 years

I thank for experiments:

- ✓ Prof Claudio Agostinelli and Prof Stefano Pileri, Hemolymphopathology, S Orsola Hospital, Bologna
- ✓ Dr Teresa Marafioti, Haematopathology, University College London Hospitals, London
- ✓ Dr Mariaserena Benassi, Dr Laura Pazzaglia, Dr Amalia Conti, Dr Serena Pollino, Research Unit "Molecular Characterization of Sarcoma, Rizzoli Orthopaedic Institute, Bologna
- ✓ Dr Enrico Lucarelli e Dr Barbara Dozza, Osteoarticular Regeneration Laboratory, Rizzoli Orthopaedic Institute, Bologna

Dr Antonio Curti, Dr Maraingela Lecciso, Dr Darina Ocadlikova, Stem Cells Research and Cells Therapy, Seragnoli Institute, S Orsola Hospital, Bologna

I thank Prof Guido Biasco, Prof Sante Tura and Prof Francesco Antonio Manzoli: with their example I learned to put passion and perseverance in what I do

I thank Dr Robert Maki, Northwell Health Cancer Institute, New York City, for his continuous scientific supervision in sarcoma research and friendship

I thank mom and dad, for believing in me

I thank my husband, Michele, for his patience and love